②

NAVAL POSTGRADUATE SCHOOL
Monterey , California

DTIC
S ELECTE
OCT 10 1990
B D

THESIS

LOCAL AND SPATIALLY AVERAGED HEAT
TRANSFER DISTRIBUTIONS IN A CURVED CHANNEL
WITH 40 TO 1 ASPECT RATIO FOR DEAN NUMBERS
FROM 50 TO 200

by

Paul E. Skogerboe

March 1990

Thesis Advisor: Phillip Ligrani

Approved for public release; distribution is unlimited

90

REPORT DOCUMENTATION PAGE

1a. REPORT SECURITY CLASSIFICATION UNCLASSIFIED	1b. RESTRICTIVE MARKINGS
2a. SECURITY CLASSIFICATION AUTHORITY	3 DISTRIBUTION/AVAILABILITY OF REPORT
2b. DECLASSIFICATION/DOWNGRADING SCHEDULE	Approved for public release; distribution is unlimited.

4 PERFORMING ORGANIZATION REPORT NUMBER(S)	5 MONITORING ORGANIZATION REPORT NUMBER(S)

6a. NAME OF PERFORMING ORGANIZATION Naval Postgraduate School	6b. OFFICE SYMBOL (If applicable) 69	7a. NAME OF MONITORING ORGANIZATION Naval Postgraduate School
6c. ADDRESS (City, State, and ZIP Code) Monterey, CA 93943-5000		7b. ADDRESS (City, State, and ZIP Code) Monterey, CA 93943-5000

8a. NAME OF FUNDING/SPONSORING ORGANIZATION	8b. OFFICE SYMBOL (If applicable)	9 PROCUREMENT INSTRUMENT IDENTIFICATION NUMBER MIPR-No. C-80019-F

8c. ADDRESS (City, State, and ZIP Code) U. S. ARMY AVIATION RES. & TECH. ACTIVITY AVSCOM NASA-LEWIS RES. CENTER CLEVELAND 45433	10. SOURCE OF FUNDING NUMBERS			
	Program Element No	Project No	Task No	Work Unit Accession Number

11 TITLE (Include Security Classification)
LOCAL AND SPATIALLY AVERAGED HEAT TRANSFER DISTRIBUTIONS IN A CURVED CHANNEL WITH 40 TO 1 APECT RATIO FOR DEAN NUMBERS FROM 50 TO 200

12 PERSONAL AUTHOR(S) SKOGERBOE, PAUL E.

13a TYPE OF REPORT Master's Thesis	13b TIME COVERED From To	14. DATE OF REPORT (year, month, day) 1990 MARCH 29	15 PAGE COUNT 131

16 SUPPLEMENTARY NOTATION
The views expressed in this thesis are those of the author and do not reflect the official policy or position of the Department of Defense or the U.S. Government.

17 COSATI CODES			18 SUBJECT TERMS (continue on reverse if necessary and identify by block number)
FIELD	GROUP	SUBGROUP	CURVED HEATING CHANNEL, HEAT TRANSFER COEFFICIENTS, NUSSELT NUMBERS, DEAN VORTICES, CENTRIFUGAL INSTABILITIES, Theses

19. ABSTRACT (continue on reverse if necessary and identify by block number)

The effects of curvature and the resulting centrifugal instabilities on local heat transfer distributions are studied in a curved channel at Dean numbers ranging from 50 to 200. The channel has a rectangular cross section of 1.27 cm by 50.1 cm giving an aspect ratio of 40 to 1. Flow is heated in a straight portion of the channel prior to the curved portion in order to obtain flow which is hydrodynamically and thermally fully developed. All baseline tests confirm techniques employed and qualify flow behavior. These consist of energy balance checks and comparison of results from the straight section to numerical and analytic solutions. Nusselt numbers in the curved section initially show an abrupt decrease after the imposition of the stabilizing influences of convex curvature. These are followed by a gradual increase as centrifugal instabilities and Dean vortices form and develop. Spatially resolved results also show significant surface Nusselt number variations across the span of a vortex pair, especially on the concave surface. On the convex surface, local Nusselt numbers are much more apt to be spanwise uniform.

20 DISTRIBUTION/AVAILABILITY OF ABSTRACT ☐ UNCLASSIFIED/UNLIMITED ☒ SAME AS REPORT ☐ DTIC USERS	21 ABSTRACT SECURITY CLASSIFICATION UNCLASSIFIED	
22a NAME OF RESPONSIBLE INDIVIDUAL PROFESOR LIGRANI	22b TELEPHONE (Include Area code) (408) 646-3382	22c OFFICE SYMBOL 69 Li

DD FORM 1473, 84 MAR   83 APR edition may be used until exhausted
All other editions are obsolete

SECURITY CLASSIFICATION OF THIS PAGE

Unclassified

i

Locally and Spacially Averaged Heat Transfer Distributions in a Curved
Channel with 40 to 1 Aspect Ratio for Dean Numbers from 50 to 200

by

Paul E. Skogerboe
Lieutenant, United States Navy
B.S., Iowa State University, 1982

Submitted in partial fulfillment of the
requirements for the degree of

MASTER OF SCIENCE IN MECHANICAL ENGINEERING

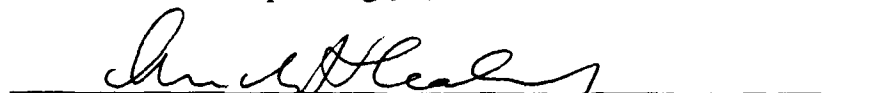from the

NAVAL POSTGRADUATE SCHOOL

March 1990

Author:

_____

Paul E. Skogerboe

Approved by:

_____

Phillip M. Ligrani, Thesis Advisor

_____

Anthony J. Healey, Chairman
Department of Mechanical Engineering

ii

ABSTRACT

The effects of curvature and the resulting centrifugal instabilities on local heat transfer distributions are studied in a curved channel at Dean numbers ranging from 50 to 200. The channel has a rectangular cross section of 1.27 cm by 50.1 cm giving an aspect ratio of 40 to 1. Flow is heated in a straight portion of the channel prior to the curved portion in order to obtain flow which is hydrodynamically and thermally fully developed. All baseline tests confirm techniques employed and qualify flow behavior. These consist of energy balance checks and comparison of results from the straight section to numerical and analytic solutions. Nusselt numbers in the curved section initially show an abrupt decrease after the imposition of the stabilizing influences of convex curvature. These are followed by a gradual increase as centrifugal instabilities and Dean vortices form and develope. Spacially resolved results also show significant surface Nusselt number variations across the span of a vortex pair, especially on the concave surface. On the convex surface, local Nusselt numbers are much more apt to be spanwise uniform.

iii

TABLE OF CONTENTS

LIST OF FIGURES

ACKNOWLEDGMENT

I. INTRODUCTION

A. DESCRIPTION OF THE PROBLEM

The effects of curvature and the resulting centrifugal instabilities on local heat transfer distributions are studied using a curved channel with an internal aspect ratio of 40 to 1. Results are presented for Dean numbers ranging from 50 to 200, resulting in laminar flow which sometimes contains pairs of Dean vortices. Other work at the Naval Postgraduate School in this area addresses the development of vortex flows due to centrifugal instabilities and the effects of these secondary flows on transition from laminar to turbulent behavior without considering heat transfer. Ligrani and Niver [Ref. 1] describe some results from this study which are also obtained in a curved channel with a similar aspect ratio of 40 to 1. These authors also review other non-thermal studies.

Several other studies focus on heat transfer in channels with turbulent flow. Johnson and Launder [Ref. 2] present local heat transfer results from a channel with a 180 degree bend and square cross section. They emphazise that instabilities from curvature produce very complex examples of turbulent flows due to substantial secondary flows. Additional studies are described by Chang, Humphrey, Johnson and Launder [Ref. 3], who employ a channel with a 180 degree bend of square cross section, and by Brinch and Graham [Ref. 4], who use a curved channel with an aspect ratio of 6. Studies dealing with the effects of heat transfer on turbulent boundary layers include ones described by Gibson, Verriopoulos and Nagano [Ref. 5], Simon and Moffat [Ref. 6] and Chang, Humphrey and Modavi [Ref. 7].

No studies, other than the present one are known to the present authors, which consider the effects of centrifugal instabilities and vortex flows on local heat transfer distributions in laminar and transitional flow in a channel with 40 to 1 aspect ratio. Understanding such curved flows is important to the design of devices such as heat exchangers and gas turbine blades.

B. OBJECTIVES

The objective of this thesis is to provide experimental evidence as to how curvature affects local heat transfer distributions on the surfaces of a curved channel for Dean numbers from 50 to 200. This is accomplished by;

1. Qualifying experimental procedures, measurement techniques and channel facilities by conducting several baseline comparisons on the straight portion of the channel.

2. Provide accurate Nusselt number data for both surfaces of the 180 degree curved channel, thus providing information as to how centrifugal instabilities and the resulting vortex pairs affect local heat transfer distributions.

C. ORGANIZATION

Subsequent to this introduction, Chapter II details the design and construction of the curved heated channel used in this study. Chapter III discusses the experimental procedures and measurment techniques. Chapter IV provides a series of baseline qualification comparisons and then presents the results of the Nusselt number measurements. Chapter V presents conclusions and recommendations.

II EXPERIMENTAL FACILITIES

A. CURVED HEATED CHANNEL

The apparatus used in this study is a rectangular curved channel shown in Figure 1. Within this facility, local surface temperatures and other quantities are measured so that the effects of curvature on local Nusselt number distributions can be studied. To coincide with work done on a transparent channel used for flow visualization, shown in Figure 2, identical internal dimensions are used for the heat transfer channel. The channel has an interior rectangular cross section of 1.27 cm by 50.1 cm, giving an aspect ratio of 40 to 1. The heat transfer channel is different from the transparent channel since it allows for thermal expansion which results from heating. This is accomplished by non-rigid securing of channel surfaces and by constructing much of the channel on skids to allow for longitudinal expansion. A detailed description of the design and construction of the channel is presented by Hughes [Ref. 8]. A brief summary of design and construction details is also given here.

1. Channel Construction

A photograph of the channel for heat transfer measurements is shown in Figure 1. Details of the inlet section are shown in Figure 3. The rectangular duct inlet section contains an aluminum honeycomb and three wire screens all placed normal to the flow direction. These devices reduce spacial non-uniformities in the flow. As the air exits the 25.4 cm by 50.8 cm rectangular duct inlet, it enters a 20 to 1 contraction ratio nozzle.The nozzle is constructed from the same two continuous pieces of lexan as used for the straight and curved test section walls, thus eliminating a seam between the nozzle and the channel. Lexan is the

3

commercial name of a polycarbonate material. The shape of the nozzle is designed using a fifth order polynomial with respect to streamwise distance to ensure that the flow remains laminar and unseparated as it enters the channel.

After exiting the inlet nozzle, air first enters a straight section, 244 cm (96 inches) in length with interior dimensions of 1.27 cm by 50.8 cm (.5 inches by 20 inches). The straight section allows hydrodynamically fully developed channel flow to develope before the flows enters the curved section. The fluid then enters a 180 degree curved channel section with a convex surface radius of 59.69 cm (23.5 inches) and a concave surface radius of 60.96 cm (24 inches). Upon exiting the curved section, air then enters a second straight section with a length of 244 cm (96 inches).

On the convex surface of the second straight section, a 5.08 cm (2.0 inches) wide slot is present which allows insertion of a probe into the channel to measure outlet mixed mean temperatures. The slot is located approximately 57.1 cm (22.5 inches) from the trailing edge of the heater on the curved convex wall, or 19.05 cm (7.5 inches) downstream of the end of curvature. A support block was constructed to support the area around the slot. Brass inserts are placed just inside the slot to allow insertion of two thin foam strips which adhere to the brass to provide an air tight seal between the channel interior and exterior as the probe is traversed. As flow leaves the second straight portion it passes through four screens, a honeycomb, a diffuser with a total angle of 3 degrees, and finally into Plenum #1.

The channel is designed to allow for thermal expansion in longitudinal and transverse directions which occurs as test surfaces are heated. As is illustrated in Figure 7 [Ref. 8], the surfaces of the channel are not rigidly secured, but are clamped onto the sidewalls to allow for such motion. In addition, both the inlet and outlet sections,including Plenum #1,

4

are constucted on two plexiglass skids to allow for longitudinal expansion.

2. Blower Assembly

The blower and plumbing connecting it to the channel are shown schematically in Figure 4 [Ref. 8]. The device itself is an ICG Industries type 10P blower, capable of producing 10.2 cm of water vacuum at 4.82 m^3/min volumetric flowrate. It is used to depressurize outlet Plenum #2 to pressures just below atmospheric pressure. In doing so, air is then drawn from Plenum #1 through a globe valve and a 5.08 cm inside diameter PVC pipe. With this system, flowrates can be varied to produce Dean numbers from 10 to 435. Flowrates are measured by means of a pressure drop across a 3.51 cm (1.5 inch) orifice plate. Details concerning the orifice plate are given in Hughes [Ref. 8] and also discussed in Chapter 3.

To reduce vibrations from the blower to the test section and to minimize disturbances to the flow, a damper is used to connect the suction side of the blower to Plenum #2 and a second damper is used to connect Plenum #2 to the orifice plate. Both dampers consist of thin sheets of plastic wrapped around the piping with air tight seals. The plastic is attached at both ends by double sided tape and then tightly secured with standard hose clamps in order to prevent any leaks. In addition, rubber mounts are used to mount the blower and blower frame to further reduce vibrations. A photograph of this assembly is shown in Figure 5.

3. Heaters

Four etched foil heaters, manufacured by the Electrofilm Corporation, are installed on each of the two lexan surfaces, as shown in Figure 6 [Ref. 8]. In the present study, these heaters provide a constant heat flux to both the concave and convex surfaces of the channel, all at the same heat rates, to produce uniform boundary conditions at the channel walls. The

5

dimensions of each heater are 38.1 cm by 152.4 cm (15.0 inches by 60.0 inches), and power capacity is 2 KW. Drawings indicating how the heaters are attached are shown in Figure 7 and Figure 8 [Ref. 8] and are discussed further by Schwartz [Ref. 9]. The leading edge of the CC1 and CV1 heaters are 88.4 cm from the channel inlet. The trailing edges of the CC2 and CV2 heaters end approximately 38.1 cm (15.0 inches) from the completion of channel curvature. This is about 57.15 cm (22.5 inches) upstream of the location of the temperature traverse probe. CC1 and CV1 refer to the two heaters on the concave and convex surfaces of the straight section, respectively, and CC2 and CV2 refer to the heaters on the concave and convex surfaces of the curved section, respectively.

Each heater is powered by a Superior Electric type 136B variac as shown in Figure 9 [Ref. 8]. With each variac, the voltage to a heater may be adjusted between 0 and 115 volts, and the current may be adjusted from 0 to 10 amps. A detailed schematic of the heater circuitry is given by Hughes [Ref. 8] and also shown in Figure 10 . Power inputs to each heater are determined by measuring voltage drops across 50 mv, 10 amp shunt resistors, as well as across each heater. The shunt resistance measurement allows for the heater current to be determined. Details in adjusting desired heat input levels are given in Chapter 3.

4 . Insulation

To minimize the loss of conducted heat to the surroundings, and maximize the amount of heat into each heater which is convected away, the outside of the entire heated portion of the channel is insulated with black foam insulation manufactured by the Halstead Company. A detailed drawing showing how various layers of insulation are attached to the channel to produce a total thickness of 6.0 cm (2.36 inches) on each side is illustrated in Figure 7

6

[Ref. 8]. For this study, an additional row of 2.5 cm (1.0 inch) insulation is attached along all edges of the heated channel to further minimize conduction from heated channel walls. Photographs of the insulation are shown in Figure 11 and Figure12.

5. Thermocouples

200 copper-constantan thermocouples are placed on channel surfaces to allow detailed spatially resolved surface temperature measurements to be made. Figure 8 [Ref. 8] shows the approximate locations of each thermocouple. The exact locations are listed in Appendix A., as determined by measurements conducted as a part of this study. Measurements are based on a coordinate system shown in Figures 13 and 14 . Here X is in the streamwise direction measured from the inlet of the straight section, Z is in the spanwise direction and measured from the centerline, and Y is normal to channel surfaces in the vertical direction measured from the channel midplane.

On the straight section,15 thermocouples are placed on each of the CC1 and CV1 surfaces in 5 spanwise rows of 3 per row. The first row is located 103.64 cm (40.8 inches) from the inlet or 15.24 cm (6 inches) from the leading edge of the heater. Each additional row is spaced 30.48 cm (12 inches) apart in the X direction. The remaining 170 thermocouples are located on the curved section walls in 5 spanwise rows of 17 per row. Again, each row is spaced 30.48 cm (12 inches) apart in the X direction. Of the 17 thermocouples in each spanwise row, two are located near the edges of the channel with the remaining 15 placed over a spanwise length of approximately 5.08 cm (2.0 inches) on each side of the centerline. The purpose of these thermocouples is to provide an accurate average local Nusselt number, as well as a means of determining local Nusselt numbers in the presence of two pairs of Dean vortices [Ref. 8].

7

Four additional thermocouples are used to measure ambient temperatures around the outside of the channel, mixed mean temperature at the air inlet and mixed mean temperature at the channel outlet. Thermocouple (TC) #200 is placed just in front of the inlet and provides the mixed mean inlet temperature. TC #201 and TC #202 are placed respectively on the outsides of the CC2 and CV2 surfaces to provide local ambient temperatures. Finally, TC #203 is used in the temperature traverse probe to provide measurement of local temperatures used to calculate outlet mixed mean temperatures.

Each of the 204 thermocouples is attached to a data acquisition channel and the corresponding channel numbers are also listed in Appendix A. Briefly, thermocouples 1 to 30 correspond to acquisition channels 0 to 29, thermocouples 31 to 115 to channels 30 to 79 and 100 to 134, and finally, thermocouples 116 to 204 correspond to channels 135 to 179 and 200 to 243.

B. DATA ACQUISITION

1. Surface Temperature Measurement

Voltages from the 204 thermocouples are read by Hewlett-Packard type T20 relay multiplexer card assemblies for T type thermocouples. These assemblies are installed in a HP3497A low-speed Data Acquisition /Control Unit and a HP3498A Extender. This system provides thermocouple compensation electronically such that voltages for type T thermocouples are given relative to 0^{0} C. This system is connected to a Hewlett-Packard 9836S computer which processes voltages from the 204 thermocouples which are then recorded into data files along with corresponding temperatures . A schematic of this system is shown in Figure 15 [Ref. 8].

8

2. Outlet Mixed Mean Temperature Measurement

The acquisition system used for exit mixed-mean temperature measurments is illustrated in Figure 16 [Ref. 8]. The thermocouple probe used to measure the mixed mean temperature at the exit of the heated test section consists of a thermocouple attached to a metal support. This support is then secured to a traversing block. An automated two-dimensional traversing device, which allows both spanwise and radial movement, is used to traverse the temperature probe and shown in Figure 17. The movements of the motors on the traversing devise are controled by signals from the HP9836S computer, which are sent to a Modulynx Mitas PMS085-CZAR Drive Controller and then to a Modulynx Mitas PMS085-D0J0 Motion Drive. The motor Drive sends signals to each of the Superior Electric M092-FD310 stepping motors, which rotate drive screws which then move two traversing blocks. The threads of the drive screws are such that one rotation gives a vertical or lateral probe movement of .127 cm (.05 inches). For each traverse, 320 local temperatures are recorded over a channel cross section area of 5.08 cm (2.0 inches) in the spanwise direction by 1.02 cm (.4 inches) in the radial direction in increments of 0.127 cm (.05 inches). Upon completion of the traverse, the controller is programmed to return the probe to its original position. Voltage readings from the traversing thermocouple are processed in the same manner as the channel surface thermocouples.

9

III. EXPERIMENTAL PROCEDURES

To obtain heat transfer distributions, flow is first induced in the channel, heater power levels are adjusted to provide a constant surface heat flux boundary condition, voltages from thermocouples are read, surface temperatures are determined, and finally Nusselt numbers are calculated. Flow is laminar for all tests. Pairs of counter rotating Dean vortices are present over a large range of the Dean numbers studied, especially at farther downstream locations.

Experimental procedures are discussed in three parts. In part one, means to set flowrate and Dean number are discussed along with details on the adjustment of thermal boundary conditions. Part two, processing of surface temperature measurements and the determination of local Nusselt numbers. Finally, part three discusses the use of the temperature traverse probe, and method used to determine local and exit mixed-mean temperatures.

A. CHANNEL PREPARATION

1. Flowrate and Dean Number Setting

Local Nusselt numbers are determined at Dean numbers ranging from 50 to 200 in increments of 25 using the software program **Nuscurv**. The first step in each run is to set the flowrate to obtain the desired Dean number. The mass flowrate, $\dot{m}$, is determined from the equation:

$$\dot{m} = De\left[\rho A_{ch}\left[\frac{v}{d}\right]\right]\sqrt{\frac{r_i}{d}}$$

Where:

De = Dean Number

ρ = Air density

A_{ch} = Channel area

r_i = Inside radius of channel curvature

d = Channel height

ν = Kinematic viscosity

The flowrate is set by regulating the pressure drop across a 3.81 cm (1.5 in) standard ASME orifice plate, located in piping between the two exit plenums. The initial value of this pressure drop is estimated using results such as the ones presented in Figure 18. The pressure drop, in inches of water, is then also measured using a digital monometer. Afterwards, an iteration process is used to determine the true Dean number.

As the iteration process is implemented, the pipe Reynolds number, Re_p, is calculated from the mass flowrate, $\dot{m}$, using the equation:

$$Re_p = \frac{\dot{m}d_p}{\rho \nu A_p}$$

Where:

d_p = Pipe diameter

A_p = Pipe cross-sectional area

A corrected mass flowrate is then calculated using the equation:

11

$$\dot{m} = KA_{OR}Y\sqrt{2\rho\Delta P}$$

Where:

K = Flow coefficient (A function of Reynolds number which is interpolated from the

ASME Tables [Ref. 10])

Y = Expansion coefficient (Calculated from Holman and Gajda [Ref. 11]

A_{OR} = Orifice Area

ΔP = Pressure drop across orifice

A corrected Reynolds number is then determined and the iterative process is continued until

the mass flowrate converges to within one percent for two successive calculations. The

final Dean number is then determined using the equation:

$$De = \frac{\dot{m}}{\rho A_{ch}}\left[\frac{d}{v}\right]\sqrt{\frac{d}{r_i}}$$

2. Constant Heat Flux Setting

The four heaters, CC1, CC2, CV1, and CV2 are designed to provide a constant

heat flux over both the concave, convex, and straight channel surfaces. The magnitude of

the heat flux is set based on two contraints. First, heat fluxes must be large enough to

obtain significant differences between surface temperatures and local mixed mean fluid

temperatures. The second constraint limits maximum surface temperatures for any location

in the channel to 60 Deg. C. This is necessary because the bonding agent used to attach

lexan sheets to cross beams is not dependable at temperatures above 65 Deg. C. For most

runs, the maximum temperature occurs at TC #199, which is located in the final spanwise

row of the convex wall of the curved section. A curve showing heat flux required per heater

12

to reach a maximum temperature of 60 Deg. C, obtained from experimental tests, is shown in Figure 19 for Dean numbers from 50 to 200.

To determine the heat flux, the voltage drops across each shunt and each heater are measured using a simple volt-ohm meter and are entered into a program called **Temcurv**. Figure 20 shows voltage drops across shunt resistors which are needed to produce desired power levels in each heater. Equations relating these voltage drops to power are given by:

$$I = \Delta V_S / R$$

and

$$P = \Delta V_H \times I$$

Where:

I   = Current (amps)

P   = Power (watts)

ΔV_S = Voltage drop across the shunt (volts)

ΔV_H = Voltage drop across the heater (volts)

R   = Shunt resistance (ohms)

B. SURFACE HEAT TRANSFER DISTRIBUTION MEASUREMENTS

1. Surface Temperature Measurements

The system is heated for approximately 8-9 hours prior to data acquisition to reach steady state and to insure that thermal equilibrium exists. Great care is taken to insure that maximum surface temperatures never exeed 60 Deg. C. by routinely checking temperatures using the temperature acquisition program, **Tcheck**. Figure 21 provides a

13

curve from Run #120689.2125 which illustrates how temperature tends to increase with time. When steady state conditions are reached, voltage readings from each thermocouple are recorded using **Temcurv** and converted into Deg. C using calibration equations determined by Hughes [Ref. 8]. For thermocouples 1 through 200, 201, 203 and 204, voltages are converted into Deg. C using the equation:

$$T = -1.988321 + 29436.53V - 2622880\ V^2 + 36932000V^3$$

For thermocouple 202 the equation is:

$$T = -1.816347 + 2928.91V - 2622880V^2 + 373752000V^3$$

Where:

T = Temperature Deg. C

V = Thermocouple voltage (volts)

These equations are utilized in the software program **Nuscurv3B**.

The surface thermocouples are attached behind Lexan surfaces exposed to the flow field. Consequently, there is a thermal contact resistance between thermocouples and convective Lexan surfaces. The temperature difference, ΔT_{wcorr}, between the actual surface and that measured by the thermocouple is given by the equation:

$$\Delta T_{wcorr} = q''_{conv}\ (CR)$$

Where:

q''_{conv} = Convected heat flux per heater area

14

CR   = Thermal contact resistance ($^oC\ m^2$ / watt)

Experimental procedures used to determine CR are described by Bella [Ref. 12]. From his

work, CR equals $3.4 \times 10^{-3}\ ^o\ cm^2$ / watt.

2. Nusselt Number Calculations

The program **Nuscurv3B** is used to determine local Nusselt numbers. The

process begins with determination of the convective power transfer using:

$$\dot{q}_{conv} = \dot{q}_{in} - \dot{q}_{cond} - \dot{q}_{rad}$$

Where:

$\dot{q}_{conv}$ = Power convected to the channel air flow

$\dot{q}_{in}$ = Power to the heaters (V x I)

$\dot{q}_{cond}$ = Power loss by conduction

$\dot{q}_{rad}$ = Power loss by radiation, set equal to zero

Power loss by conduction is given by Bella [Ref. 12], who conducted tests on a

full scale prototype model of the curved heated section. His results show that conduction

losses are given by:

$$\dot{q}_{cond} = -0.0294 + 0.4222\ (T_{wcorr} - T_{ambient}) - 0.0015\ (T_{wcorr} - T_{ambient})^2$$

Where:

T_{wcorr} = Corrected local surface temperature

$T_{ambient}$ = Ambient temperature for surroundings

15

The convective heat flux is then determined using:

$$\dot{q}''_{conv} = \dot{q}_{conv} / A_{sec}$$

Where:

A_{sec} = Surface area for each of the four heater surfaces, CC1, CC2, CV1 and CV2

With the convective heat flux known, the local mixed mean temperature at any streamwise channel location is determined using:

$$t_{mm}(x) = t_{mmin} + [\dot{q}''_{conv}(x) \, b \, x] / Cp \, (\dot{m})$$

Where:

$t_{mm}(x)$ = Local mixed mean Temperature

t_{mmin} = Inlet mixed mean temperature

b = Spanwise width

x = Streamwise distance

$\dot{q}''_{conv}$ = Heat flux over streamwise distance x

C_P = Specific heat of air

Local heat transfer coefficients are then determined using the equation:

$$h = \dot{q}_{conv} / (T_{wcorr} - t_{mm})$$

16

Finally, the local Nusselt number, Nu, is calculated from:

$$Nu = h(D_H) / k$$

Where:

D_H = Hydraulic diameter (2 x channel width = .0254 m)

k = Thermal conductivity of air at 20° Celcius (.02563 W / m K)

C. EXIT MIXED MEAN TEMPERATURE MEASUREMENTS AND DETERMINATION

1 . EXIT Mixed-Mean Temperature Determination

A two step procedure is used to determine the local mixed-mean temperature from the convective heat flux. This temperature is determined at the location of the two-dimensional traverse slot, which is 57.1 cm from the trailing edge of the heater on the convexly curved wall. First, the mixed-mean temperature is estimated at the downstream edge of the heaters using procedures described in the previous section. This temperature is noted as, t_{mmi} . In the second step, an energy balance is then used to estimate the heat loss from the flow to the unheated portion of the channel, which extends from the trailing edge of the heater to the traversing slot. This energy balance is given by:

$$\dot{m} C_P t_{mmi} = \dot{m} C_P t_{mmo} + A_{tot} h[(t_{mmi} + t_{mmo})/2 - T_W]$$

Where:

t_{mm} = Local mixed-mean temperature at the traverse slot.

T_W = Temperature of the unheated channel surface (approximately equal to ambient temperature).

17

A_{tot} = Concave and convex surface area for this portion of the channel.

h = Heat transfer coefficient at last spanwise row of thermocouples

This equation is employed in the software plotting program **Tmxdmean**, in the form where slot temperature t_{mmo} is given by:

$$t_{mmo} = \frac{\dot{m}C_p t_{mmi} - hA_{tot}(\frac{t_{mmi}}{2} - T_w)}{\dot{m}C_p + \frac{hA_{tot}}{2}}$$

2. Exit Mixed-Mean Temperature Measurement

After the channel is thermally steady state, TC #204 is set in place into the temperature traversing carriage. Using the program **Temtrav**, 320 voltage readings are taken over a 5.08 cm (2.0 inch) by 1.02 cm (0.4 inch) area as the probe moves in the traverse slot. Voltage readings are transformed into Deg. C using the equation described in the previous section. The mixed mean temperature is then given by:

$$t_m = \frac{1}{A_{ch}U} \int u t \, dA$$

Where:

t_m = Mixed mean temperature

A_{ch} = Channel traversed cross section area

U = Bulk velocity (spacially averaged)

u = Local mean streamwise velocity

18

t = Local mean temperature

The software program **Tmxdmean** is used to determine the mixed-mean temperature. This is accomplished using an approach which assumes that the area corresponding to each temperature measurement is the same:

$$t_m = \frac{1}{320} \sum_{i=1}^{320} \frac{u_i}{v} t_i$$

Velocity data, U and u_i , were obtained using a miniature five-hole pressure probe described by Baun [Ref. 13]. The velocity data used to determine mixed-mean temperatures in the present study are the same as given by Hughes [Ref. 8] and Tuzzolo [Ref. 14].

IV. RESULTS AND DISCUSSION

The objective of the present channel study is to examine the effects of curvature and the resulting centrifugal instabilities on local heat transfer distributions. Flows at Dean numbers ranging from 50 to 200 are investigated. The results of these tests are discussed in four parts. First, two types of baseline tests are discussed, which qualify measuring procedures and apparatus. This section includes discussion of spanwise-averaged Nusselt numbers from the straight portion of the channel as well as comparison of measured exit mixed-mean temperatures with values determined from energy balances. Second, spanwise-averaged Nusselt number distributions from concave and convex surfaces are presented. Third, the effects of counter-rotating Dean vortex pairs on the local Nusselt number distributions are detailed. Finally, in the fourth section, surveys of local temperatures used to determine the mixed mean temperature are presented in conjunction with mean velocity data obtained by Hughes [Ref. 8] and Tozzolo [Ref. 14].

A. BASELINE RESULTS

1. Spanwise-Averaged Nusselt Numbers From the Straight Portion of the Channel.

The walls of the straight portion of the channel are heated to insure that flow is thermally and hydrodynamically fully developed prior to entering the curved section.Because this portion of the channel is straight, much information is available on the behavior and distributions of local Nusselt numbers. First, because the flow is symmetic in the direction normal to the walls. Nusselt numbers should be the same on the top and bottom walls at each streamwise location. Second, the analytical solution for flow between two infinite parallel plates with constant heat flux boundary conditions gives the fully

20

developed Nusselt number value. Third, a numerical solution is used to predict thermal entry length behavior. All three of these are now discussed in regard to measured Nusselt number distributions.

a. Comparison of Results from the Straight CC1 and CV1 Surfaces

Figure 22 and Figure 23 show spanwise-averaged Nusselt numbers for Dean numbers of 100 and 125 for the CC1 and CV1 surfaces, respectively. The graphs show that the Nusselt number distributions are nearly identical over the entire lengths of the straight sections, from x/d of 82.1 cm, which is the location of the first spanwise row of thermocouples, to x/d of 178.6 cm, the beginning of curvature.

b. Comparison of Experimental Data with the Analytic Solution for Thermally Fully Developed Flow

Kays and Crawford [Ref. 15], indicate that the average Nusselt number is 8.24 for fully developed laminar flow between two infinite parallel plates with constant heat flux boundary conditions. Figures 22 and 23 show measured Nusselt numbers ranging from 8.45 to 8.11, which agree excellently with the value of 8.24, for x/d from 130.4 to 178.6. As indicated earlier, these data are obtained for Dean numbers of 100 and 125 and are approximately constant with x/d only after thermal entry length effects disappear and the flow becomes thermally fully developed.

c. Comparison of Thermal Development Effects with Numerical Solutions

Spanwise-averaged Nusselt numbers for Dean Numbers of 100 and 125 are compared to results from numerical predictions in Figures 24 and 25.The numerical prediction results are obtained using the STAN5 boundary layer program, described by Kays and Crawford [Ref. 15]. Exact experimental conditions are used as initial conditions

and boundary conditions, and include the effects of the unheated starting length between the nozzle exit and heater leading edges. The data and predictions show excellent agreement along the entire length of the straight portion of the channel, from x/d of 70.0 to 178.64, which validates measurements made in the thermal entry length region of the channel.

Predicted Nusselt numbers for the straight portion of the channel for all Dean Numbers studied are given in Figure 26. At each Dean number, Nusselt numbers are infinite at the initial heating point. With streamwise development, Nusselt numbers then decrease. At each particular streamwise location, spanwise-averaged Nusselt numbers increase with Dean number because the entry length needed for flow to become thermally fully developed increases. The same Nusselt numbers are non-dimensionalized in Figures 27 and 28. Predicted and measured non-dimensional Nusselt numbers for the concave surfaces are compared in Figures 29 and 30. Figures 31 and 32 then give the same type of infomation for the convex surface.

2. Mixed-Mean Temperature Comparison

Figures 33 through 39 present mixed-mean temperature distributions along the length of the channel, which are determined from the convected heat flux into the flow. These figures also compare these distributions to mixed-mean temperatures determined from local measurements of temperature and velocity obtained from probes placed in a slot located downstream of the last heater. In figures 33-39, results are given for Dean numbers of 58.5, 73.7, 98.1, 126.0, 149.8, 173.5 and 198.4. In all cases, mixed-mean temperatures measured at the exit of the curved portion closely match values at x/d of 356.6 from the energy balance. This further validates experimental procedures, experimental apparatus, and the energy balances employed, and confirms that the conduction loss estimates used in determining the convected heat fluxes are accurate. Small differences in

22

the two exit mixed-mean temperatures sometimes result from small uncertainties in measured temperatures and velocities. Mean temperature distributions, mean velocity distributions and distributions of the mean temperautre/mean velocity product used to determine the local mixed-mean termperature are presented in Part D. of Chapter 4.

3. Baseline Data Summary

All baseline test results validate experimental procedures, the measurement approach, the energy balances employed, and the facilities used in this study, and provide confidence that the measurements taken in the curved portion of the channel, located just downstream of the straight portion, represent actual flow behavior.

B. SPANWISE-AVERAGED NUSSELT NUMBER DISTRIBUTIONS

In this section, spanwise-averaged Nusselt numbers are presented, which are non-dimensionalized using the spanwise-averaged Nusselt number at x/d of 130.4. This is done to minimize some of the scatter in dimensional Nusselt numbers measured at Dean numbers lower than 100 and higher than 125.

Figures 40, 41, 42 and 43 present Nusselt number ratios for concave and convex surfaces at seven Dean Numbers. At x/d values between 0 and 82.1, no Nusselt numbers are plotted because this portion of the channel is unheated. Between x/d of 82.1 and approximately 110, Nusselt numbers increase with Dean number, with trends consistant with predictions which account for thermal entry length effects. At x/d of about 110 to 130, flow is hydrodynamically and thermally fully developed and Nusselt numbers are approximately constant with streamwise distance. As shown in Figure 22, the spanwise-averaged Nusselt number is about 8.24 for Dean numbers of 100 and 125, which is in agreement with the theory for the same flow. The same behavior exists for Dean numbers up to about 150, whenever the flow is fully laminar and no transition phenomenon are

23

present. As x/d approaches 160-180, spanwise-averaged Nusselt number ratios increase for Dean numbers of 175 and 200, as a result of initiation of transition phenomena. Peak values exist at x/d of about 178.6, which is just at the begining of curvature. Here, some mixing of flow is present that does not occur otherwise. This trend occurs on both concave and convex surfaces, but it is more pronounced on the convex surface.

As x/d becomes greater than 180, effects of curvature are evident in measurements from both the concave and convex surfaces. These effects are complex and vary not only with the Dean number, but also with the surface considered. On the concave surface at Dean numbers of 50, 75, 100 and 125, Nusselt number ratio distributions are the same for x/d of 178.6 to approximately 226.9. For each case, the Nusselt numbers decrease drastically as a result of the stabilizing influence of convex curvature, which causes a stabilizing effect initially near the convex surface before propagating across the width of the channel.

At x/d greater then 226.9 for both surfaces, the presence of Dean vortices is evident in local Nusselt number ratios, which gradually increase with streamwise development. These vortices develop because of the imposition of centrifugal instabilities. For x/d from 226.9 to 299.4, the lowest Nusselt number ratios correspond to a Dean numbers of 50, and the highest correspond to Dean numbers of 100 and 125. At these higher Dean numbers, centrifugal instabilities and the accompanying Dean vorices are more intense, and thus, Nusselt numbers are also higher.

At Dean numbers of 150, 175 and 200, results from both the concave and convex surfaces show evidence of transition phenomena resulting in the onset of some chaotic motions. This is particularly so for x/d ranging from 154.5 to 178.6, just prior to curvature,where Nusselt number ratios are locally higher. At x/d from 178.6 to 300, ratios

24

from the convex surface are generally lower than from the concave surface. This occurs because of the stabilizing and destabilizing influences of the convex and concave surfaces, respectively. Flow visualization results for the same experimental conditions show considerable mixing.

C. EFFECTS OF COUNTER-ROTATING DEAN VORTEX PAIRS ON LOCAL NUSSELT NUMBER DISTRIBUTIONS

Local Nusselt numbers versus non-dimensional spanwise length, z/d, for both concave and convex surfaces at Dean numbers of 58.5, 73.7, 98.1, 126.0, 149.8, 173.5 and 198.4, are given in Figures 44-57. These data, especially those from the concave surface, illustrate the effects of pairs of counter-rotating Dean vortices on local Nusselt number distributions.

In general, local Nusselt numbers on the convex surface are generally spanwise uniform, regardless of Dean number. Exceptions occur at Dean numbers of 149.8, 173.5 and 198.4, where some slight variations are present probably due to vortex pairs. On the concave surface, local Nusselt numbers develop significant variations in the spanwise direction as the flows develop downstream as a result of vortex upwash and downwash regions. Local Nusselt number values are augmented near downwash regions and diminished in upwash regions. Such spanwise variations coincide with increases of spanwise-averaged Nusselt numbers, and are most significant for Dean numbers of 98.6 and greater. Such behavior is also consistant with flow visualization results which show counter-rotating vortex pairs for the same experimental conditions.

Focussing on Nusselt number results for a Dean number of 98.6 and comparing them to the spanwise averaged Nusselt number data presented in section B, interesting conclusions are made. Data at x/d of 202.8 to 226.9 show that local Nusselt numbers are

25

spanwise uniform. These locations coincide with regions where spanwise averaged Nusselt numbers are lower than values at other x/d, as a result of the imposition of centrifugal instabilities. As x/d increases to 251.1, 275.2 and 299.4, spanwise-averaged Nusselt numbers increase and local Nusselt numbers show considerable spanwise variations due to the formation of Dean vortex pairs.

Such trends are present at all Dean numbers greater than or equal to 98.6. However, at Dean numbers of 173.5 and 198.4, local Nusselt numbers show spanwise variations at x/d as low as 202.8 to 226.9.

D. LOCAL MIXED-MEAN TEMPERATURE SURVEY DATA

1. Local Mean Temperature Distributions

Mean temperature surveys are presented for Dean numbers of 58.5, 73.7, 98.1, 126.0, 149.8, 173.5 and 198.4 in Figures 58-64. Here, mean refers to a time-average. For Dean numbers of 58.5 and 73.7, spanwise periodicities result due to vortex pairs. At Dean numbers from 98.1 to 198.4, the local mean temperature distributions are fairly spanwise uniform, with only slight variations due to vortex pairs. Such variations are present at lower Dean numbers because Dean vortices form only after a considerable amount of streamwise development. Such vortices continue to exist at higher Dean numbers, but they are unsteady over spanwise distances greater than the spacing between vortex pairs, which makes them appear spanwise uniform in the time-averaged flow field.

2. Local Mean Velocity Distributions

Mean velocity distributions are given by Hughes [Ref. 8] and Tuzzolo [Ref. 14]. Results for Dean numbers of 50, 75, 100 and 150 are shown in Figures 65-68. Qualitative trends of the velocity contours coincide nicely with local mean temperature contours; velocity profiles at low Dean numbers show some spanwise variations, while at higher

26

Dean numbers the profiles are fairly spanwise uniform.

3. Distributions of the Mean Temperature-Mean Velocity Product

Mean temperature-mean velocity product distributions are presented in Figures 69-75 for Dean numbers of 58.5, 73.7, 98.1, 126.0, 149.8, 173.5 and 198.4. The graphs show good spanwise uniformity for all Dean numbers, except for some of the lower values, as expected. As mentioned in Part C of Chapter 3, these temperature-velocity product data are used to compute the local mixed mean temperatures discussed in Chapter 4, Part A., Section 2.

V. CONCLUSIONS AND RECOMMENDATIONS

A. CONCLUSIONS

The effects of curvature and the resulting centrifugal instabilities on local heat transfer distributions are studied in a curved channel at Dean numbers ranging from 50 to 200. The channel is designed with a rectangular cross section of 1.27 cm by 50.1 cm giving an aspect ratio of 40 to 1. These interior dimensions coincide with those of another channel which is transparent and used for flow visualization. In the channel used for thermal studies, the flow is heated in a 2.44 m straight portion, located just prior to the curved portion to obtain flow which is hydrodynamically and thermally developed. The flow then enters a 180 degree heated curved section with a convex surface radius of 59.69 cm and a concave surface radius of 60.96 cm. Surface temperatures and ambient temperatures are measured using 204 thermocouples, whose outputs are used to determine local Nusselt numbers as constant heat flux boundary conditions are maintained on all heated surfaces.

Several baseline comparisons qualify flow behavior as well as the experimental procedures and measurement techniques. In the first of these, spanwise-averaged Nusselt numbers from the two walls of the straight portion of the channel match with each other very well. As thermal entry length effects disappear, dimensional Nusselt numbers approach 8.24 as expected from the theory for thermally fully developed flow between two parallel infinite plates with constant heat flux boundary conditions. In the thermally developing region, measured Nusselt numbers match results from numerical predictions. Finally, measured mixed-mean temperatures at the exit of the curved section match values determined from energy balances. These baseline comparisons thus validate experimental procedures, the measurement approach and the facilities used, and provide confidence of

the accuracy of measurements from the curved portion of the channel.

Spanwise-averaged Nusselt numbers are non-dimensionalized with respect to the Nusselt number determined at x/d of 130.4. For Dean numbers of 50, 75, 100 and 125, these ratios approach constant values on the straight portion of the channel for x/d from 110 to 180. At smaller x/d, Nusselt number ratios increase with Dean number as a result of thermal entry length effects. For Dean Numbers of 150, 175 and 200 increases in Nusselt number ratios are present for $160 \leq x/d \leq 180$ as a result of transition phenomena.

The stabilizing influences of convex curvature are evidenced at the onset of curvature by drastic decreases in Nusselt number ratios for both surfaces at Dean numbers of 50, 75, 100 and 125. These effects initially produce a stablilizing effect, which occurs primarily near the convex surface and then propagates across the width of the channel. As x/d increases, the formation of Dean vortices as a result of centrifugal instabilities is evidenced by gradual increases of the local Nusselt number ratios. Here, Nusselt number ratios are generally lower on the concave surface, where the lowest Nusselt number ratios are present at a Dean number of 50 and the highest values exist at Dean Numbers of 100 and 125. Higher Nusselt numbers are expected at higher Dean numbers because centrifugal instabilities and the resulting Dean vortices are more intense. Higher Nusselt numbers are expected near the concave surface because of the intensity of secondary flows from counter rotating vortex pairs, which are much less intense near convex surfaces.

At Dean numbers of 150, 175 and 200, effects of transition phenomena are considerably more apparent. Nusselt number ratios show local increases on the straight portion of the channel just prior to curvature. After curvature is imposed, trends are generally similar ones observed at the lower Dean numbers, except that Nusselt number ratios are higher probably because of increased flow mixing associated with transition

29

phenomena.

Local Nusselt numbers from the convex surface are fairly spanwise uniform, regardless of Dean number. On the concave surface, however, significant spanwise variations are evident, especially at Dean numbers of 98.6 or greater, which result from upwash and downwash regions in vortex pairs. Such spanwise variations correspond to increases in spanwise-averaged Nusselt numbers which occur with streamwise development.

Mean temperature and mean velocity survey data show some spanwise periodicity at the lower Dean numbers due to upwash and downwash regions formed by vortex pairs. As the Dean number increases, these surveys show distributions which are fairly spanwise uniform.

B . RECOMMENDATIONS

Recommendations are, first, repeat the present study at Dean numbers from 200 to 450 to obtain additional information on the connections between centrifugal instabilities, Dean vortices and transition from laminar flow to turbulent flow. Second, Nusselt numbers should be measured in situations where the heat flux differs on the two surfaces of the channel.

APPENDIX A
THERMOCOUPLE PLACEMENT TABLES

TC#	CH#	X(cm)	Z(cm)	TC#	CH#	X(cm)	Z(cm)
1	0	103.64	15.36	24	23	164.60	-15.12
2	1	103.64	.12	25	24	195.08	15.36
3	2	103.64	-15.12	26	25	195.08	.12
4	3	134.12	15.36	27	26	195.08	-15.12
5	4	134.12	.12	28	27	225.56	15.36
6	5	134.12	-15.12	29	28	225.56	.12
7	6	164.6	15.36	30	29	225.56	-15.12
8	7	164.6	.12	31	30	256.04	15.36
9	8	164.6	-15.12	32	31	256.04	1.575
10	9	195.08	15.36	33	32	256.04	1.270
11	10	195.08	.12	34	33	256.04	.991
12	11	195.08	-15.12	35	34	256.04	.737
13	12	225.56	15.36	36	35	256.04	.483
14	13	225.56	.12	37	36	256.04	.254
15	14	225.56	-15.12	38	37	256.04	.025
16	15	103.64	15.36	39	38	256.04	-.127
17	16	103.64	.12	40	39	256.04	-.330
18	17	103.64	-15.12	41	40	256.04	-.610
19	18	134.12	15.36	42	41	256.04	-.864
20	19	134.12	.12	43	42	256.04	-1.092
21	20	134.12	-15.12	44	43	256.04	-1.346
22	21	164.60	15.36	45	44	256.04	-1.575
23	22	164.60	.12	46	45	256.04	-1.829

31

TC#	CH#	X(cm)	Z(cm)	TC#	CH#	X(cm)	Z(cm)
47	46	256.04	−15.12	70	69	317.00	.559
48	47	286.52	15.36	71	70	317.00	.305
49	48	286.52	1.549	72	71	317.00	.127
50	49	286.52	1.295	73	72	317.00	−.064
51	50	286.52	1.067	74	73	317.00	−.381
52	51	286.52	.787	75	74	317.00	−.660
53	52	286.52	.508	76	75	317.00	−.914
54	53	286.52	.279	77	76	317.00	−1.219
55	54	286.52	.025	78	77	317.00	−1.473
56	55	286.52	−.229	79	78	317.00	−1.778
57	56	286.52	−.508	80	79	317.00	−2.083
58	57	286.52	−.813	81	100	317.00	−15.12
59	58	286.52	−1.041	82	101	347.48	15.36
60	59	286.52	−1.270	83	102	347.48	1.778
61	60	286.52	−1.524	84	103	347.48	1.448
62	61	286.52	−1.727	85	104	347.48	1.143
63	62	286.52	−1.981	86	105	347.48	.864
64	63	286.52	−15.12	87	106	347.48	.610
65	64	317.00	15.36	88	107	347.48	.356
66	65	317.00	1.651	89	108	347.48	.051
67	66	317.00	1.372	90	109	347.48	−.229
68	67	317.00	1.118	91	110	347.48	−.432
69	68	317.00	.838	92	111	347.48	−.635

TC#	CH#	X(cm)	Z(cm)	TC#	CH#	X(cm)	Z(cm)
93	112	347.48	-.914	116	135	256.04	15.36
94	113	347.48	-1.194	117	136	256.04	1.981
95	114	347.48	-1.448	118	137	256.04	1.702
96	115	347.48	-1.702	119	138	256.04	1.397
97	116	347.48	-1.981	120	139	256.04	1.118
98	117	347.48	-15.12	121	140	256.04	.914
99	118	377.96	15.36	122	141	256.04	.635
100	119	377.96	1.653	123	142	256.04	.356
101	120	377.96	1.321	124	143	256.04	.051
102	121	377.96	1.041	125	144	256.04	-.279
103	122	377.96	.787	126	145	256.04	-.533
104	123	377.96	.533	127	146	256.04	-.787
105	124	377.96	.356	128	147	256.04	-.991
106	125	377.96	.051	129	148	256.04	-1.118
107	126	377.96	-.178	130	149	256.04	-1.397
108	127	377.96	-.457	131	150	256.04	-1.676
109	128	377.96	-.737	132	151	256.04	-15.12
110	129	377.96	-1.016	133	152	286.52	15.36
111	130	377.96	-1.245	134	153	286.52	2.134
112	131	377.96	-1.489	135	154	286.52	1.854
113	132	377.96	-1.727	136	155	286.52	1.549
114	133	377.96	-2.011	137	156	286.52	1.270
115	134	377.96	-15.12	138	157	286.52	.965

TC#	CH#	X(cm)	Z(cm)	TC#	CH#	X(cm)	Z(cm)
139	158	286.52	.737	162	201	317.00	-.864
140	159	286.52	.508	163	202	317.00	-1.168
141	160	286.52	.229	164	203	317.00	-1.397
142	161	286.52	-.051	165	204	317.00	-1.626
143	162	286.52	-.305	166	205	317.00	-15.12
144	163	286.52	-.533	167	206	347.48	15.36
145	164	286.52	-.787	168	207	347.48	1.956
146	165	286.52	-1.090	169	208	347.48	1.727
147	166	286.52	-1.321	170	209	347.48	1.499
148	167	286.52	-1.575	171	210	347.48	1.194
149	168	286.52	-15.12	172	211	347.48	.914
150	169	317.00	15.36	173	212	347.48	.635
151	170	317.00	1.930	174	213	347.48	.381
152	171	317.00	1.600	175	214	347.48	.178
153	172	317.00	1.295	176	215	347.48	-.178
154	173	317.00	1.067	177	216	347.48	-.457
155	174	317.00	.838	178	217	347.48	-.686
156	175	317.00	.584	179	218	347.48	-.940
157	176	317.00	.305	180	219	347.48	-1.270
158	177	317.00	.102	181	220	347.48	-1.549
159	178	317.00	-.127	182	221	347.48	-1.829
160	179	317.00	-.457	183	222	347.48	-15.12
161	200	317.00	-.584	184	223	377.96	15.36

TC#	CH#	X(cm)	Z(cm)	TC#	CH#	X(cm)	Z(cm)
185	224	377.96	1.981	201	240	0.0	0.0
186	225	377.96	1.727	202	241	Ambient Convex	
187	226	377.96	1.448	203	242	Ambient Concave	
188	227	377.96	1.219	204	243	450.27	0.0
189	228	377.96	.939				
190	229	377.96	.635				
191	130	377.96	.356				
192	131	377.96	.127				
193	132	377.96	-.229				
194	133	377.96	-.457				
195	134	377.96	-.686				
196	135	377.96	-.914				
197	136	377.96	-1.194				
198	137	377.96	-1.473				
199	138	377.96	-1.727				
200	139	377.96	-15.12				

APPENDIX B
FIGURES

The following pages contain the figures used in the development of this thesis.

Figure 1.   Curved Heat Transfer Channel
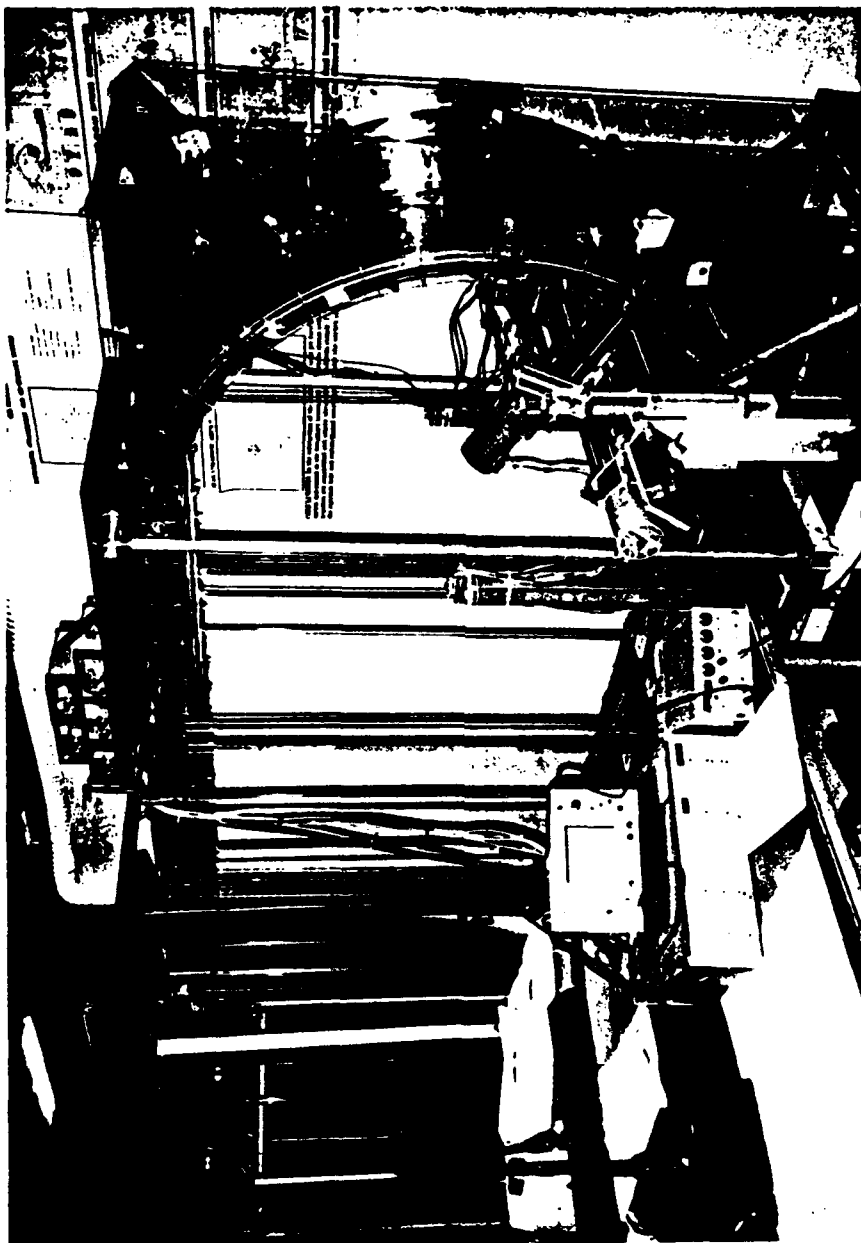
Figure 2.   Curved Transparent Channel
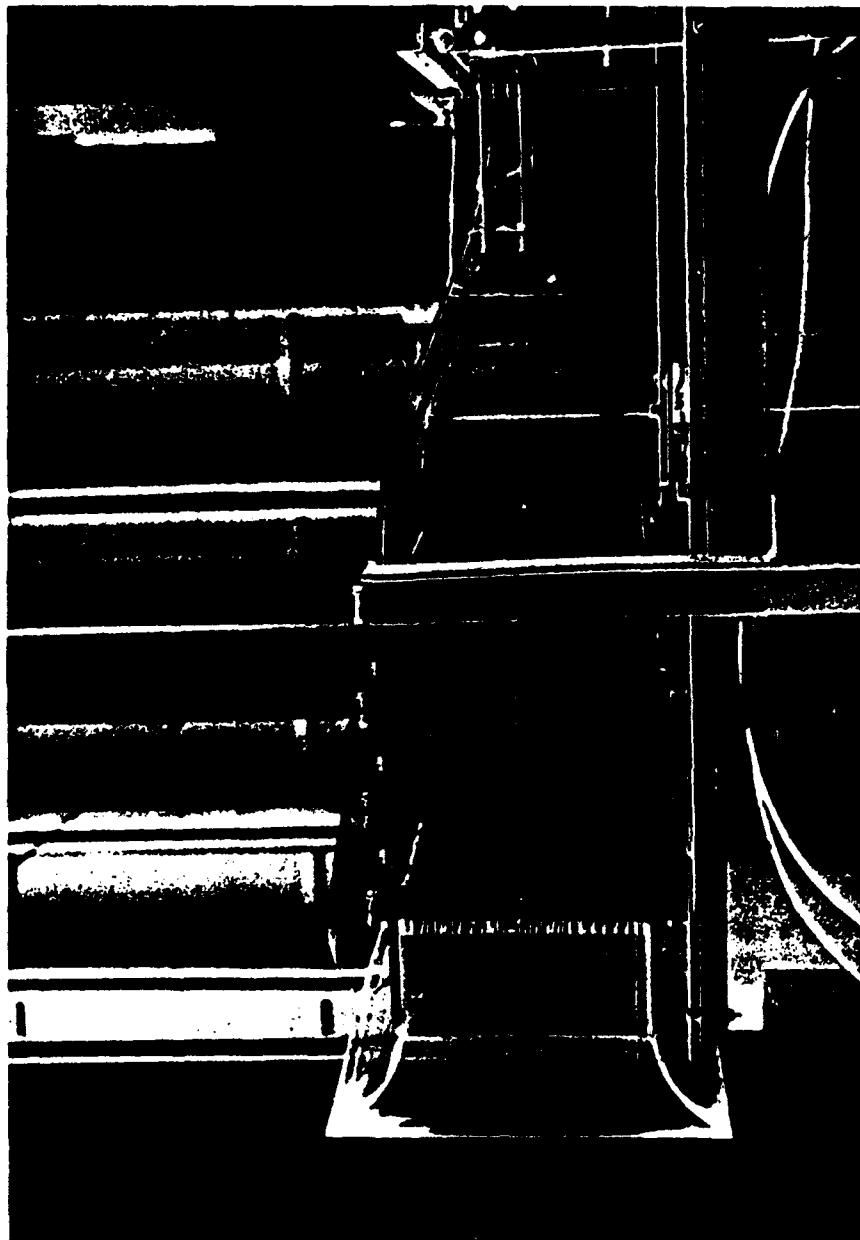
Figure 3. Channel Inlet Section
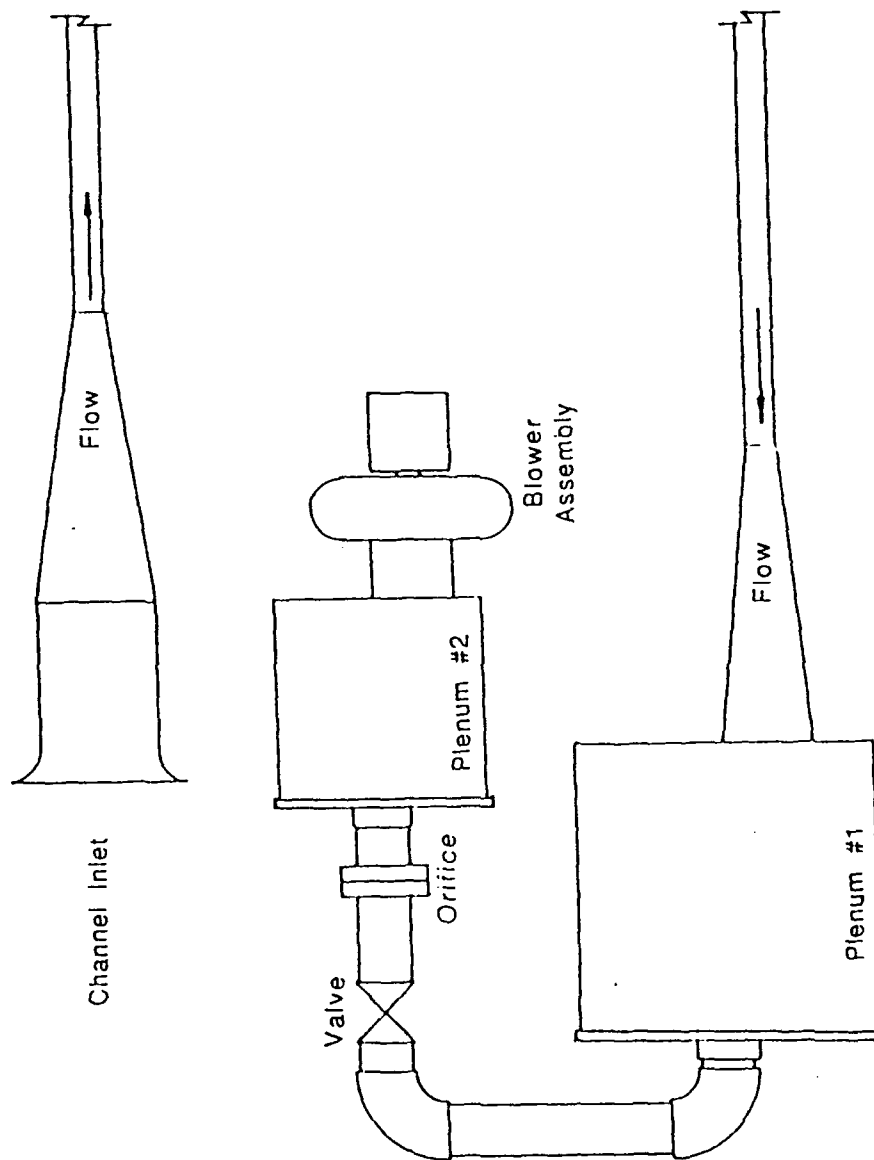
Figure 4.   Schematic of Blower Assembly

40
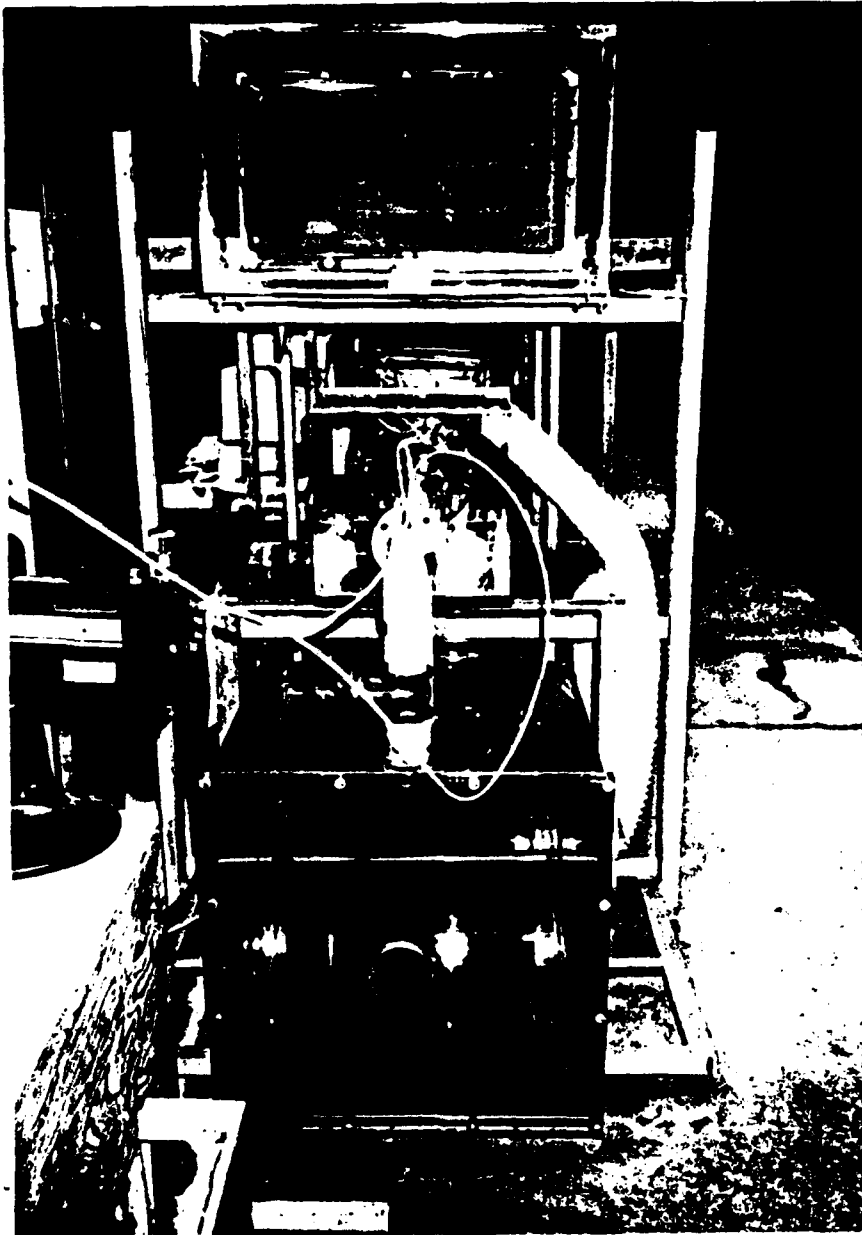
Figure 5.   Photograph of Blower Assembly

41
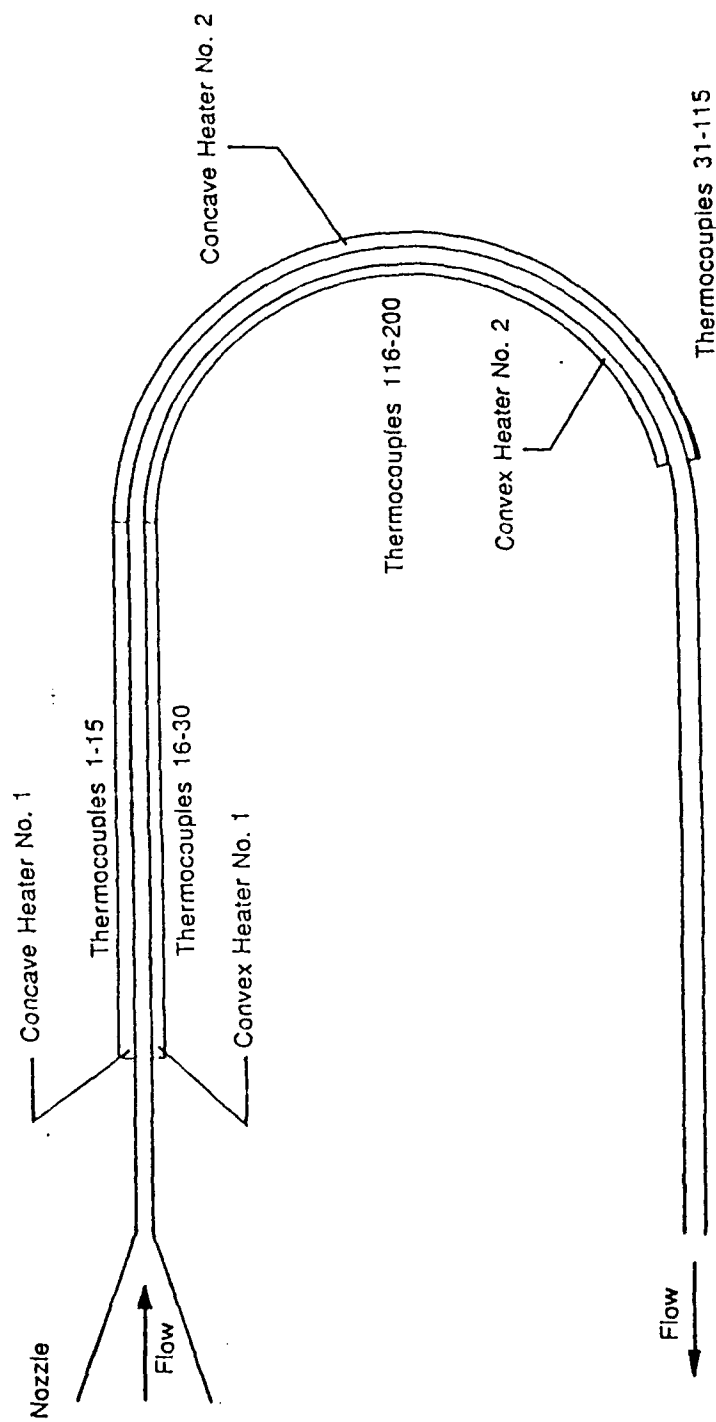
Figure 6. Channel Heater Identification
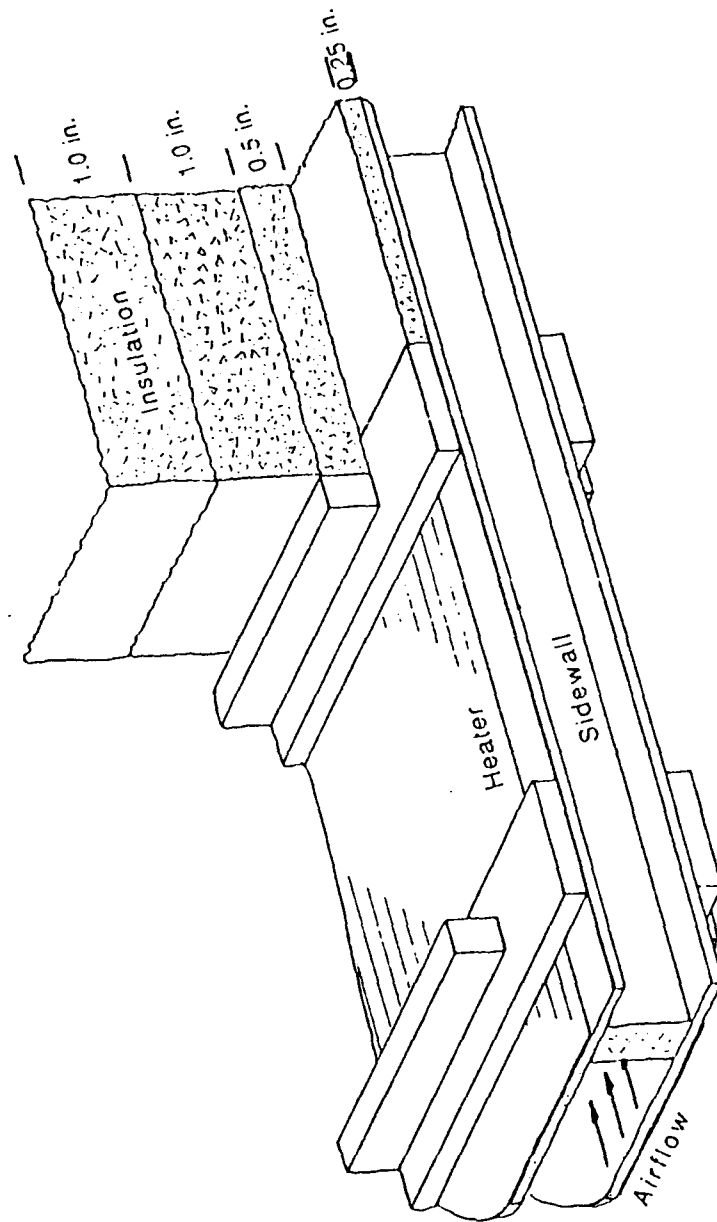
Figure 7. Heat Transfer Insulation Drawing

43
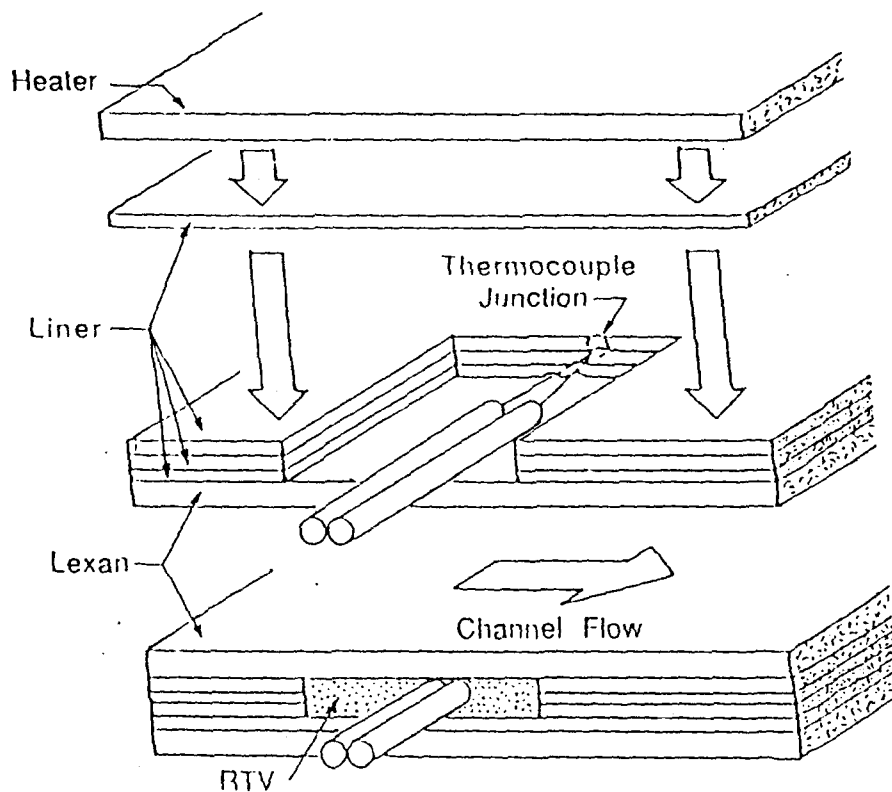
Figure 8. Channel Thermocouple Installation
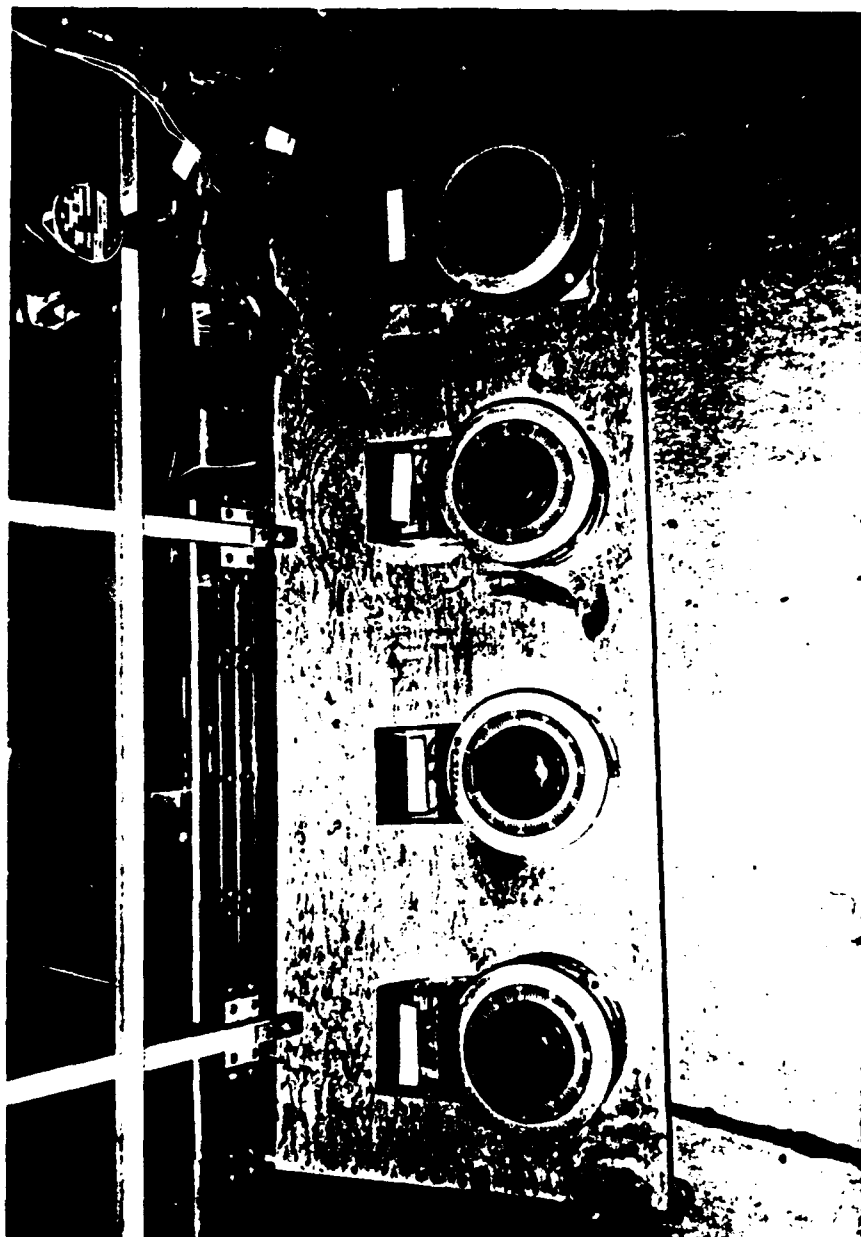
Figure 9.   Channel Heater Control Variacs
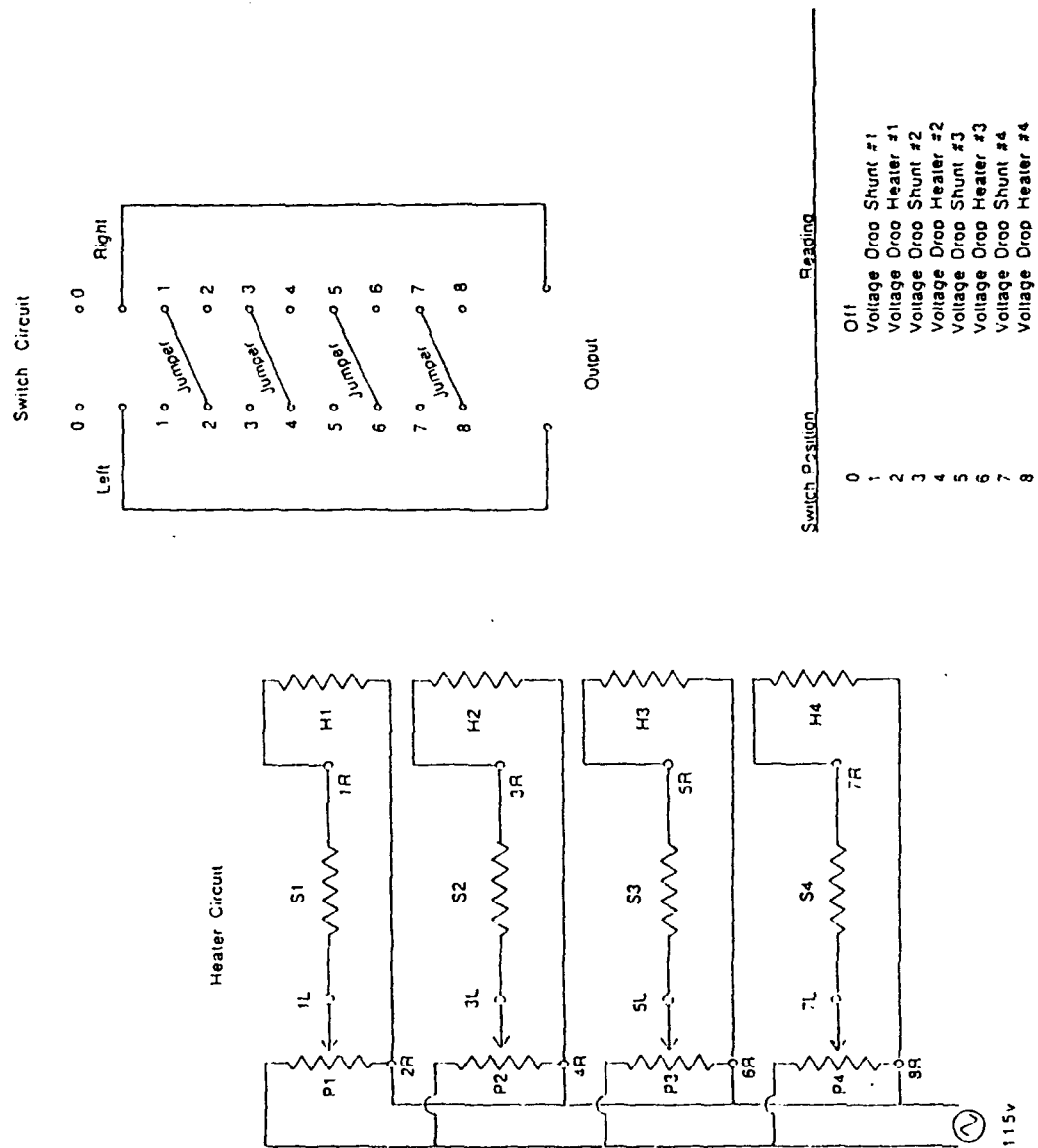
Figure 10. Heater and Control Circuit Wiring Diagram

46
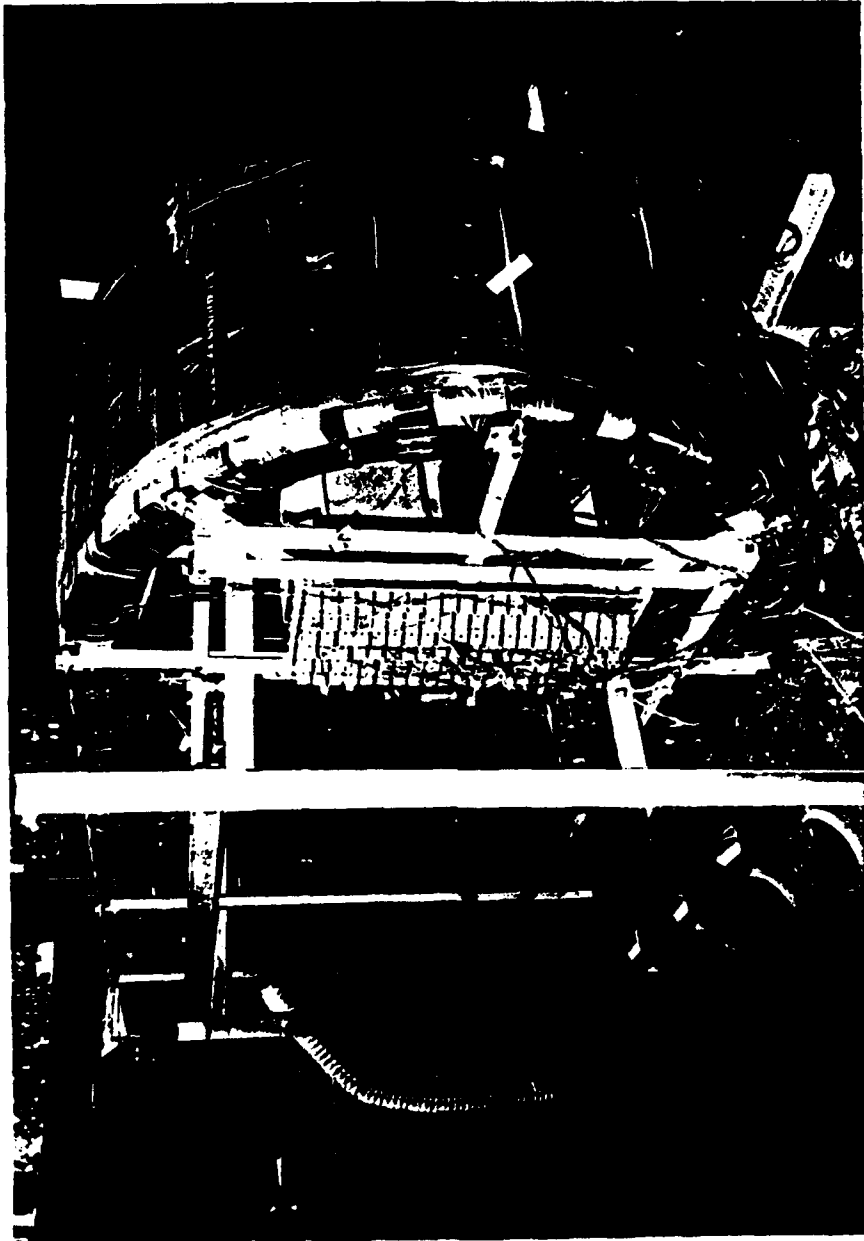
Figure 11. Photograph of Channel Insulation

Figure 12. Photograph of Channel Insulation

48

Concave Heater No. 2
Thermocouple Arrangement
Top View

Concave Heater No. 1
Thermocouple Arrangement
Top View
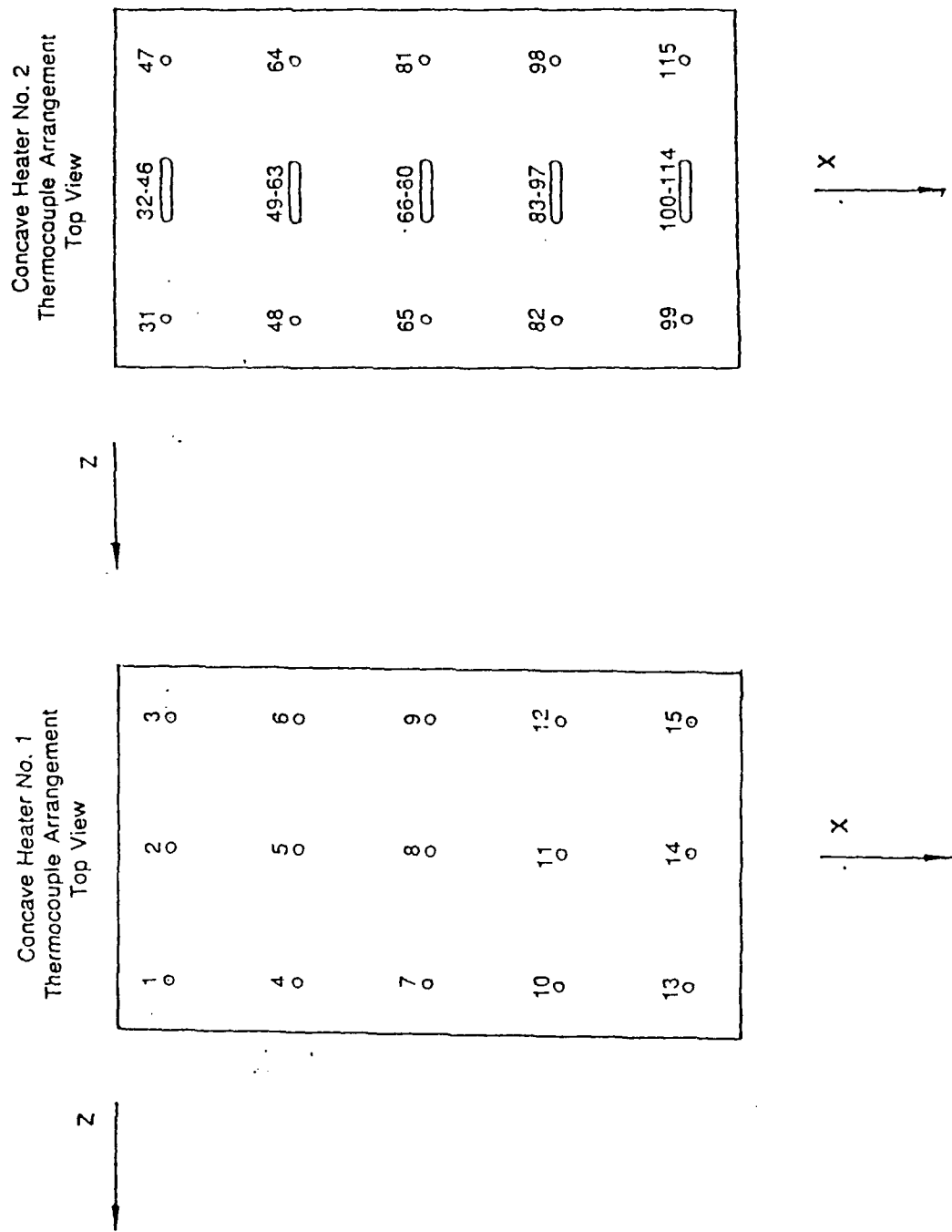
Figure 13. Concave Heater Thermocouple Placement

49
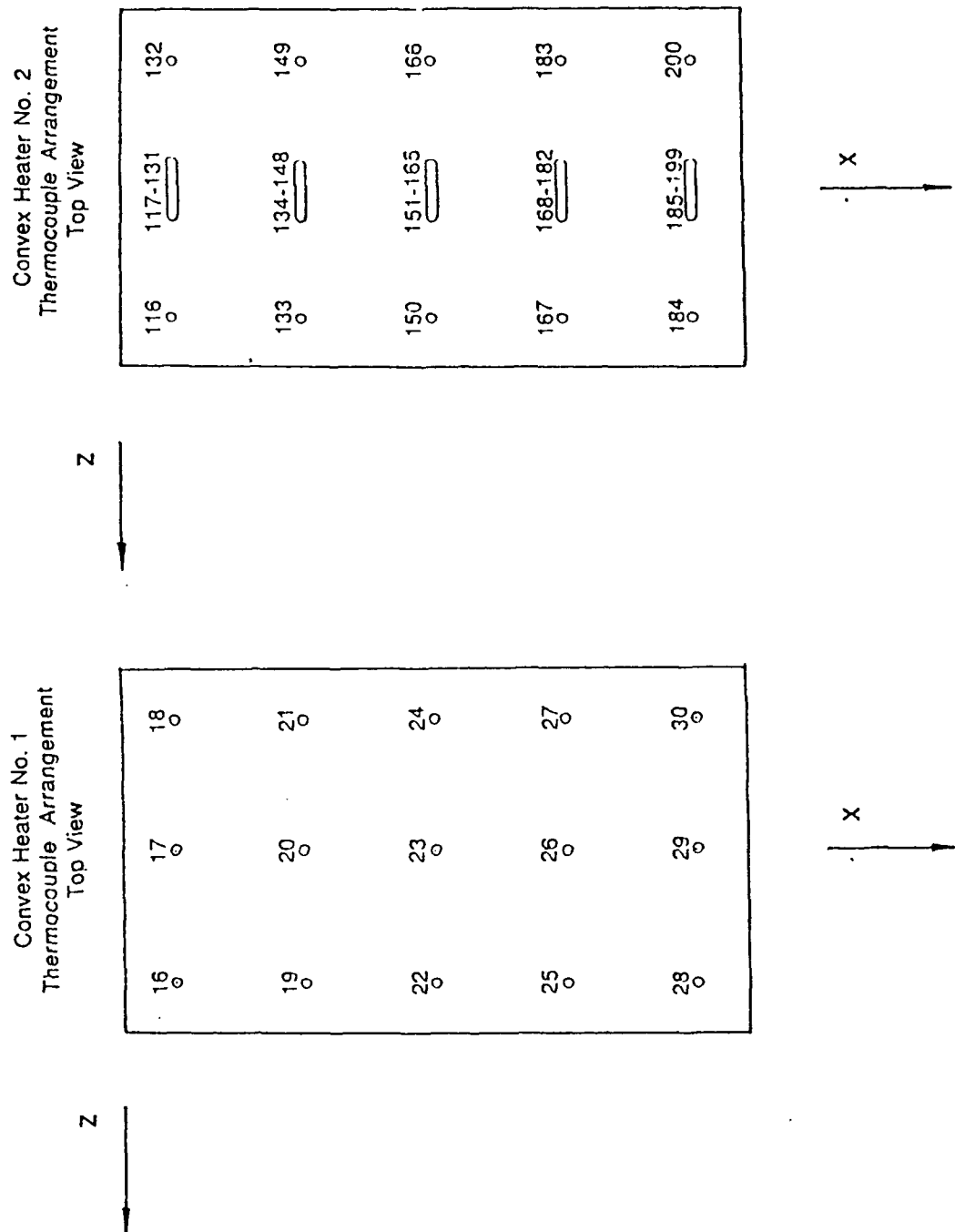
Figure 14. Convex Heater Thermocouple Placement

50
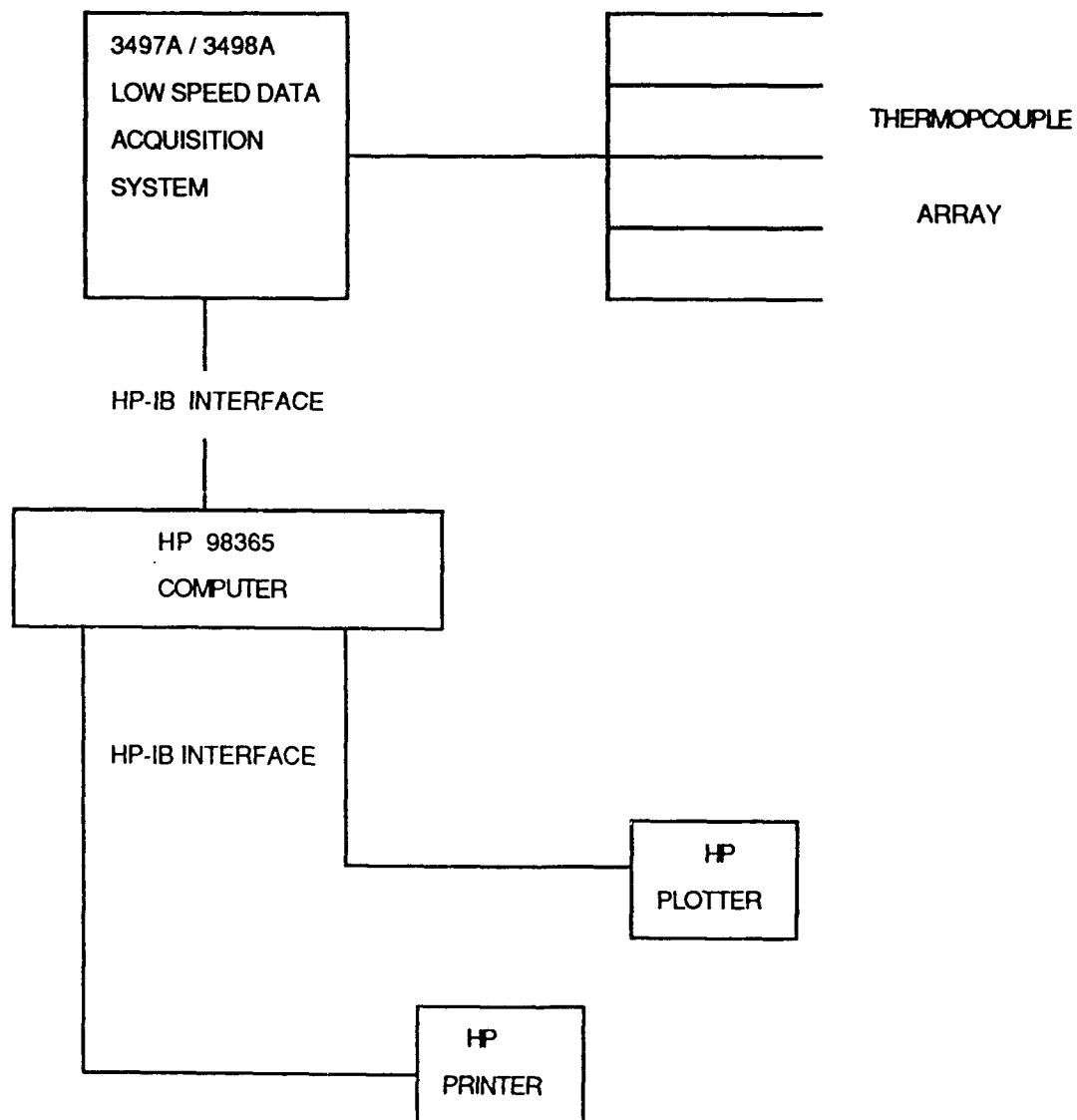
Figure 15. Data Acquisition System For Surface Temperature
Measurement
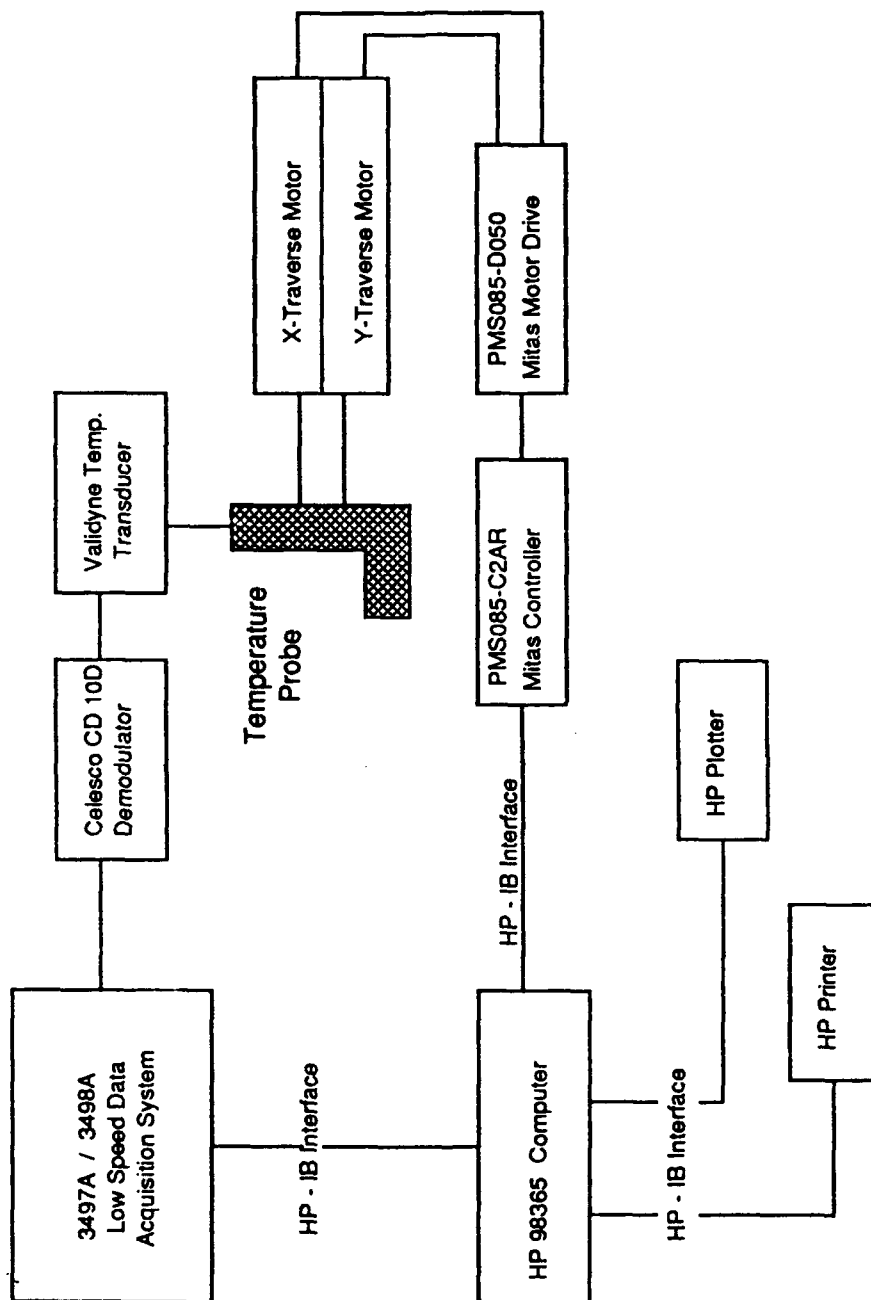
Figure 16. Data Acquisition System For Mixed-Mean
Temperature Measurement

52
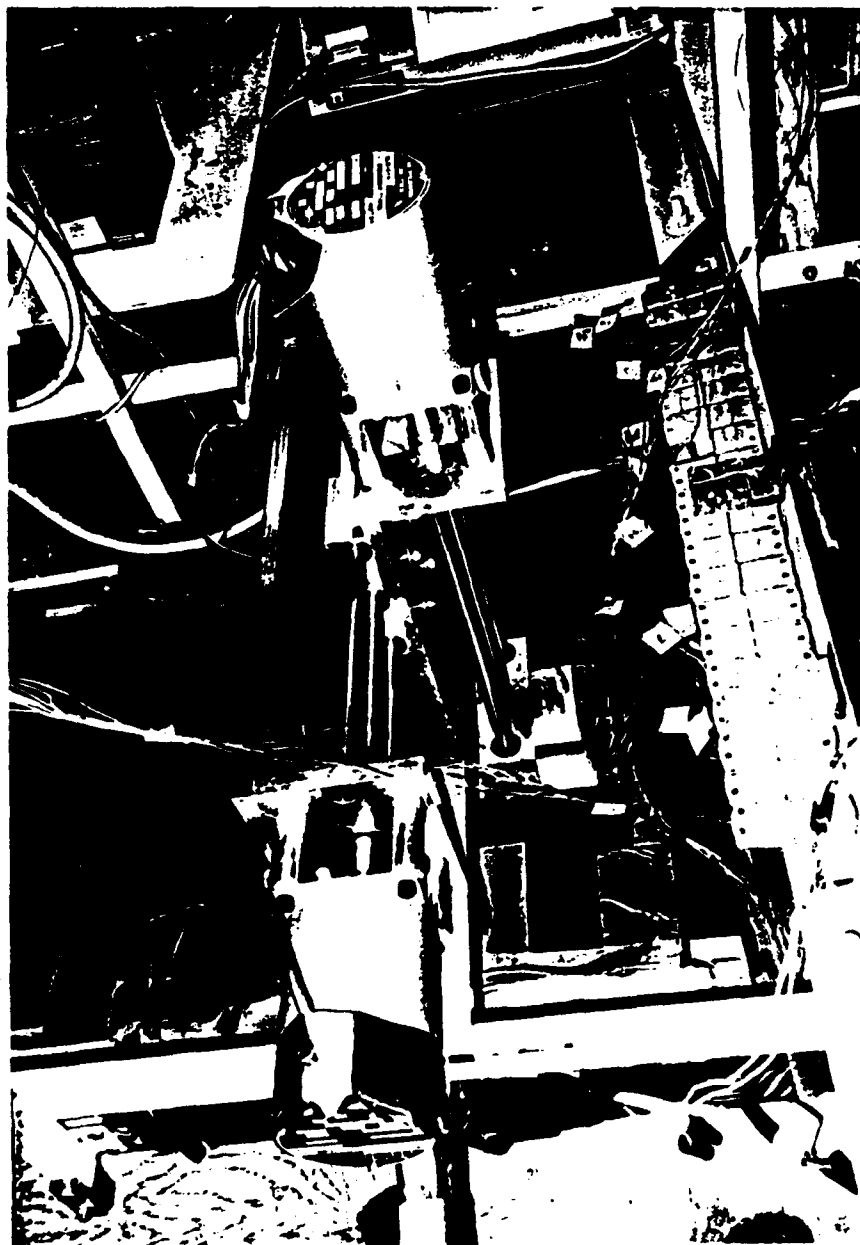
Figure 17. Photograph of Temperature Traversing Mechanism

PRESSURE DROP VS DEAN NUMBER
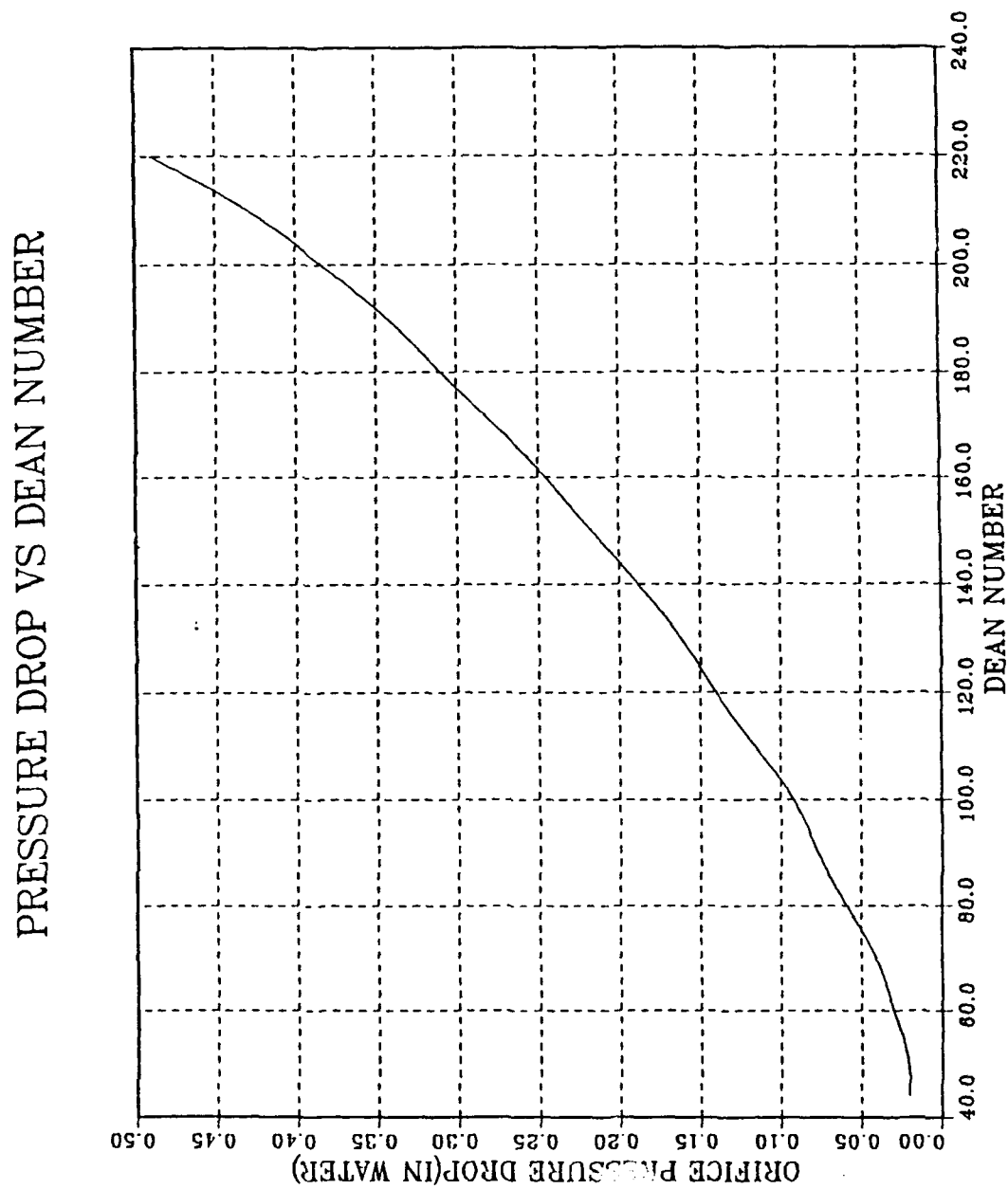
Figure 18. Pressure Drop Across Orifice Plate vs. Dean
Number

POWER INPUT VS DEAN NUMBER
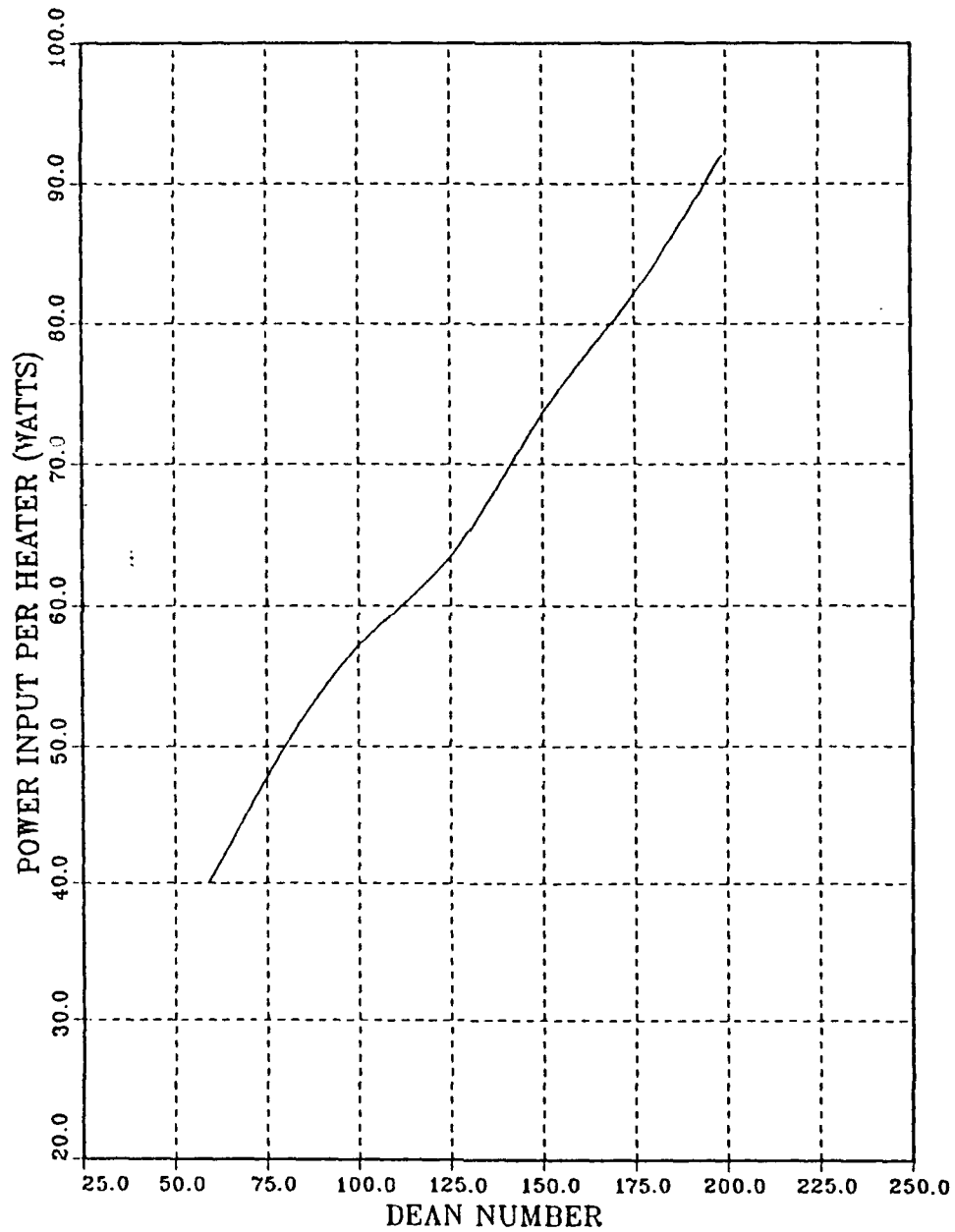
Figure 19.   Dean Number Versus Power Input Per Heater

55

VOLTAGE DROP VS POWER
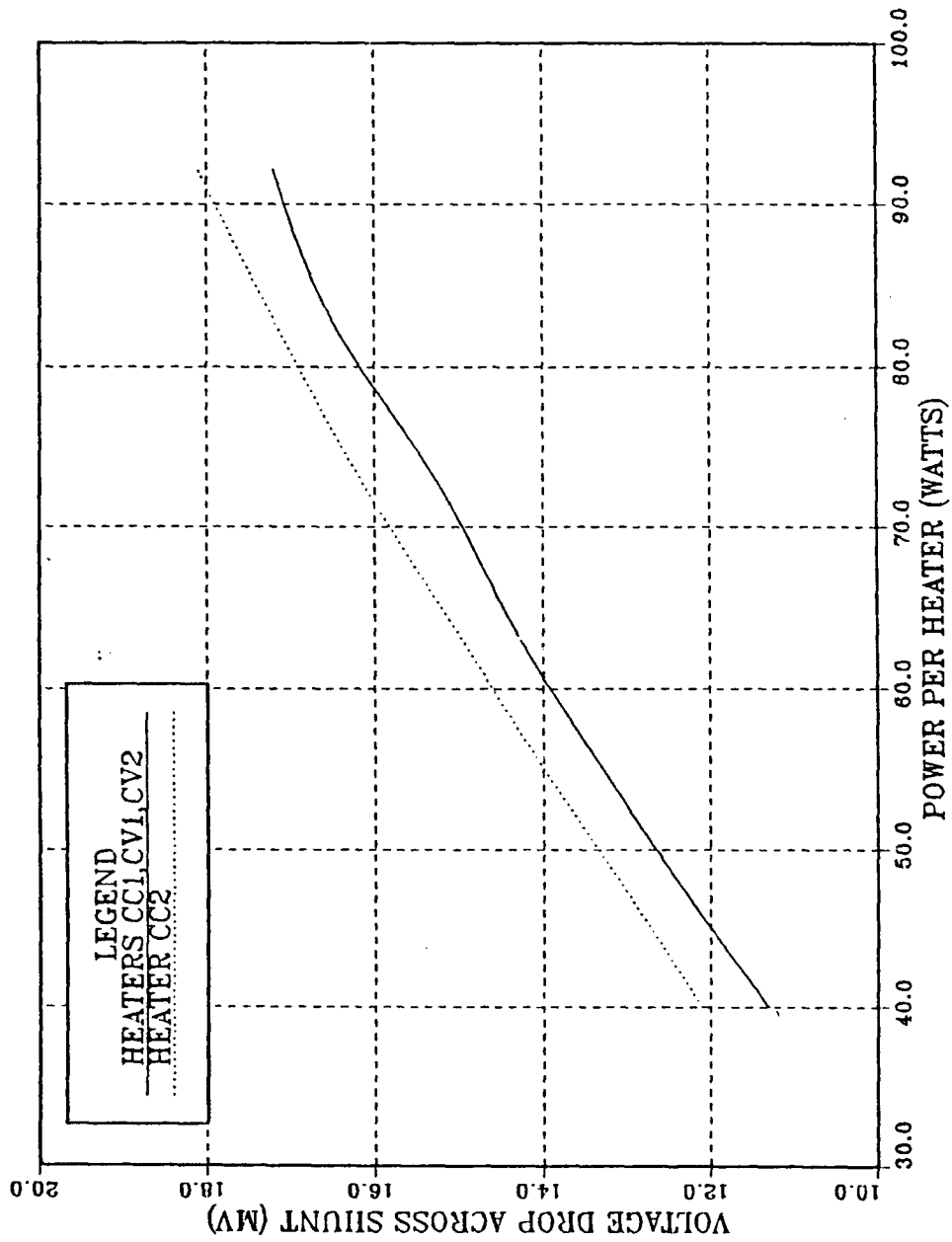
Figure 20. Voltage Drop Across Shunt Versus Heat Flus Per
Heater

56

MAXIMUM TEMPERATURE RISE VS TIME
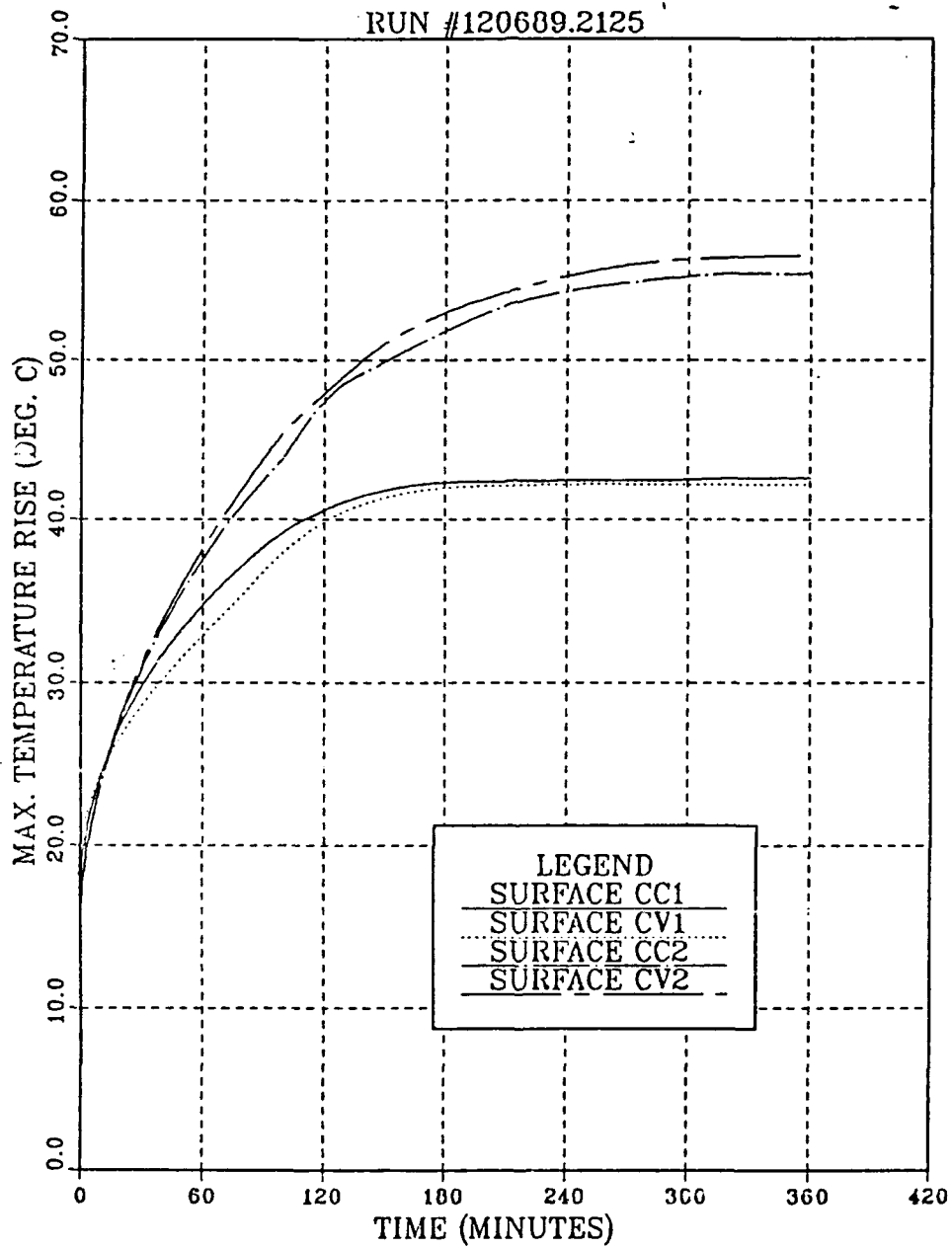
Figure 21. Temperature Increase vs. Time For Run#120689

CONCAVE SURFACE
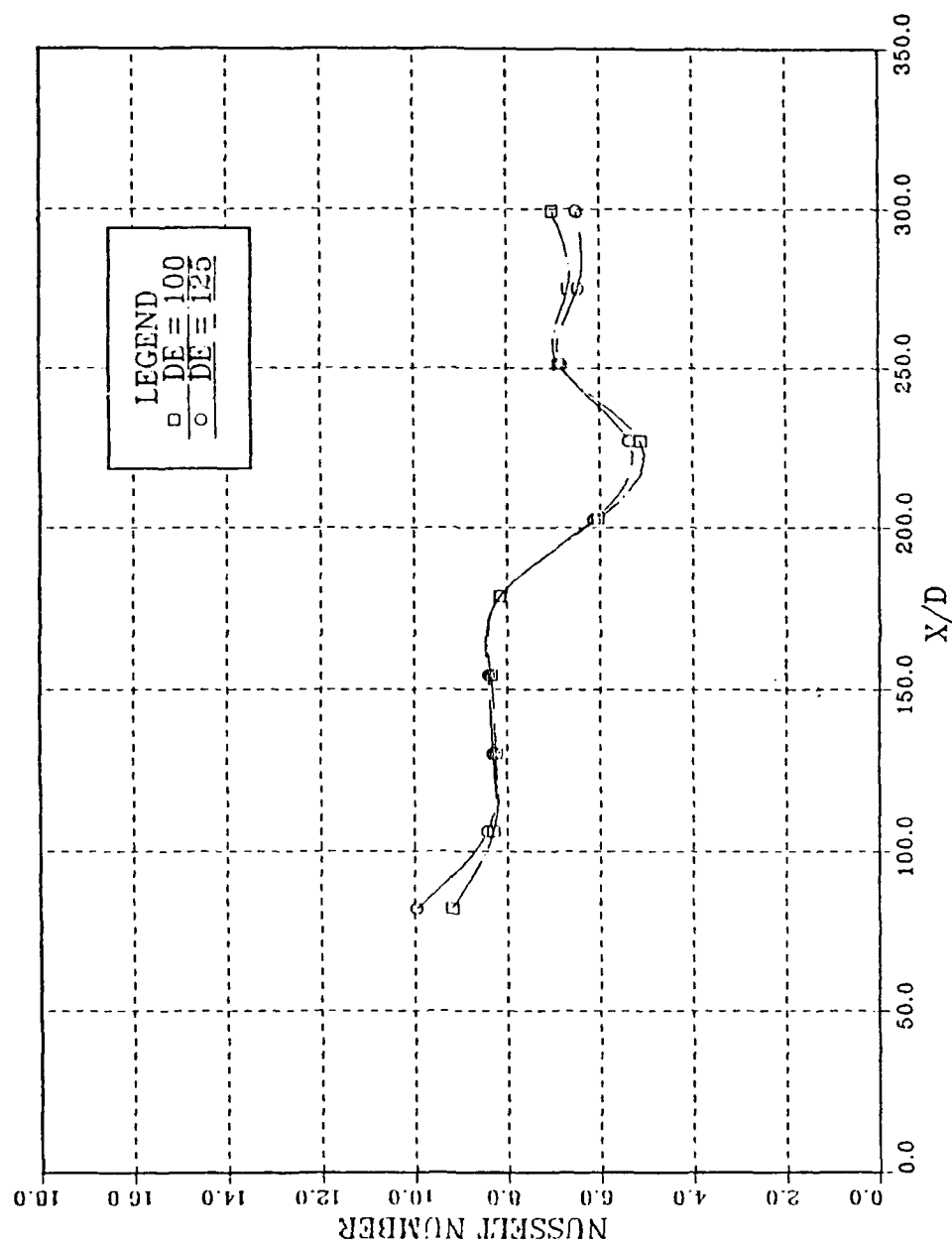
Figure 22. Spanwise Average Nusselt Number Distribution vs.
x/d , Concave Surface, De = 100 and 125

58
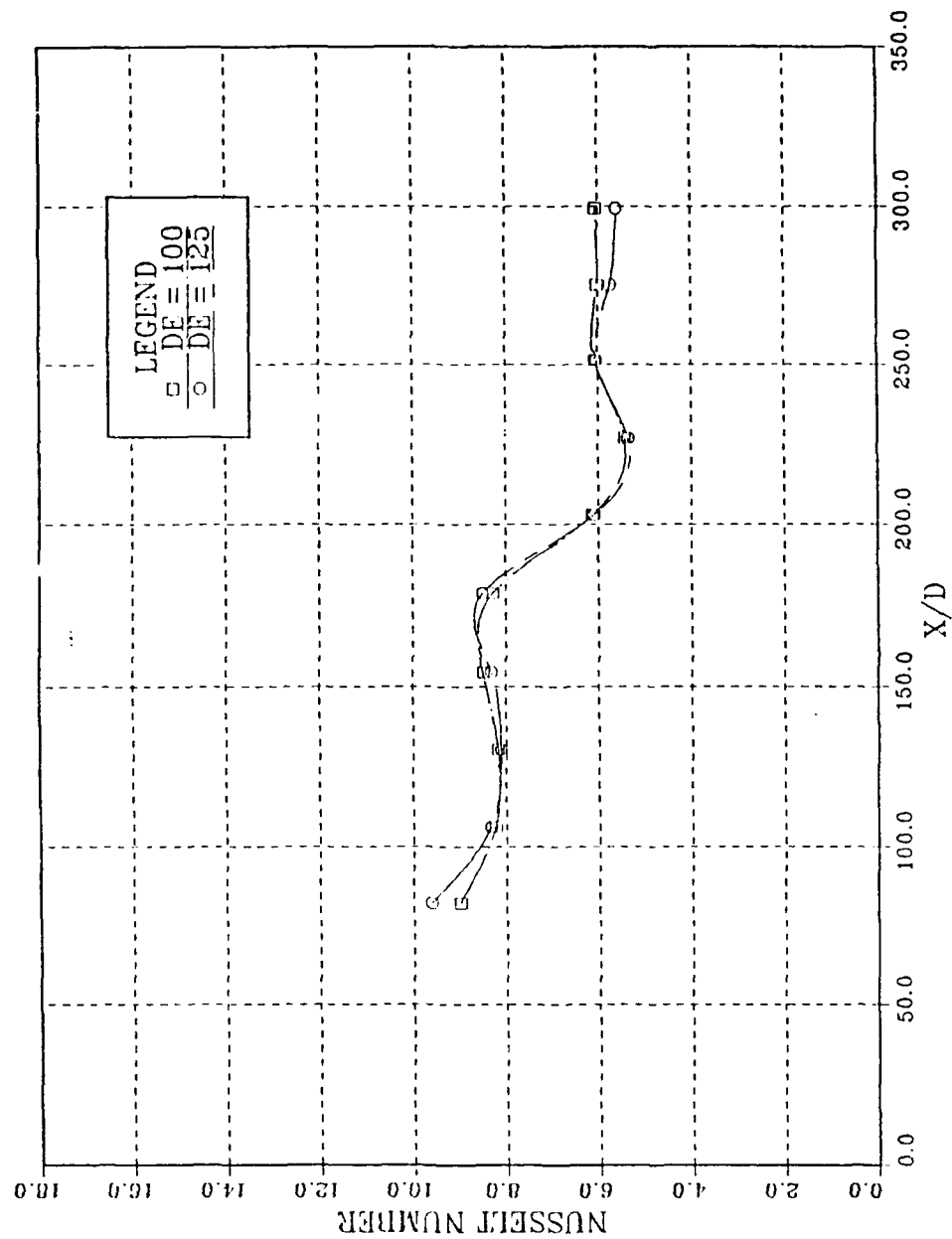
CONVEX SURFACE

Figure 23. Spanwise Averaged Nusselt Number Distribution vs.
x/d, Convex Surface, D~ = 100 and 125

59
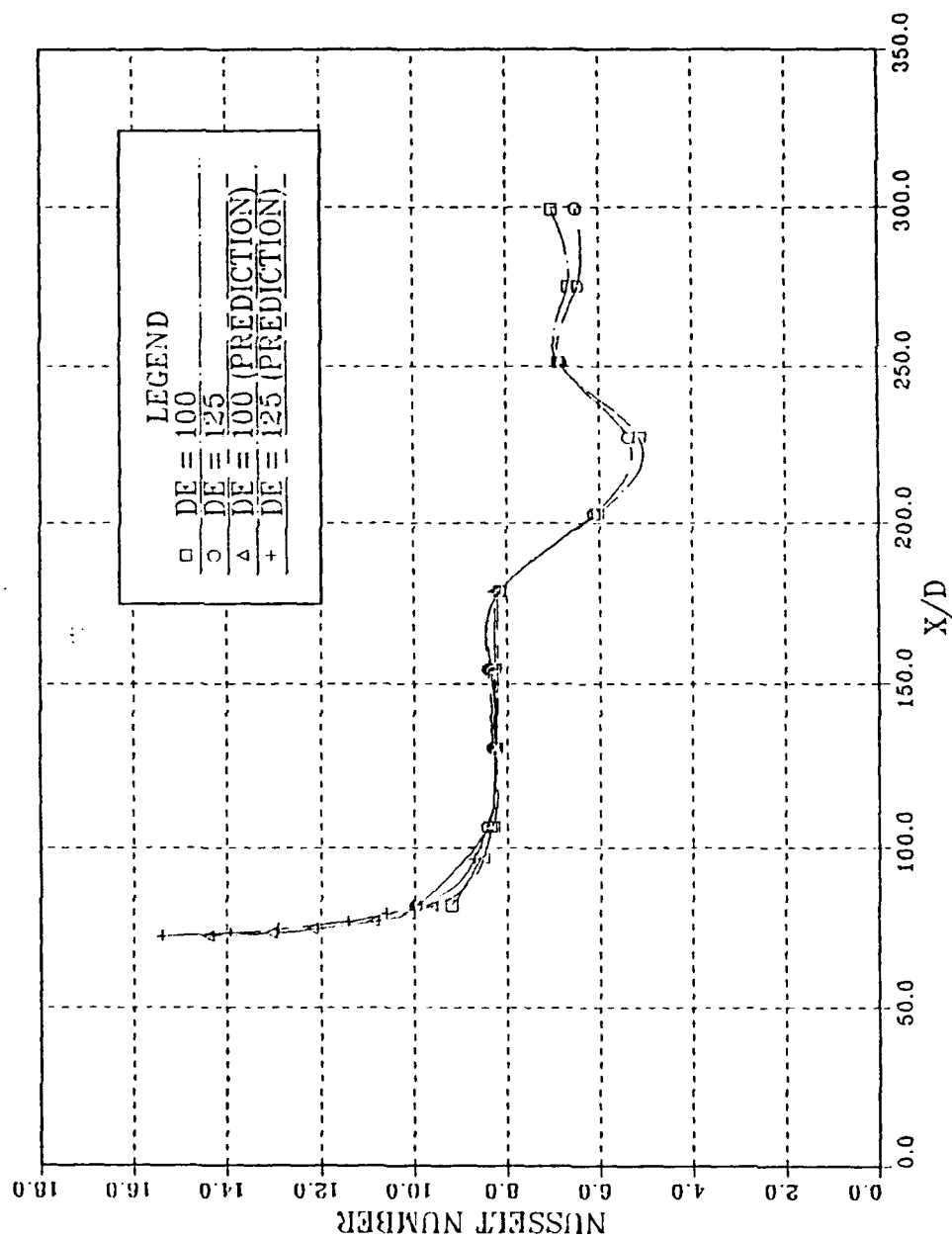
Figure 24. Spanwise Averaged Nusselt Number vs. x/d,
Comparison Of Experimental And Analytical Values,
Concave Surface, De = 100 and 125

60
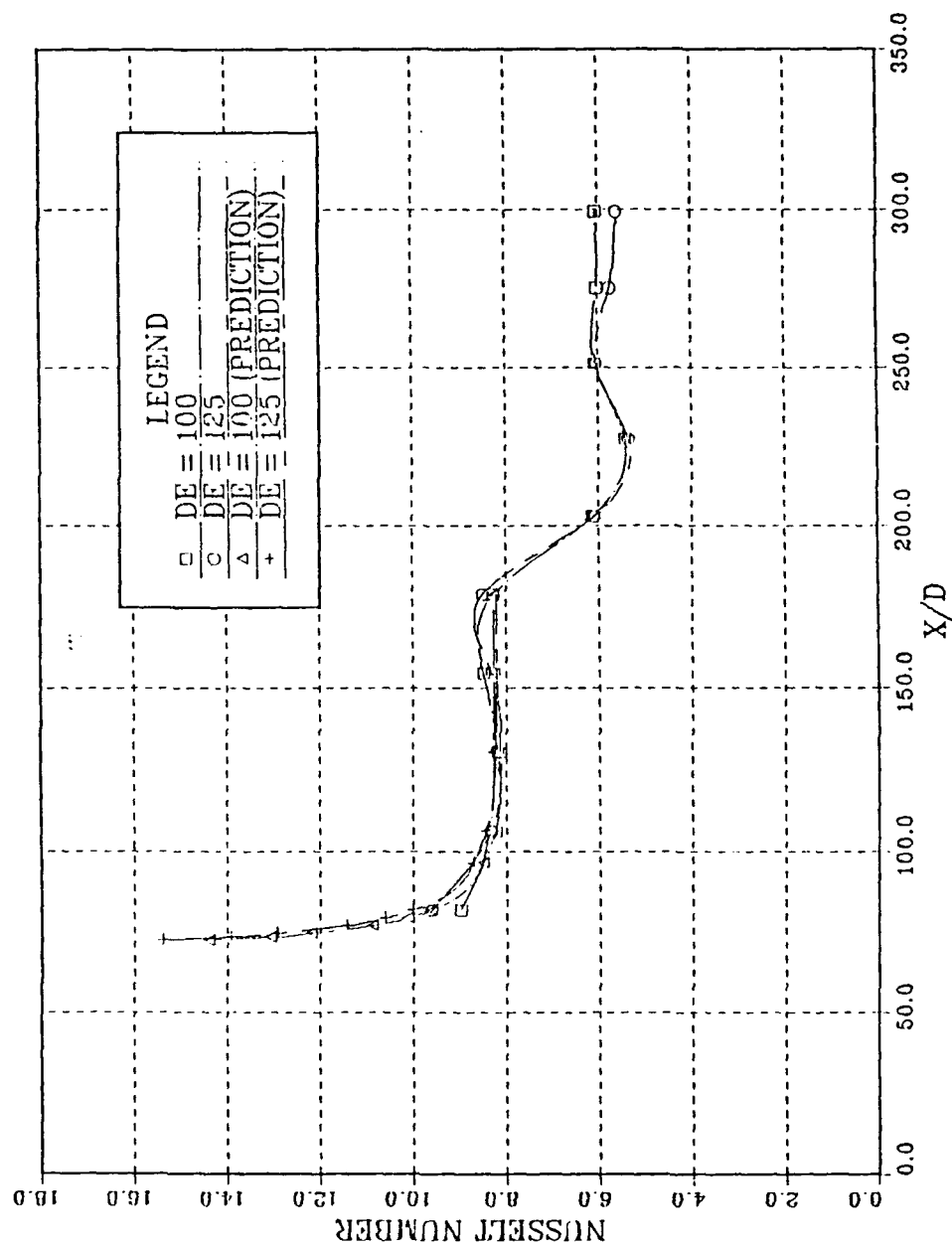
CONVEX SURFACE

Figure 25. Spanwise Averged Nusselt Number xs. x/d,
Experimental and Analytical Values, Convex Surface,
De = 100 and 125

61

PREDICTED STRAIGHT CHANNEL FLOW
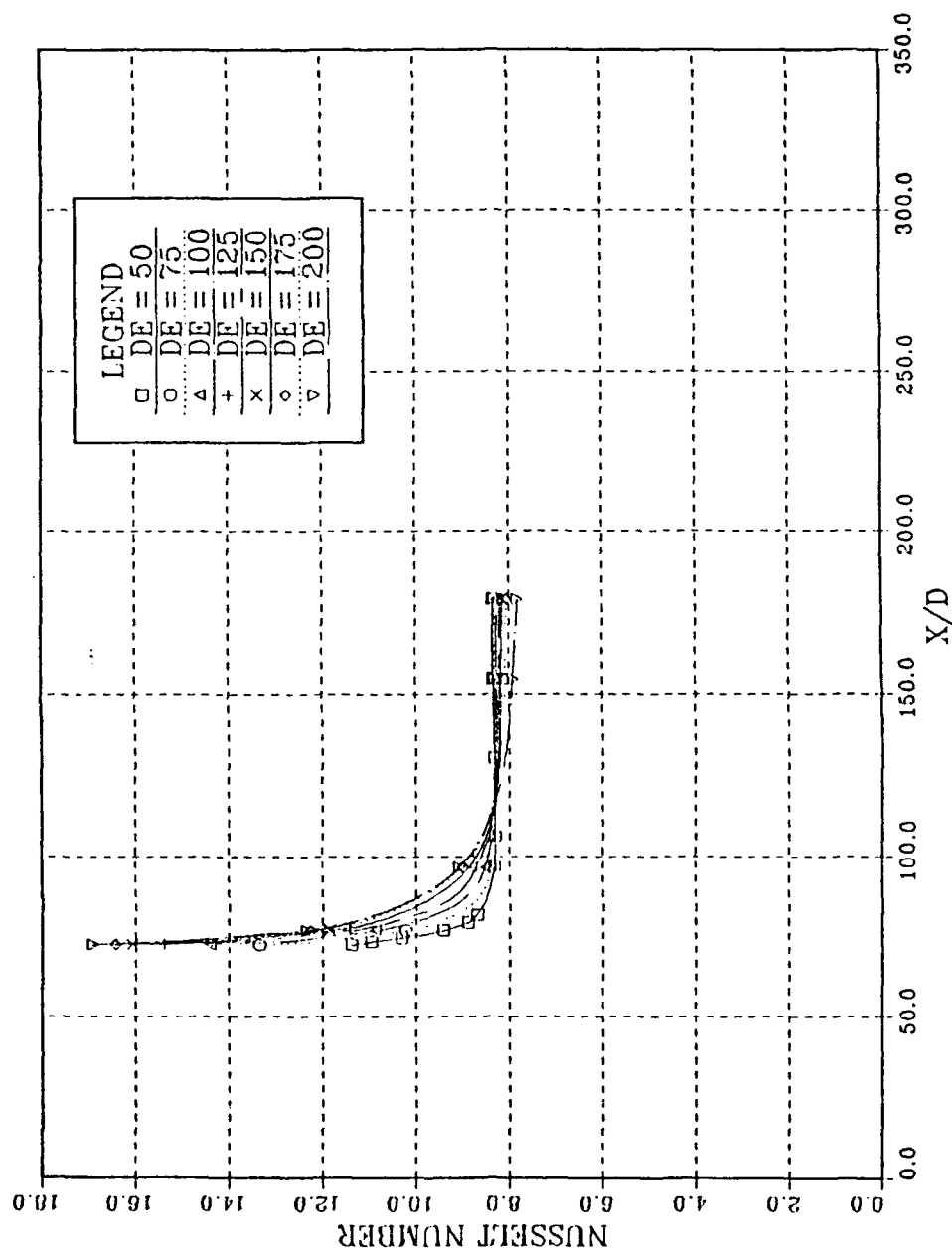
Figure 26. Predicted Straight Channel Flow For Averaged
Nusselt Number vs. x/d

62

PREDICTED STRAIGHT CHANNEL FLOW
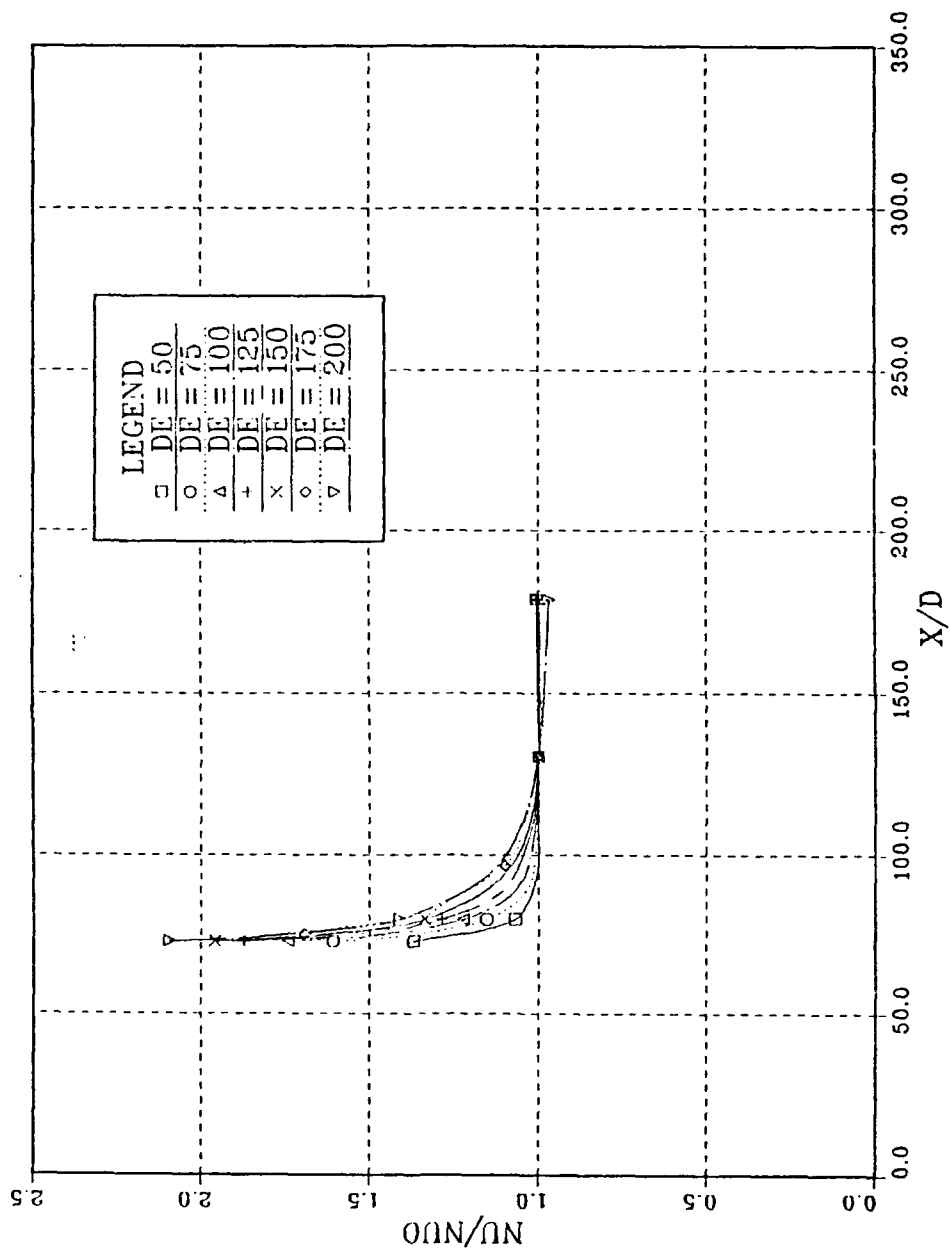
Figure 27. Predicted Straight Channel Flow For Non-Dimensional Nusselt Number vs. x/d

63
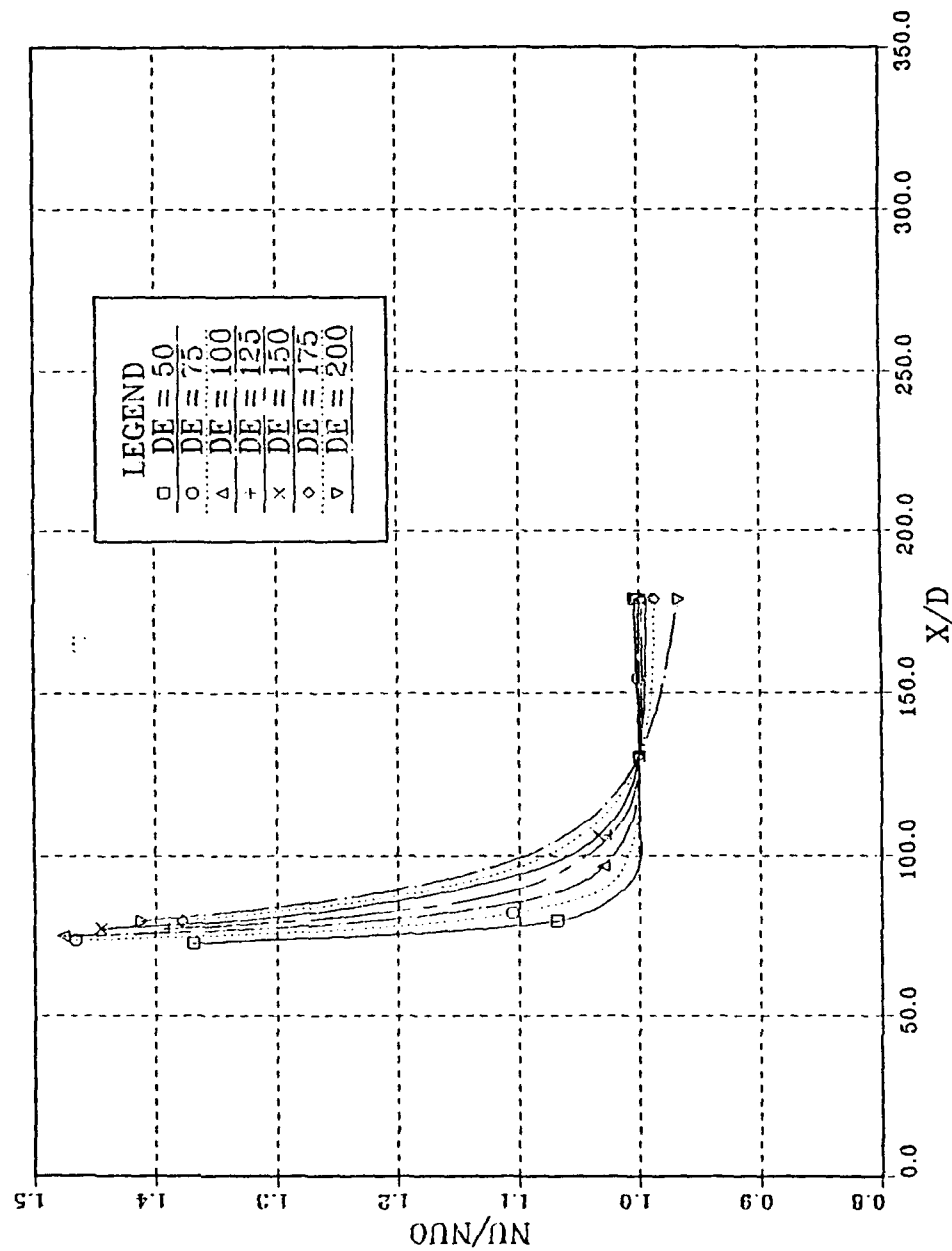
Figure 28. Predicted Staight Channel Flow For Non-Dimensional
Nusselt Number vs. x/d

64

Figure 29. Nu/Nuo vs. x/d, Concave Surface, Experimental and
Predicted Values For De = 50, 75, 100 and 125

65
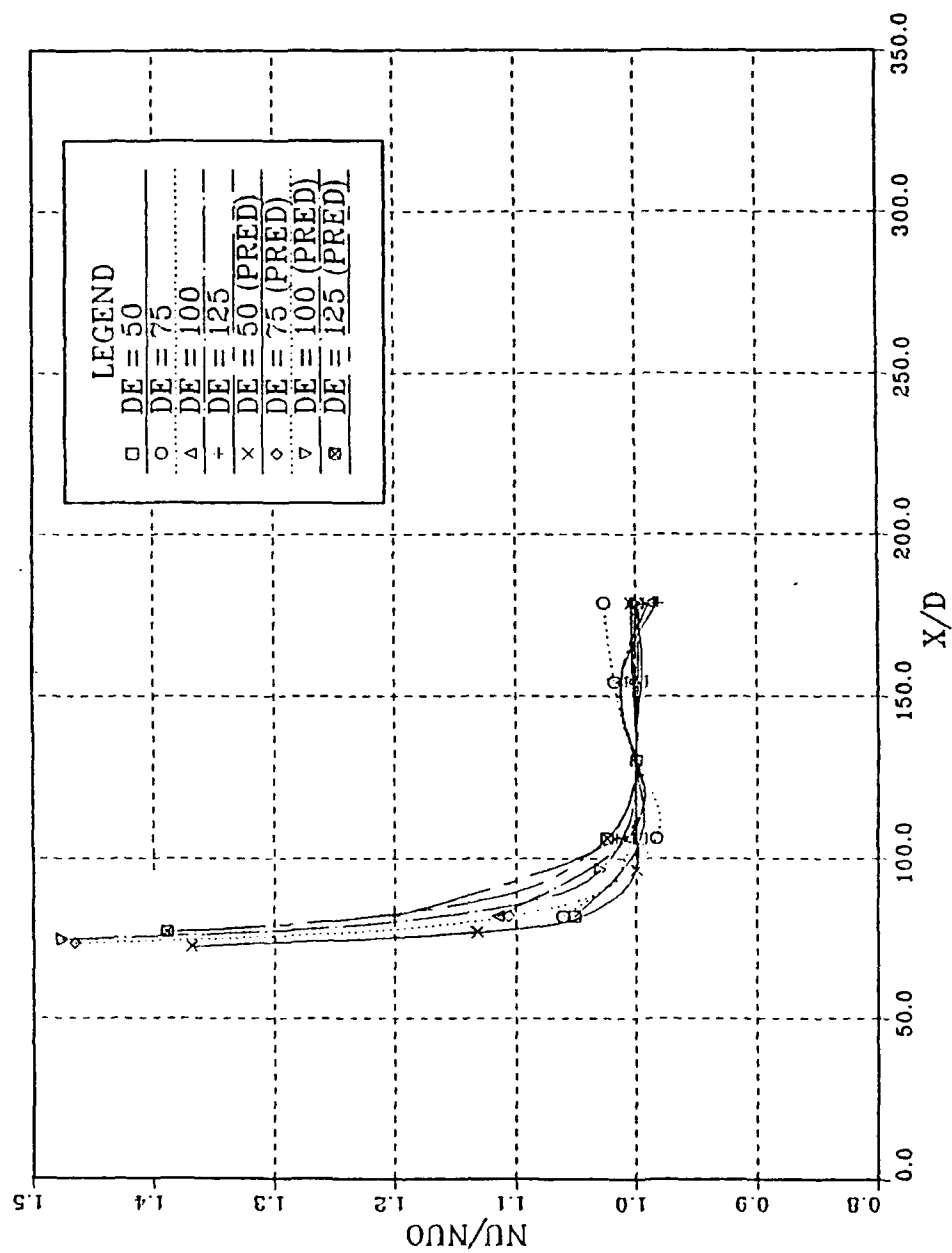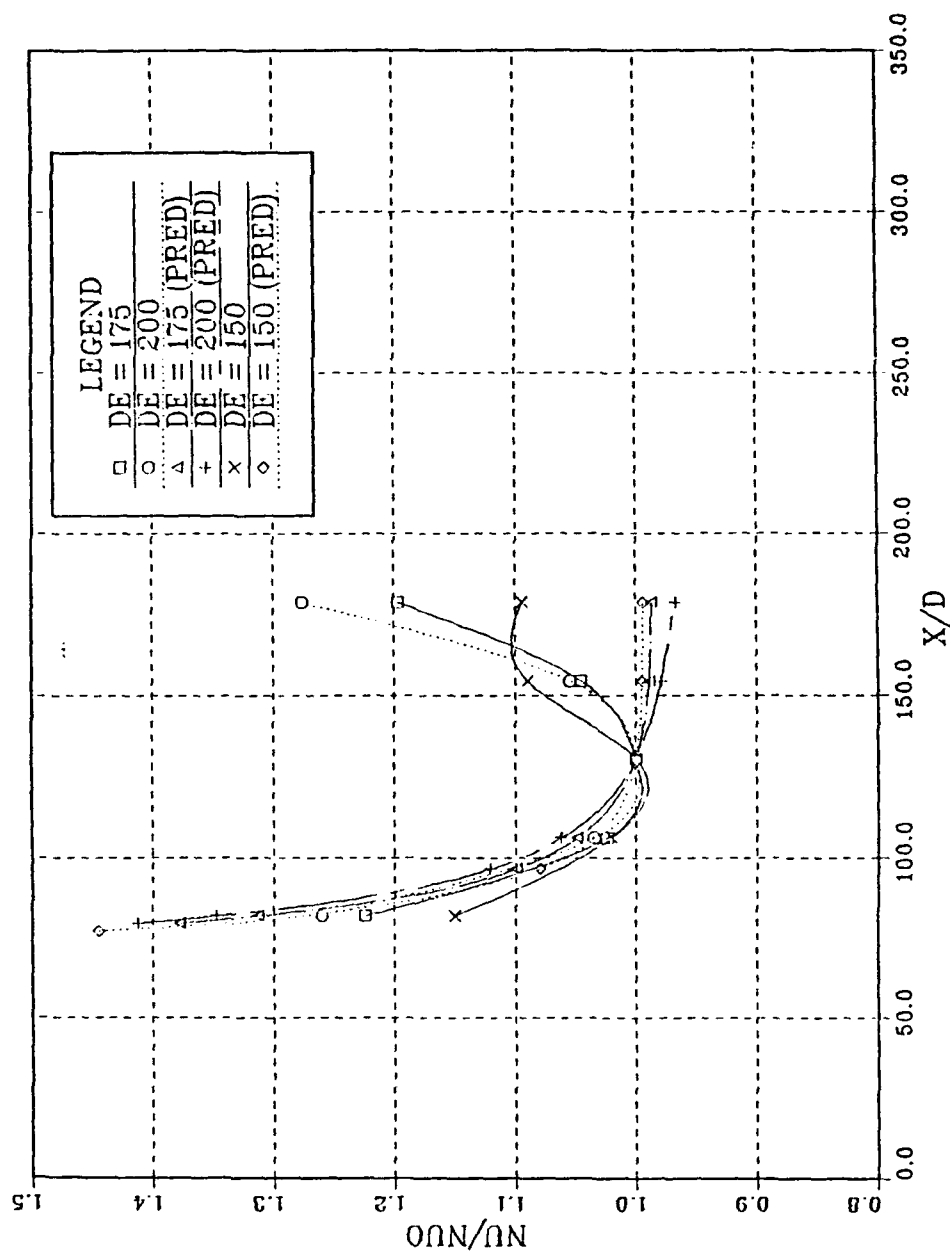
CONCAVE SURFACE

Figure 30. Nu/Nuo vs. x/d, Concave Surface, Experimental and
Predicted Values For De = 150, 175 and 200

66
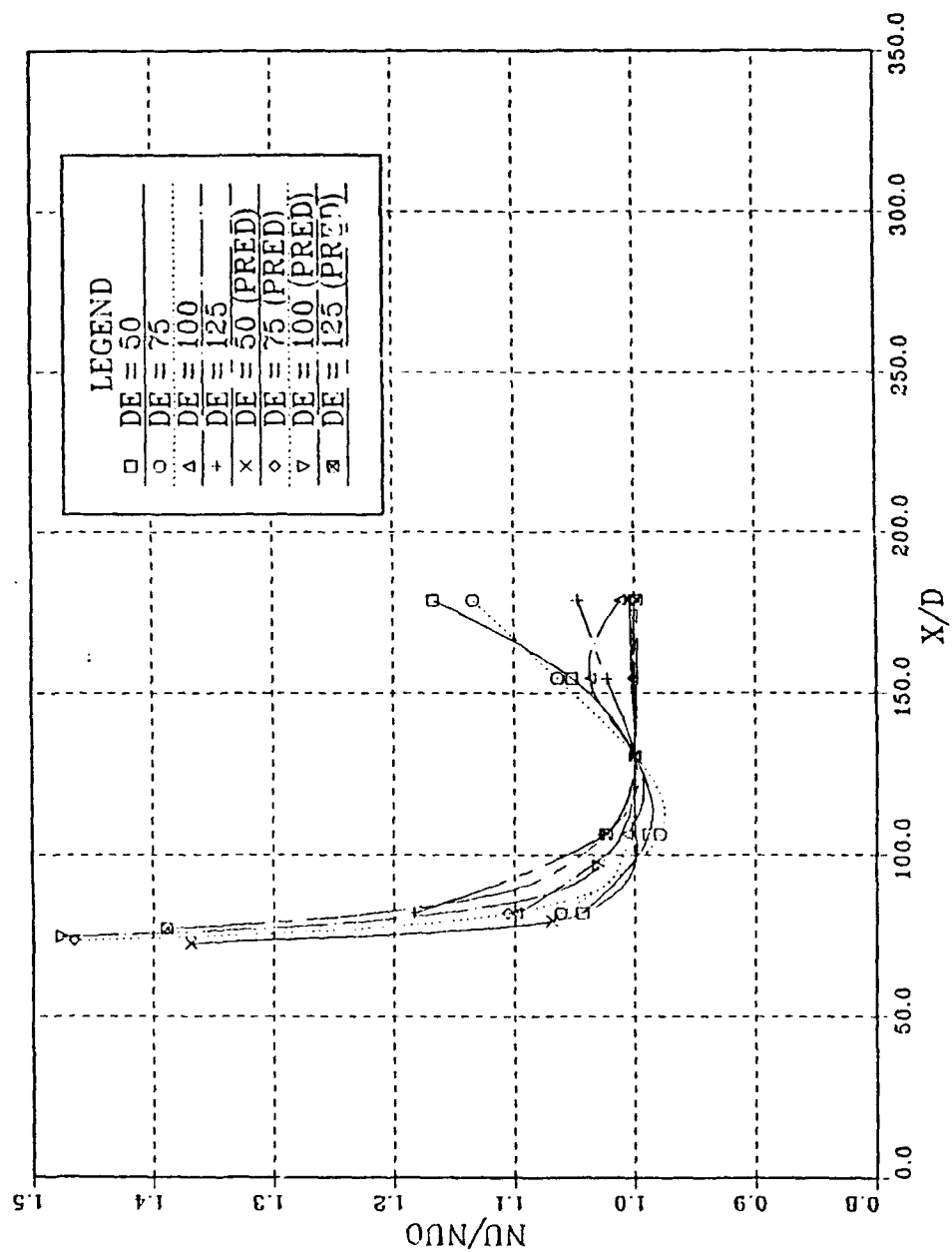
CONVEX SURFACE

Figure 31. Nu/Nuo vs. x/d, Convex Surface, Experimental and
Predicted Values For De = 50, 75, 100 and 125

67
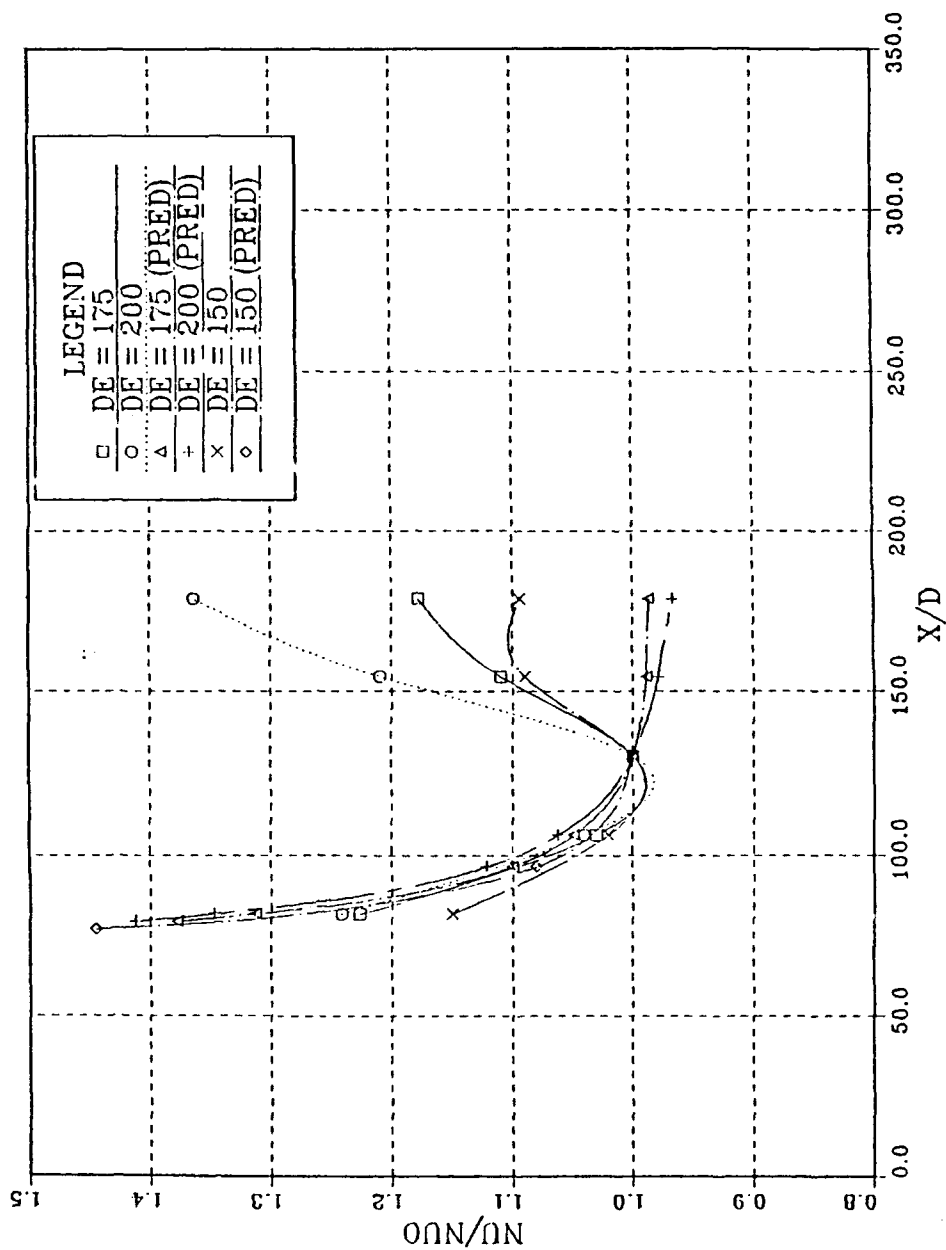
CONVEX SURFACE

Figure 32. Nu/Nuo vs. x/d, Convex Surface, Experimental and
Predicted Values For De = 150, 175 and 200

68
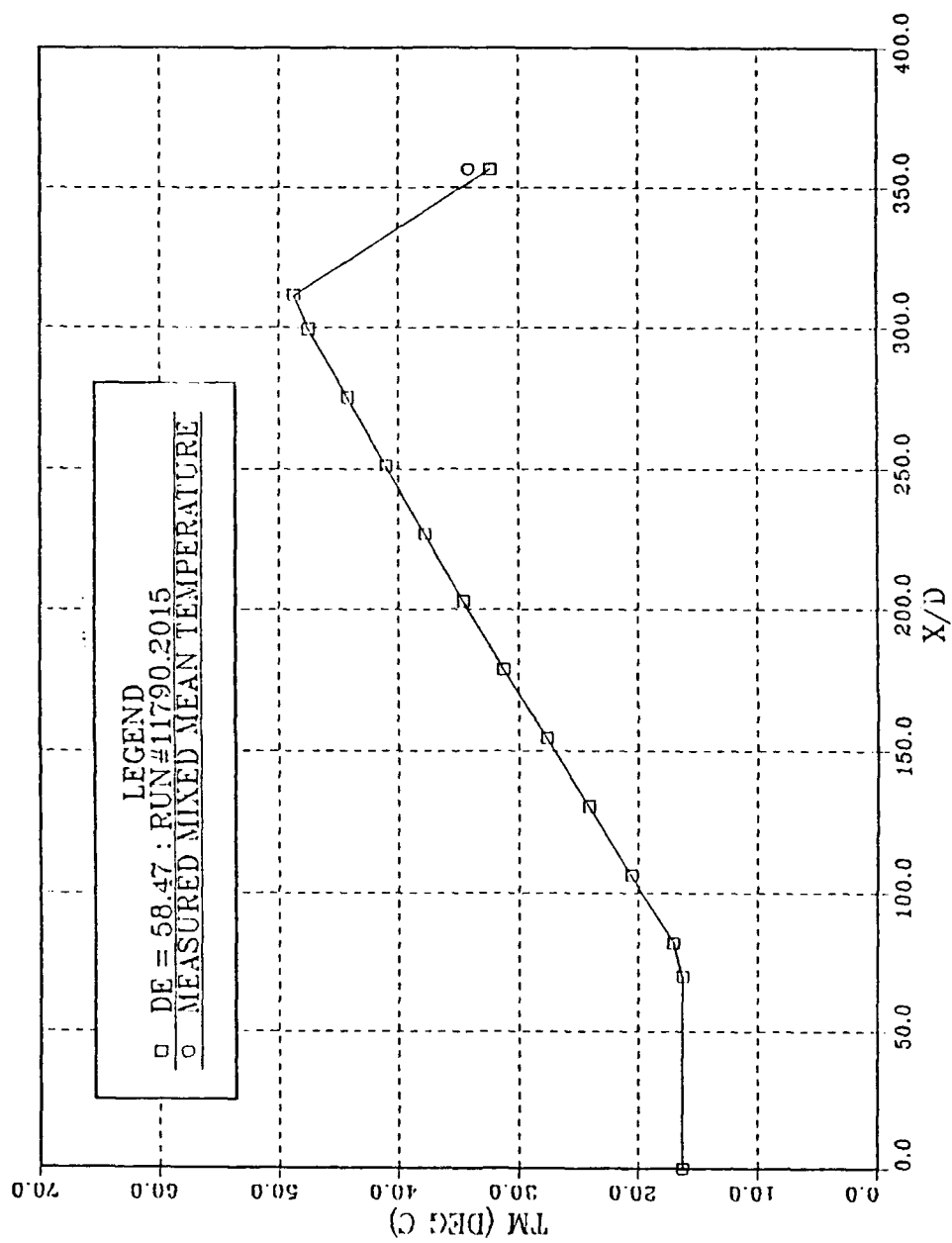
Figure 33. Mixed-Mean Temperature vs. x/d Comparison, De = 58.5

69
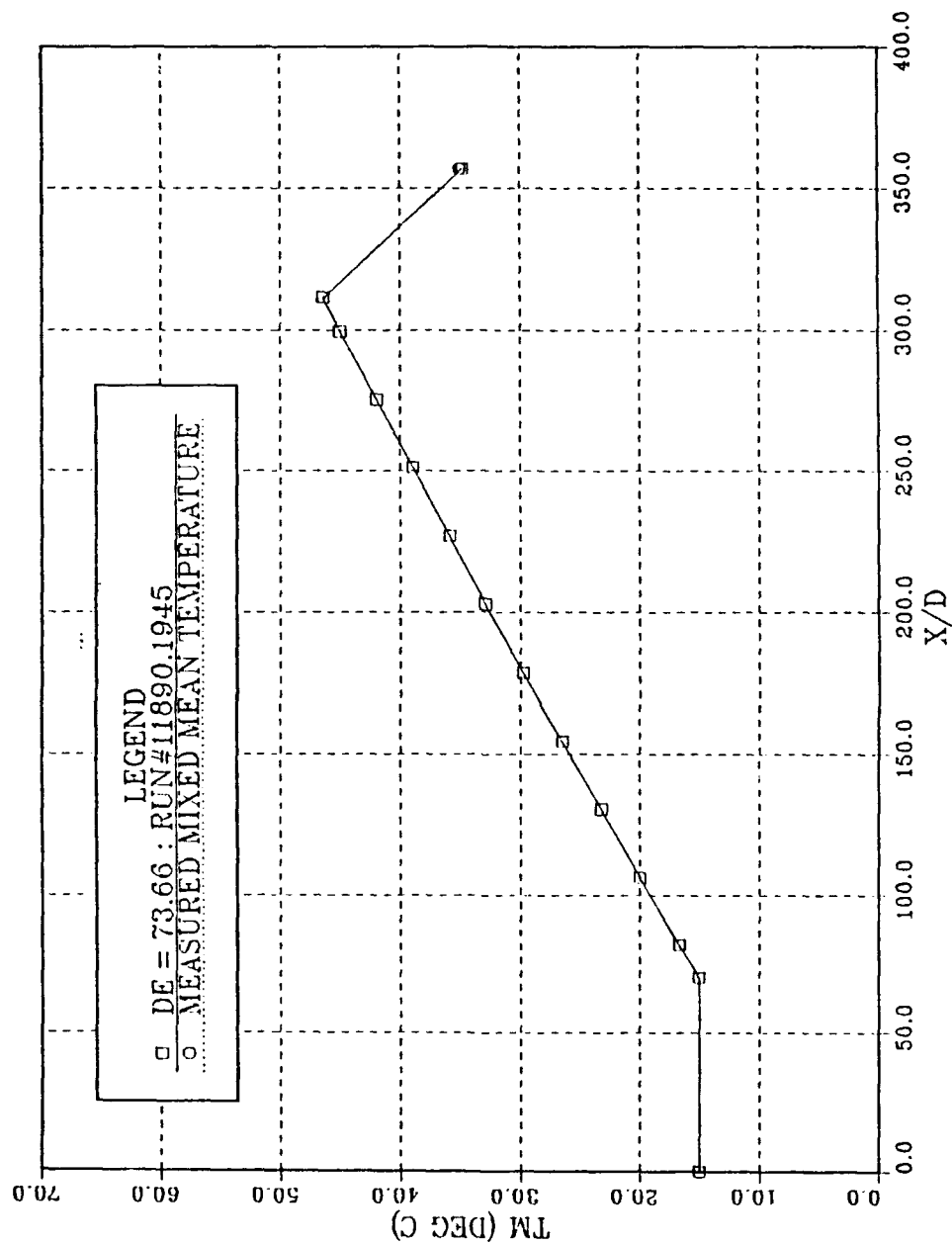
Figure 34. Mixed-Mean Temperature vs. x/d Comparison,
De = 73.7

70
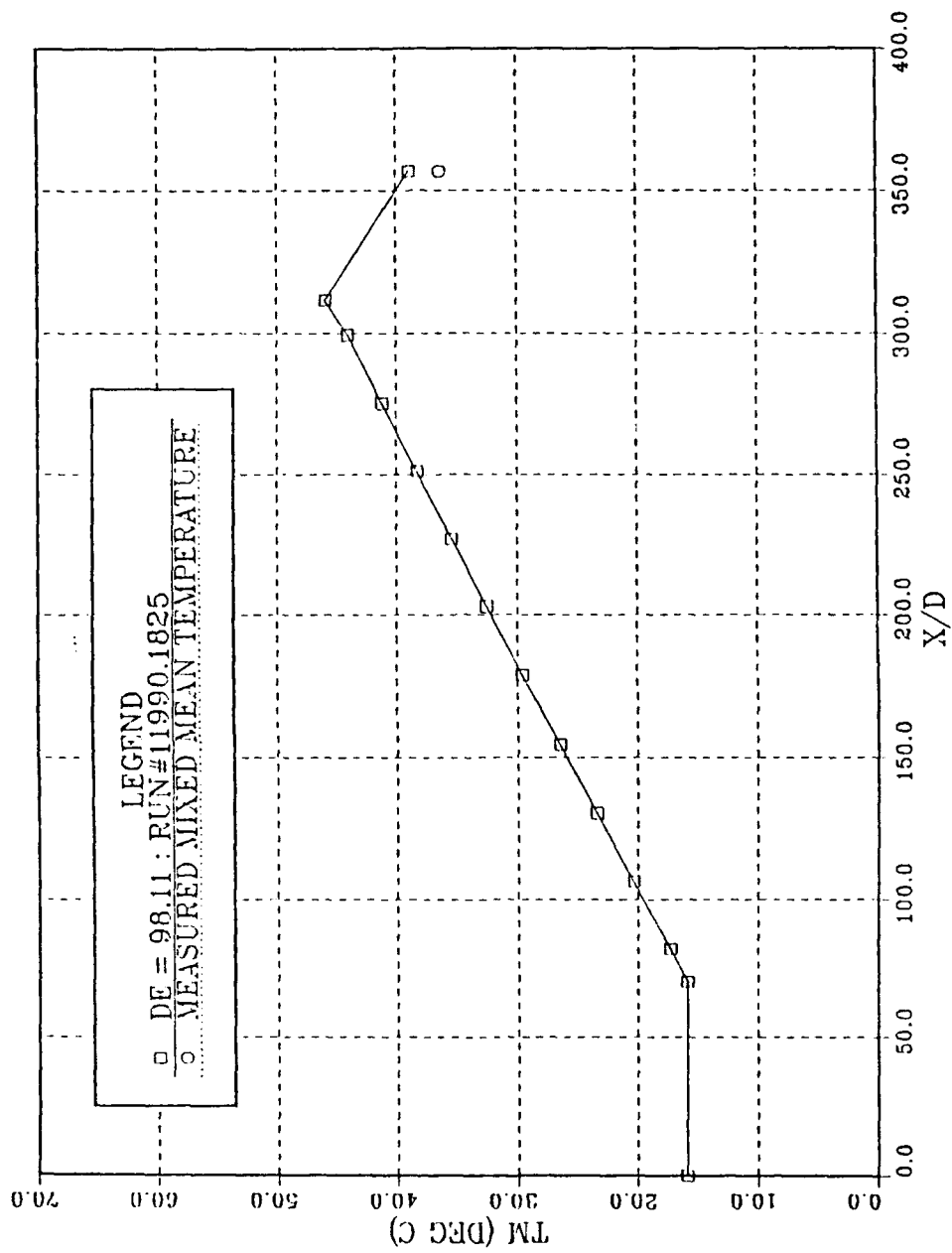
Figure 35. Mixed-Mean Temperature vs. x/d Comparison,
De = 98.1

71
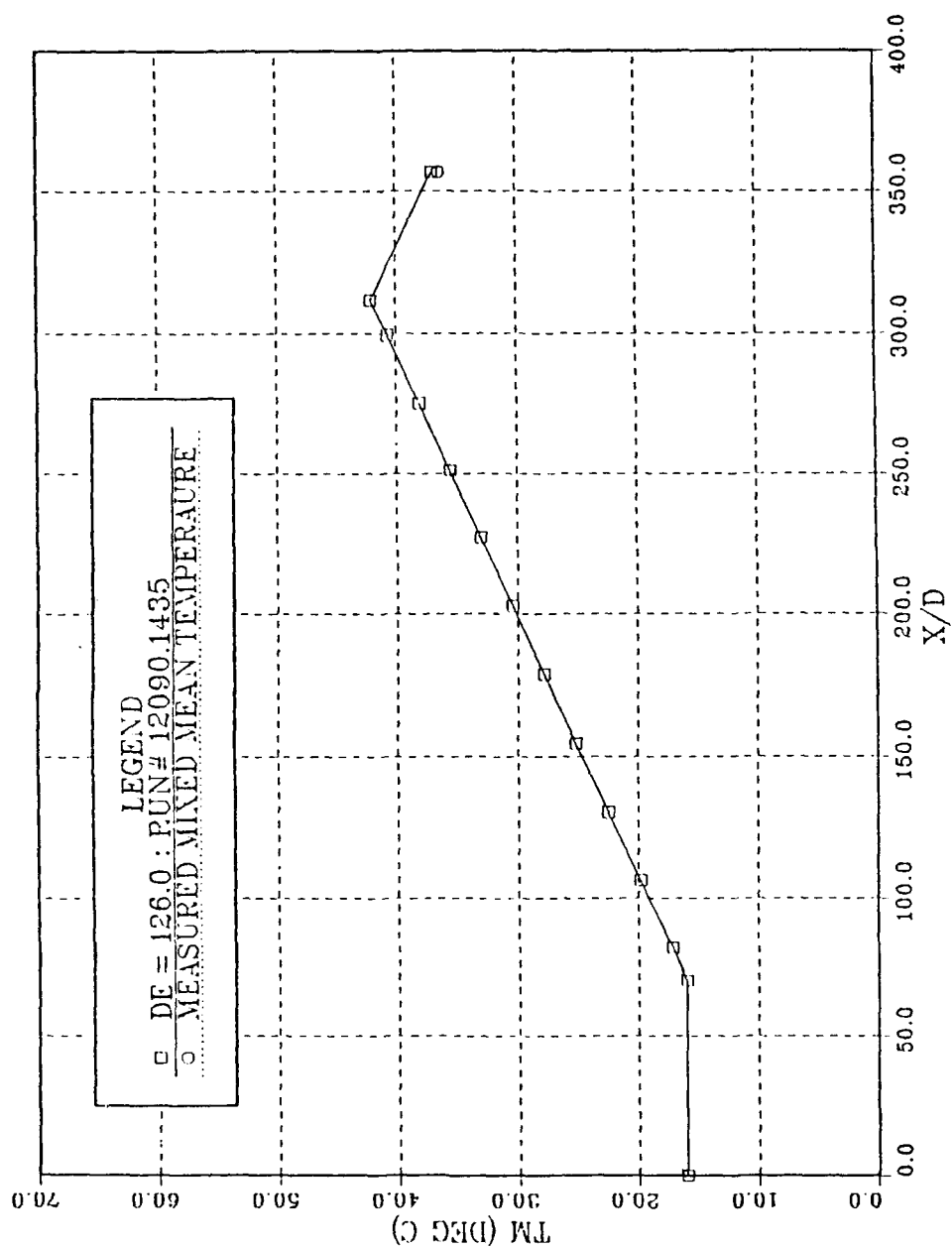
Figure 36. Mixed-Mean Temperature vs. x/d Comparison,
De = 126.0

72
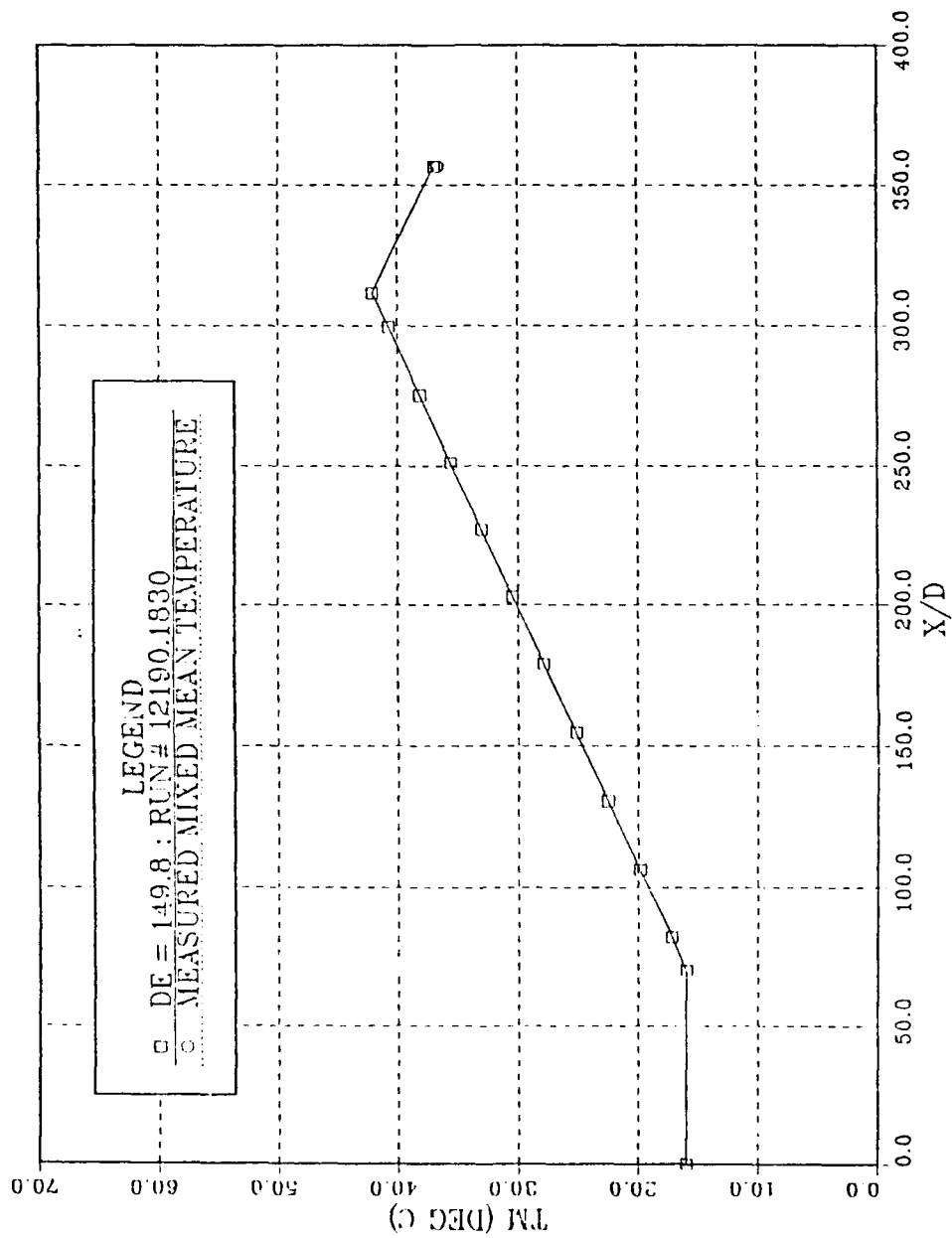
Figure 37. Mixed-Mean Temperature vs. x/d Comparison,
De = 149.8

73
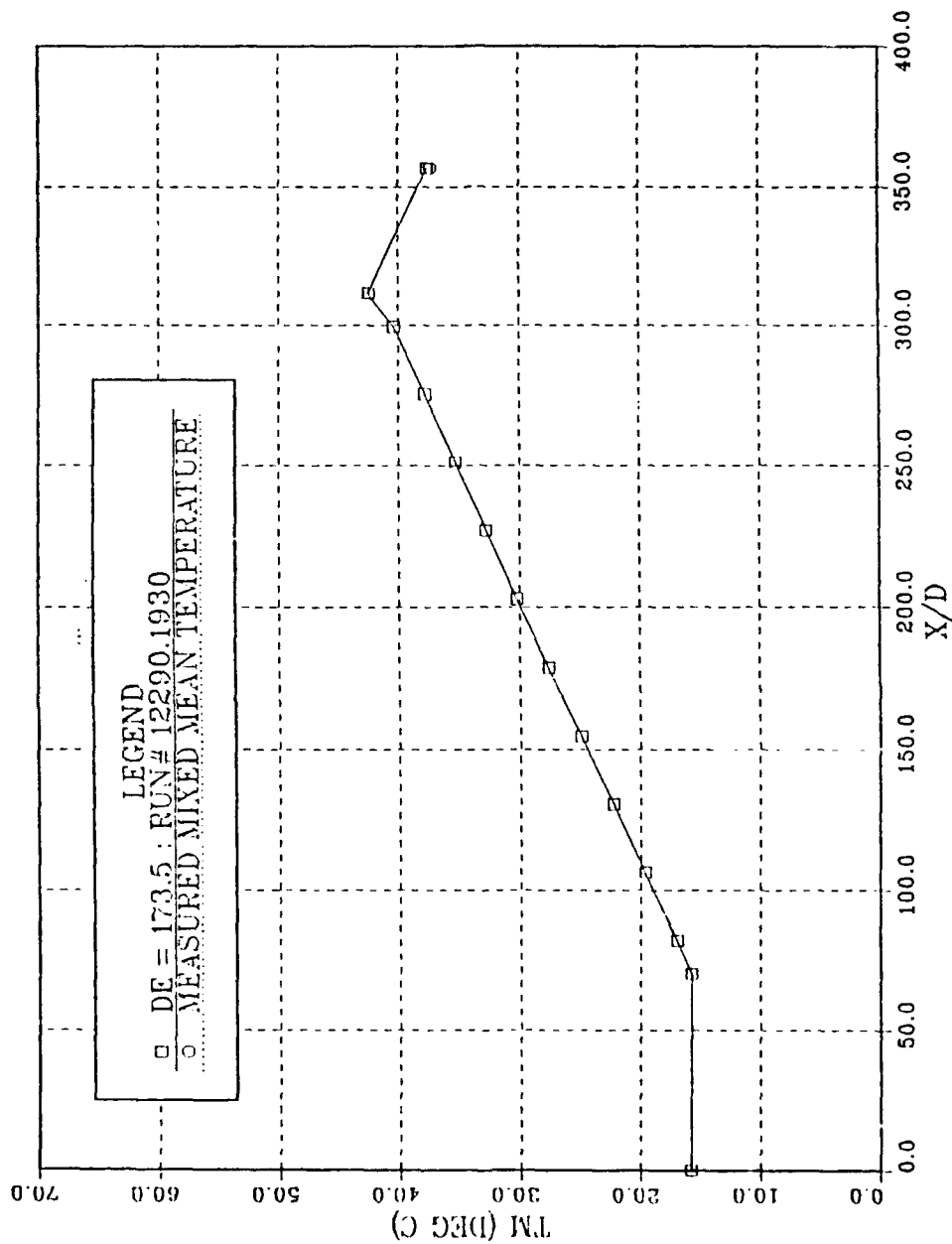
Figure 38. Mixed-Mean Temperature vs. x/d Comparison,
De = 173.5

74
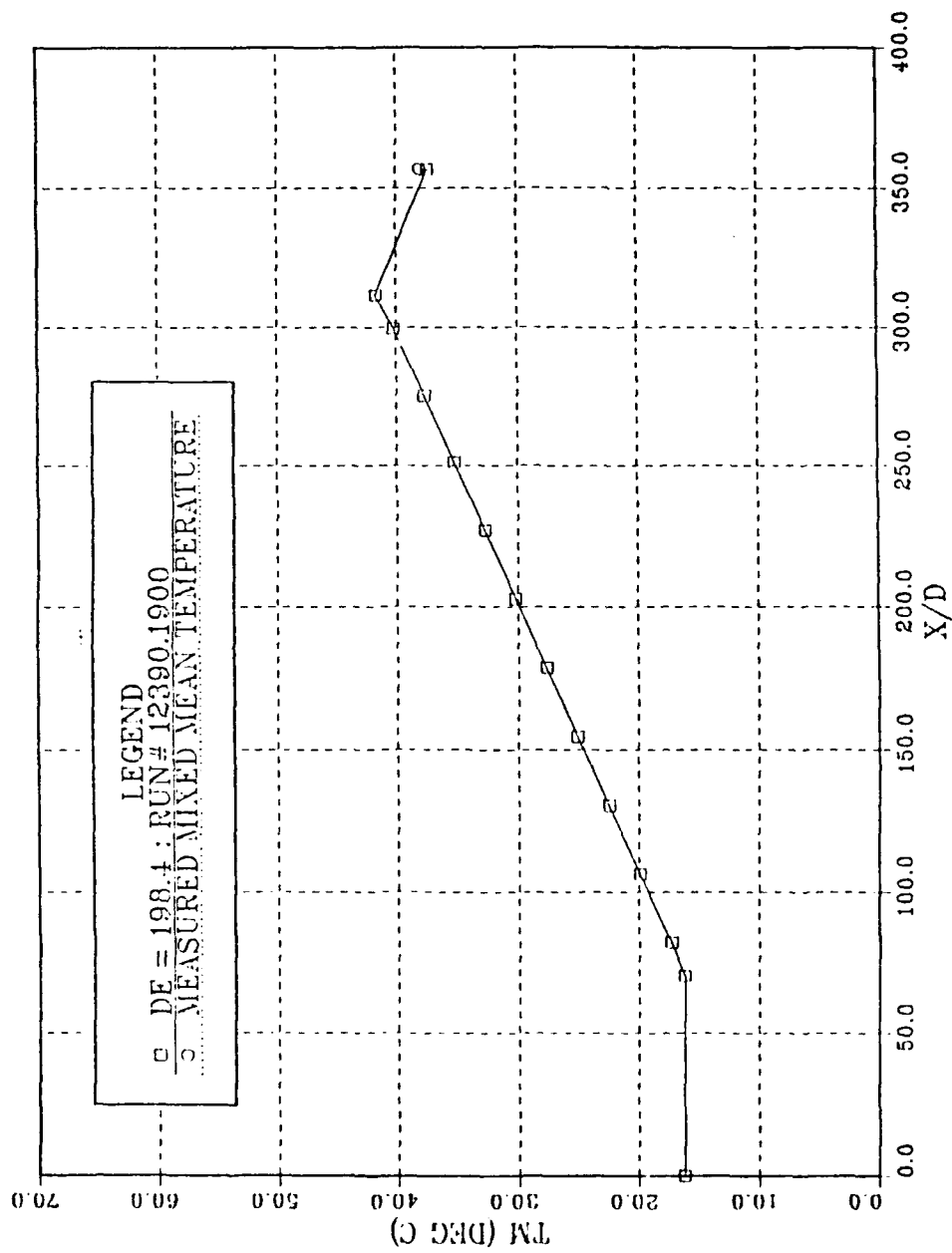
Figure 39. Mixed-Mean Temperature vs. x/d Comparison,
De = 198.4

75
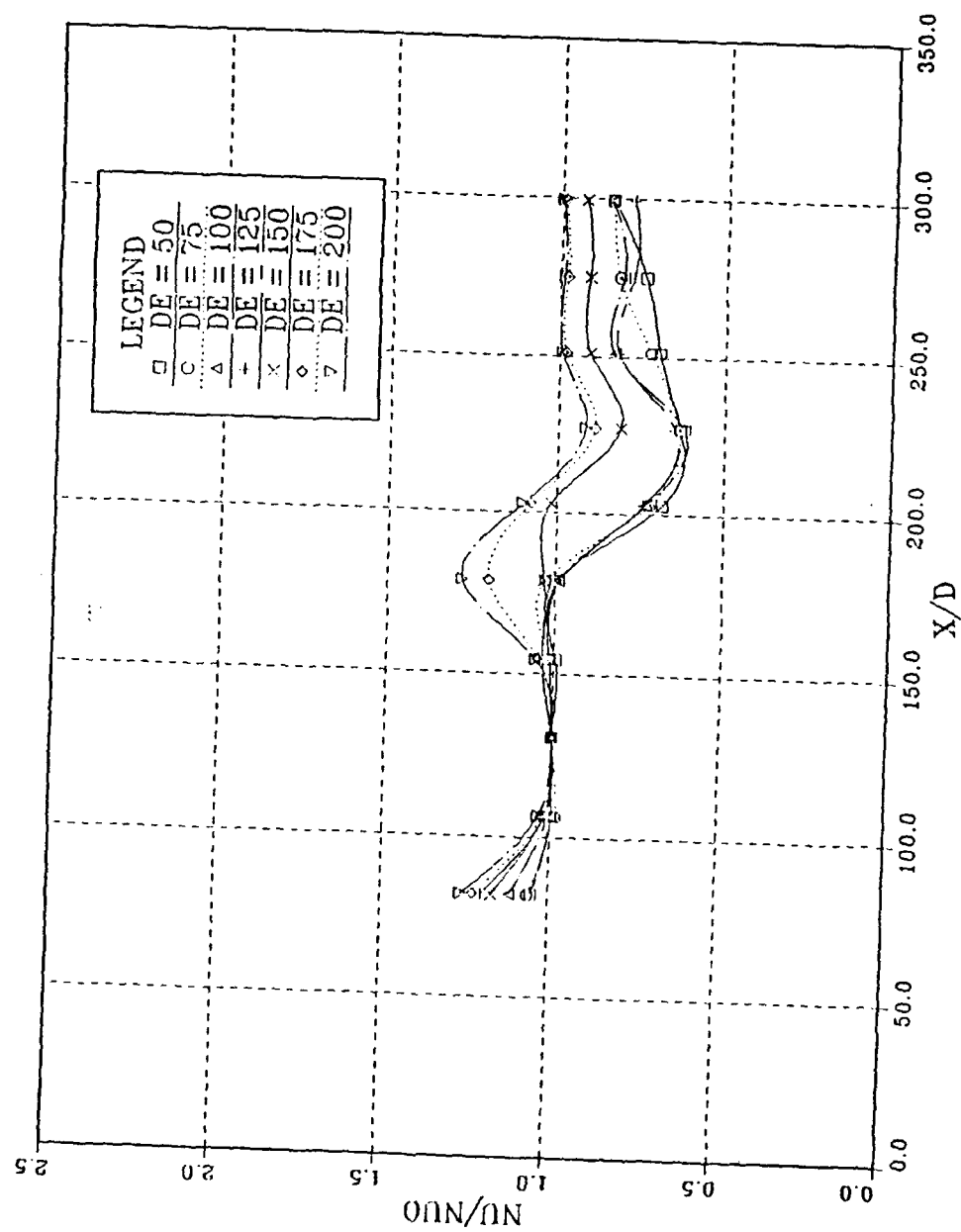
CONCAVE SURFACE

Figure 40. Nu/Nuo vs. x/d, Concave Surface, All Dean Numbers

76
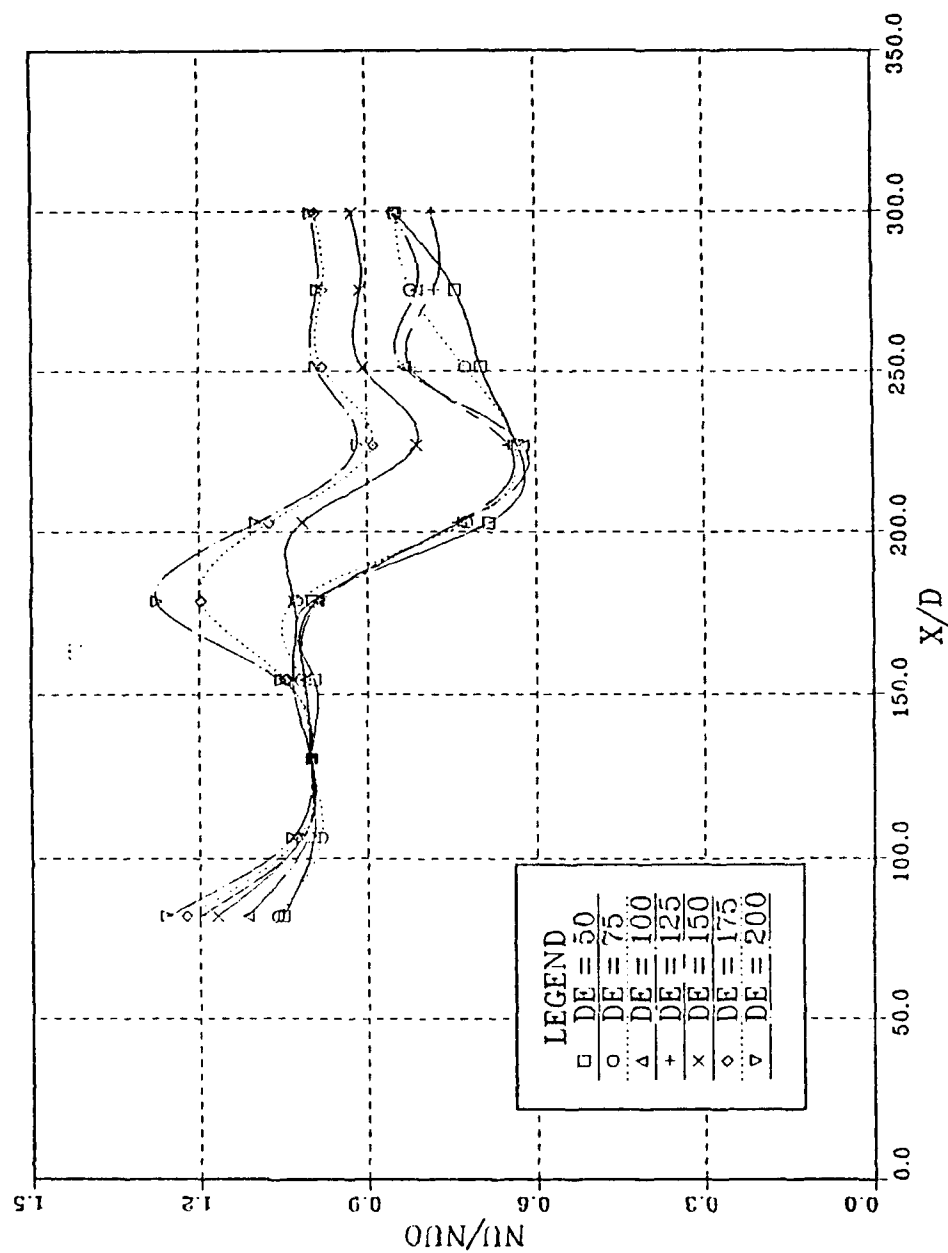
Figure 41. Nu/Nuo vs. x/d, Concave Surface, All Dean Numbers

77
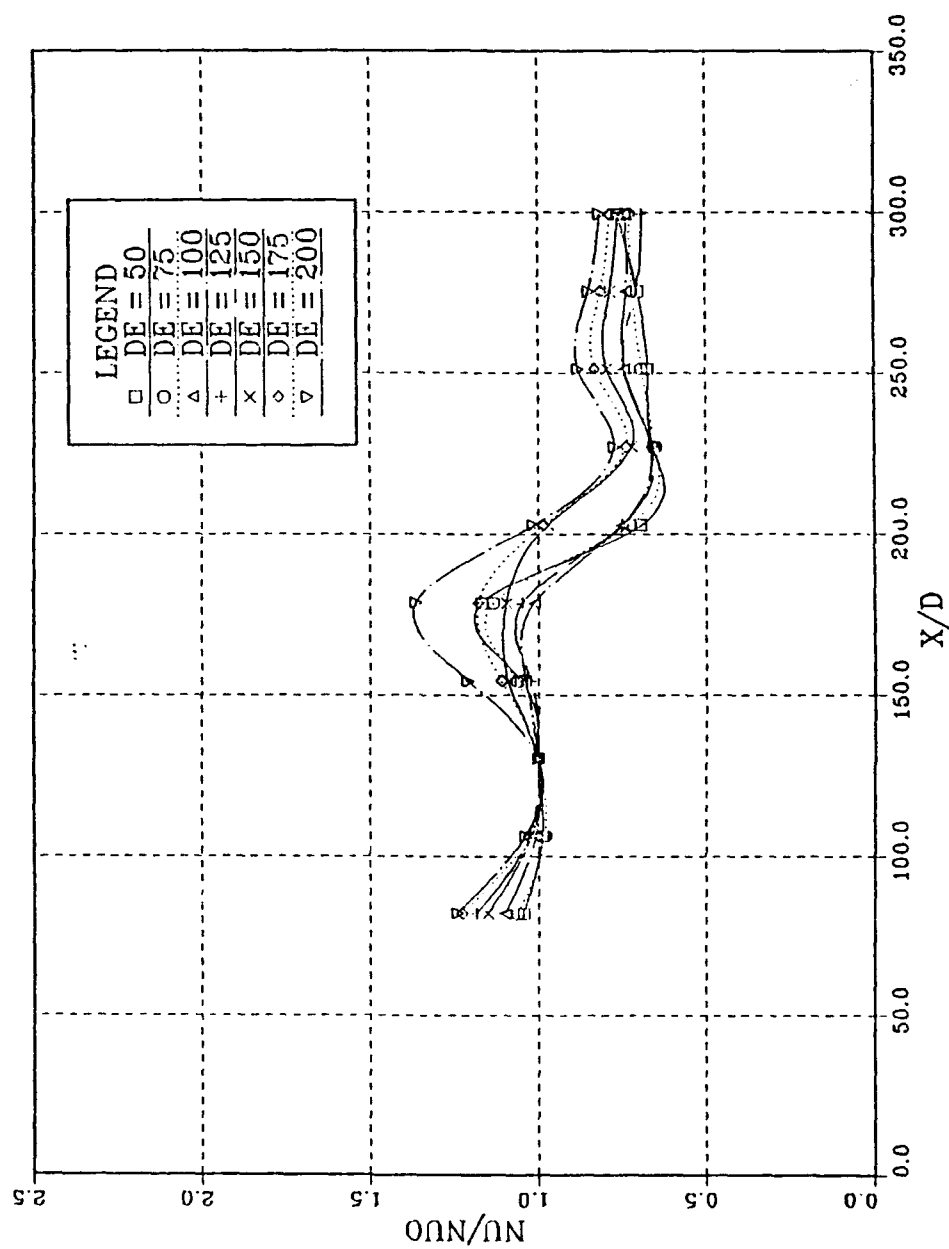
CONVEX SURFACE

Figure 42. Nu/Nuo vs. x/d, Convex Surface, All Dean Numbers

78
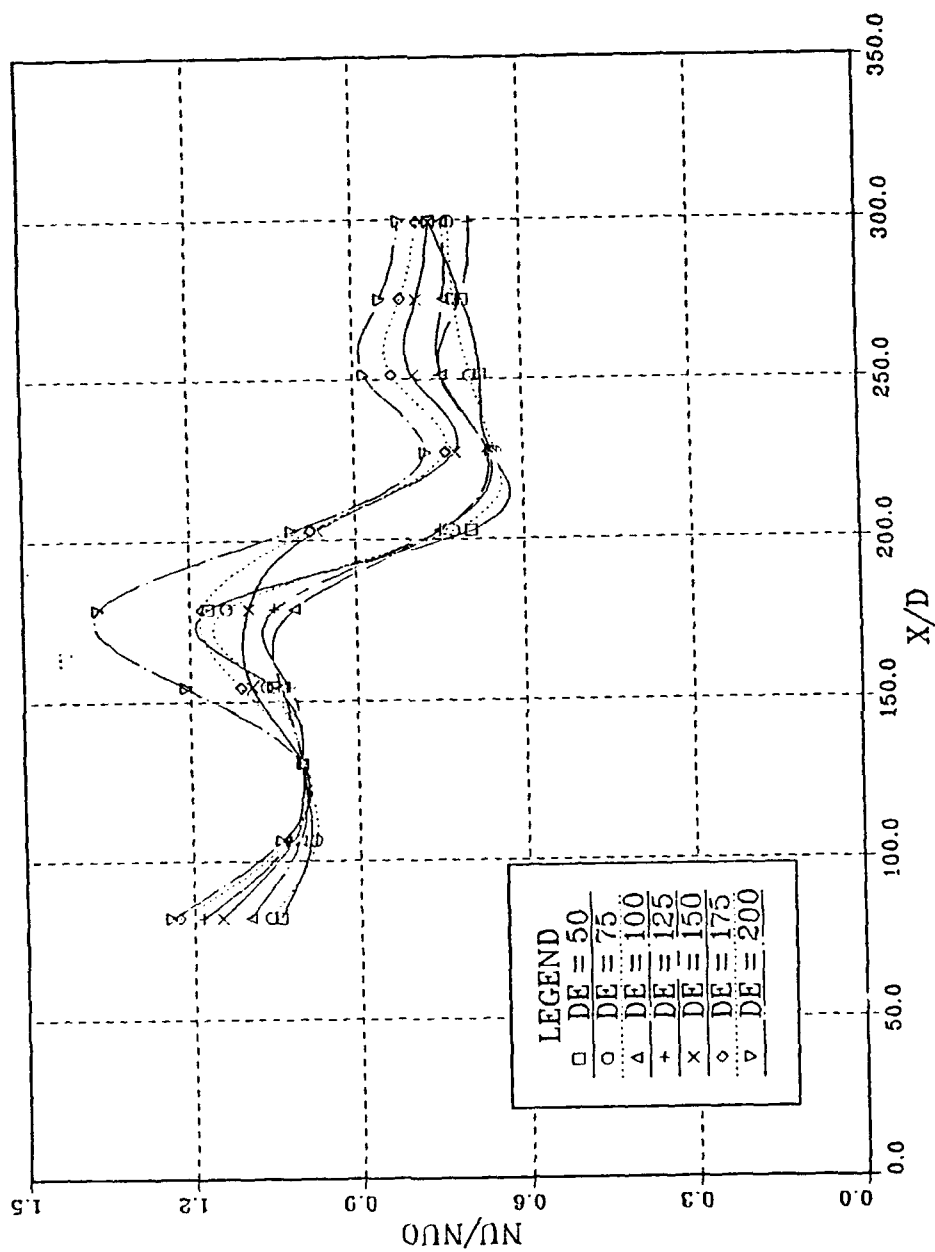
CONVEX SURFACE

Figure 43. Nu/Nuo vs. x/d, Convex Surface, All Dean Numbers

79
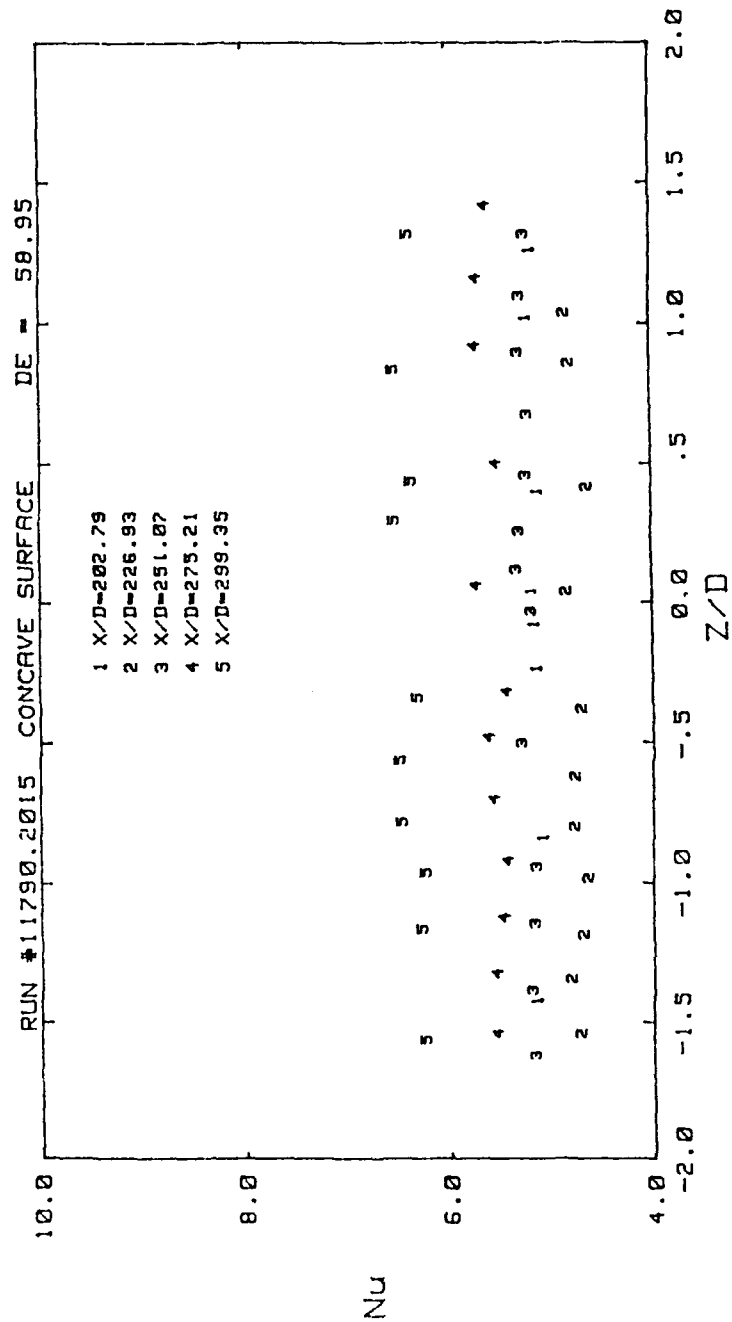
Figure 44. Spanwise Nusselt Number Distributions vs. z/d For
Curved Concave Surface, De = 58.9

80
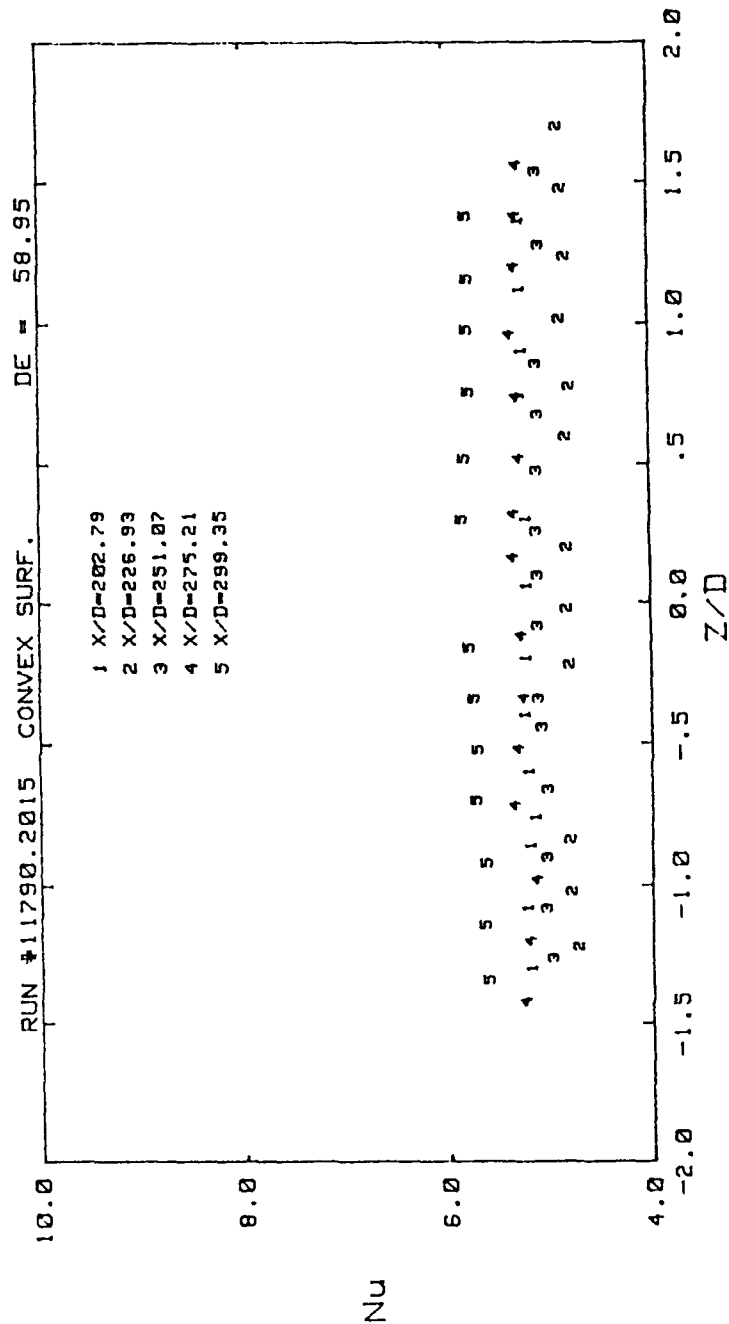
Figure 45. Spanwise Nusselt Number Distributions vs. z/d For Curved Convex Surface, De = 58.9

81
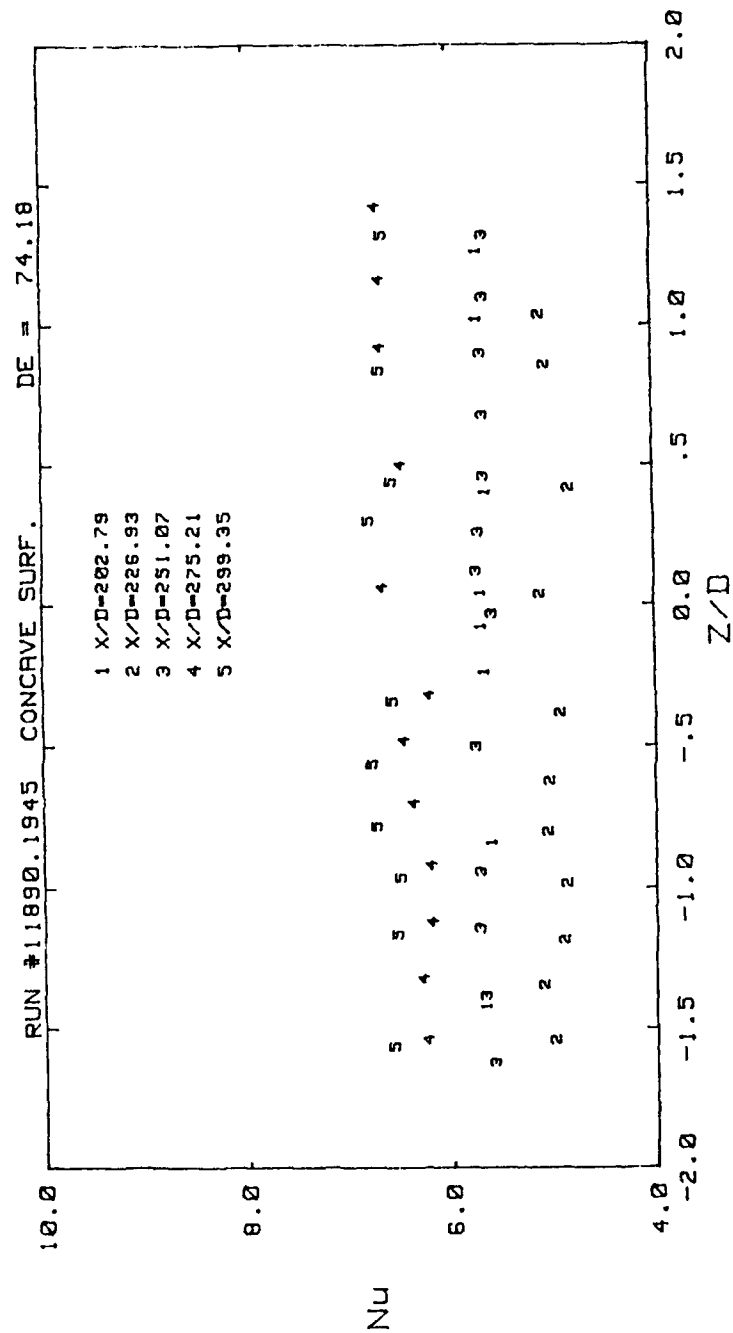
Figure 46. Spanwise Nusselt Number Distributions vs. z/d For Curved Concave Surface, De = 74.2
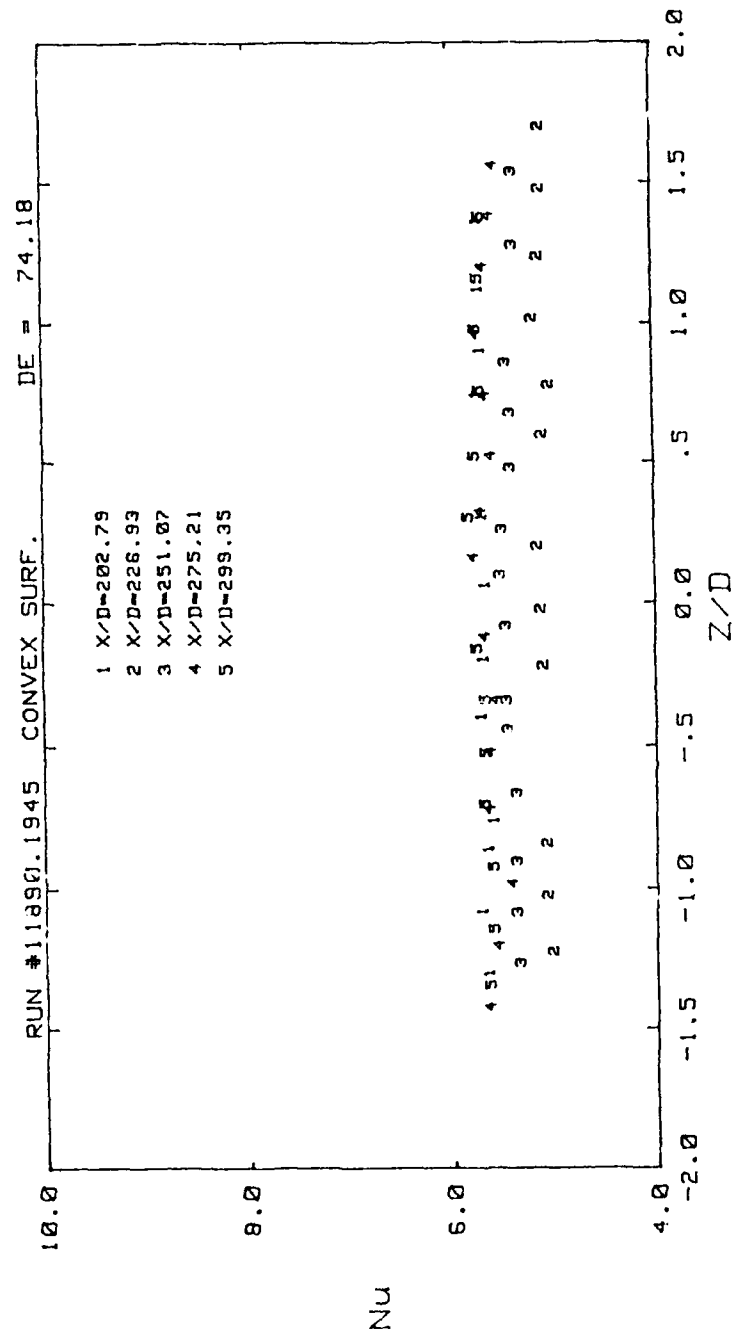
Figure 47. Spanwise Nusselt Number Distributions vs z/d For
Curved Convex Surface, De = 74.2

83
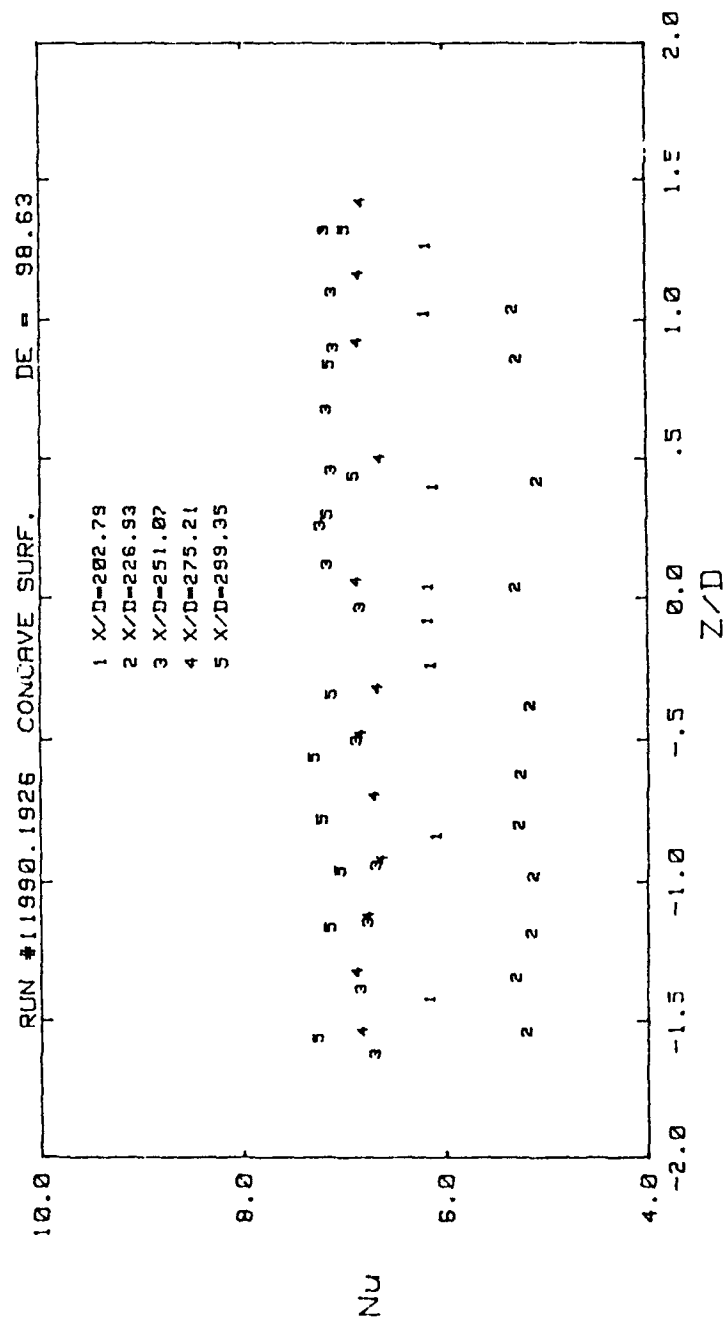
Figure 48. Spanwise Nusselt Number Distributions vs. z/d For Curved Concave Surface, De = 98.6

84
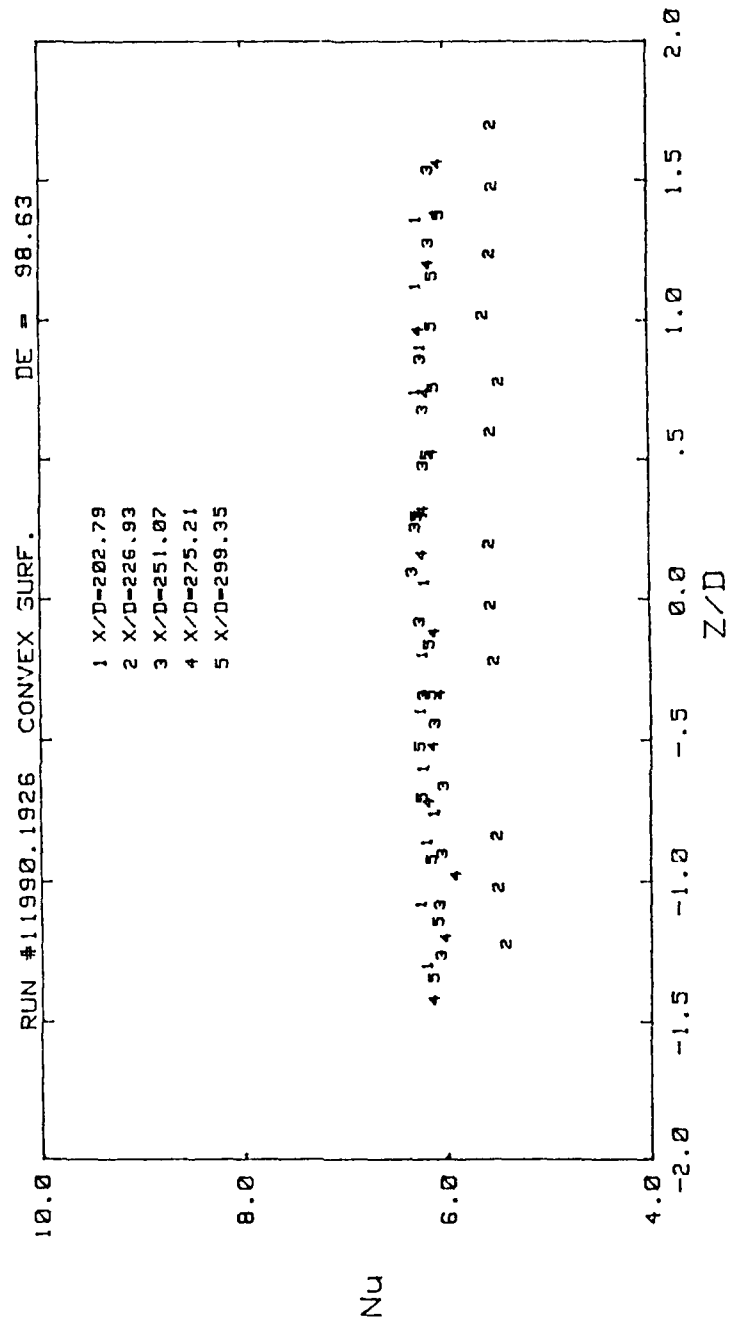
Figure 49. Spanwise Nusselt Number Distributions vs. z/d For Curved Convex Surface, De = 98.6

85
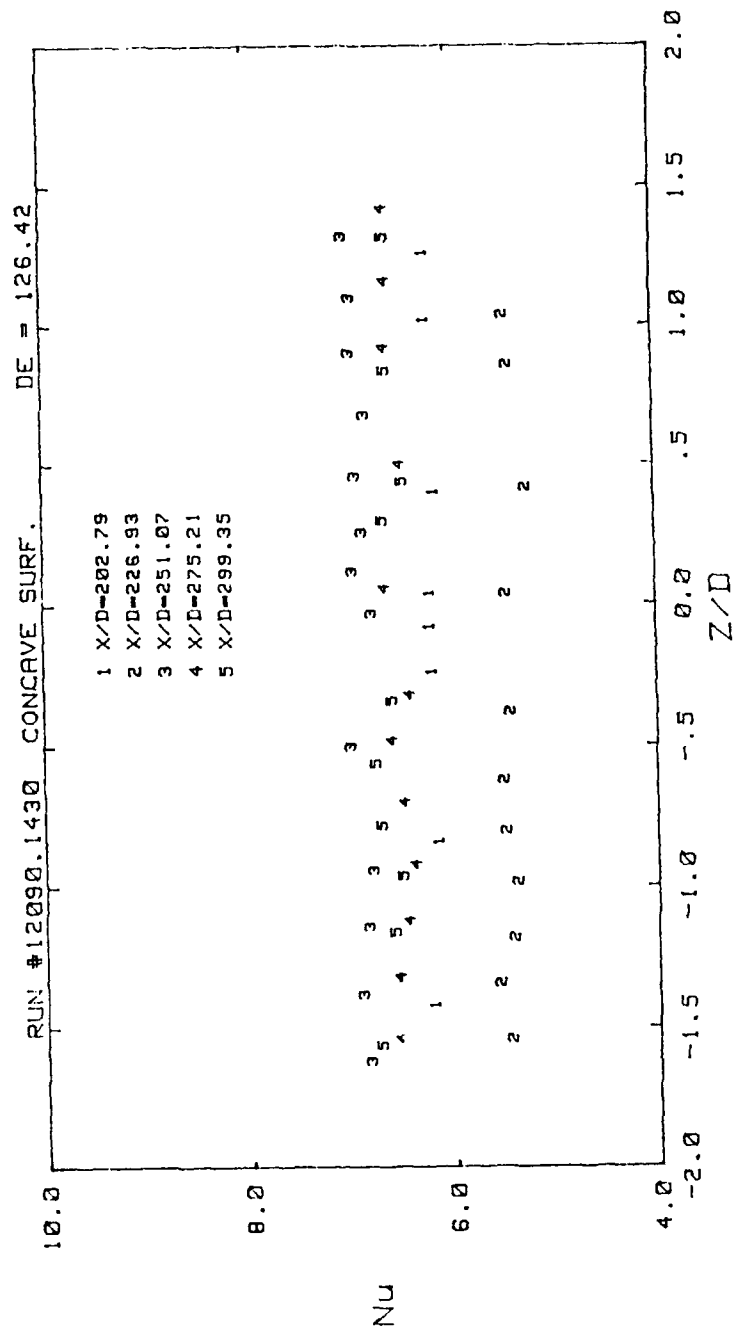
Figure 50. Spanwise Nusselt Number Distributions vs. z/d For
Curved Concave Surface, De = 126.4
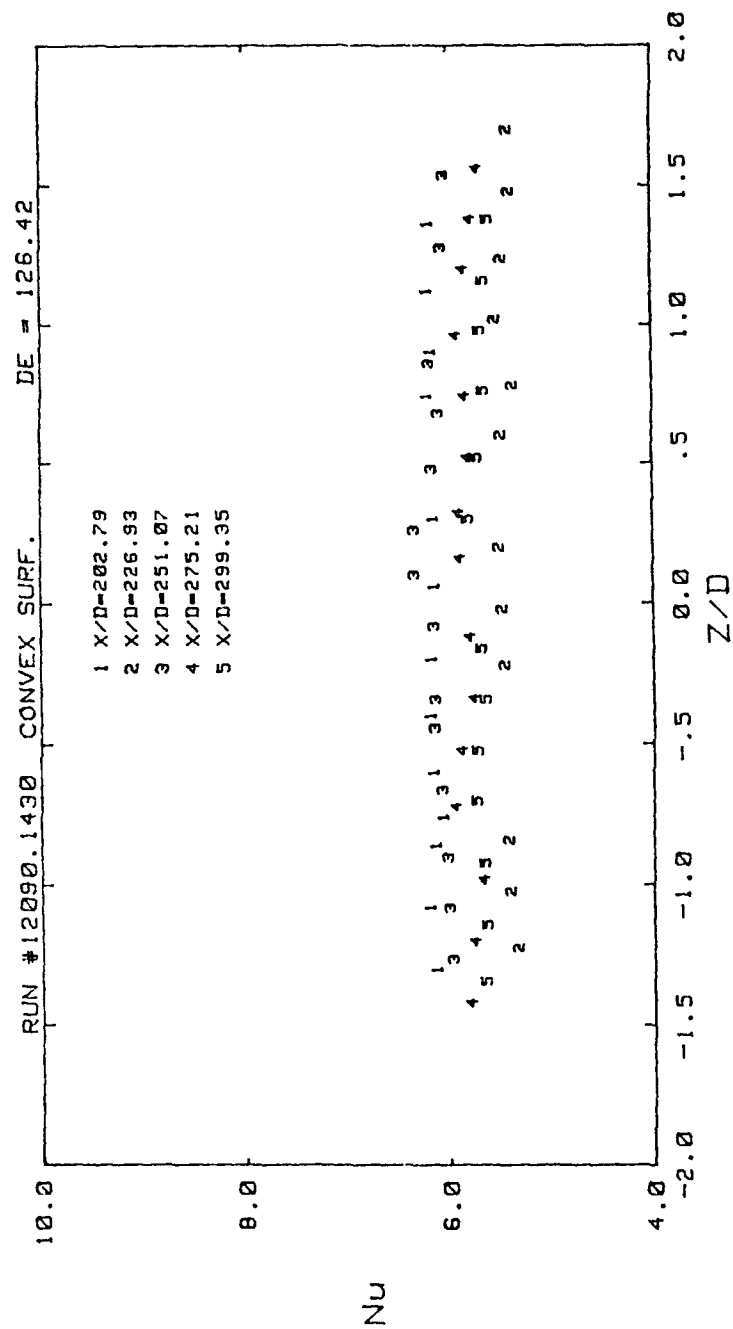
Figure 51. Spanwise Nusselt Number Distributions vs. z/d For Curved Convex Surface, De = 126.4

87
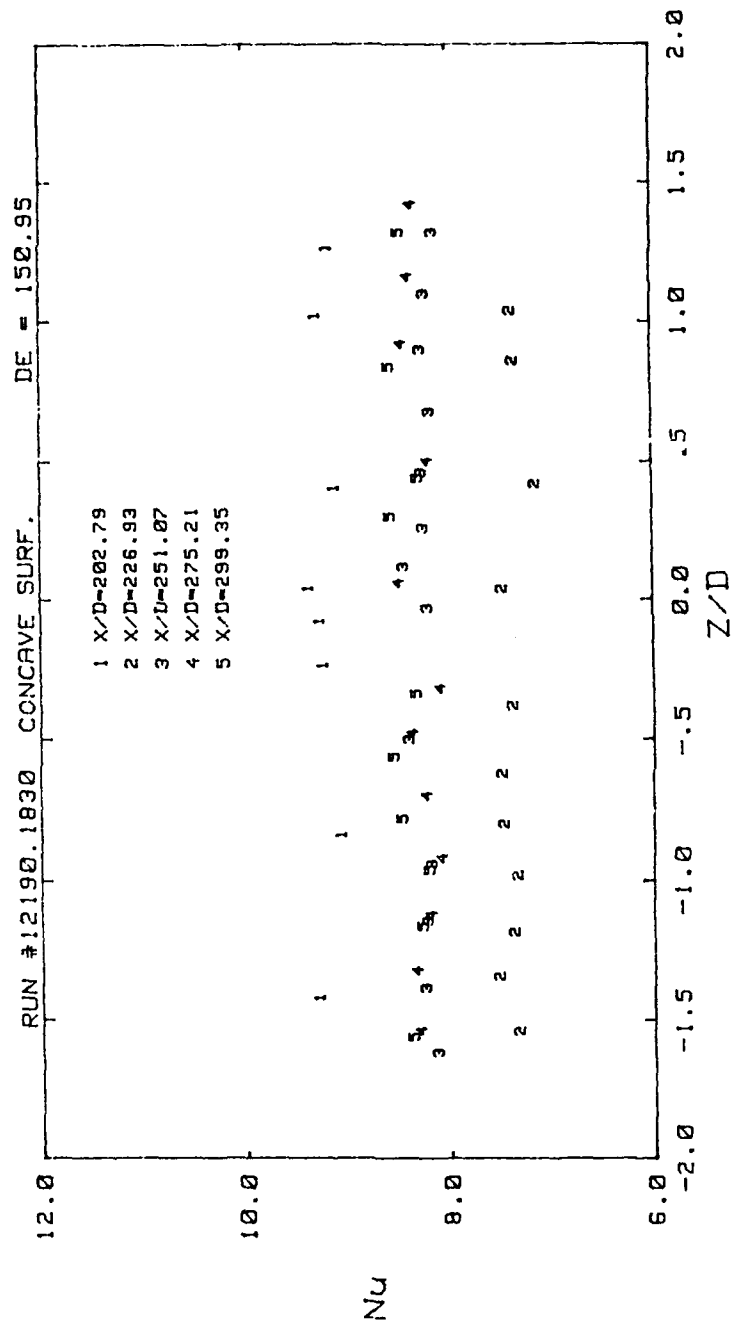
Figure 52. Spanwise Nusselt Number Distributions vs. z/d For Curved Concave Surface, De = 150.9

88
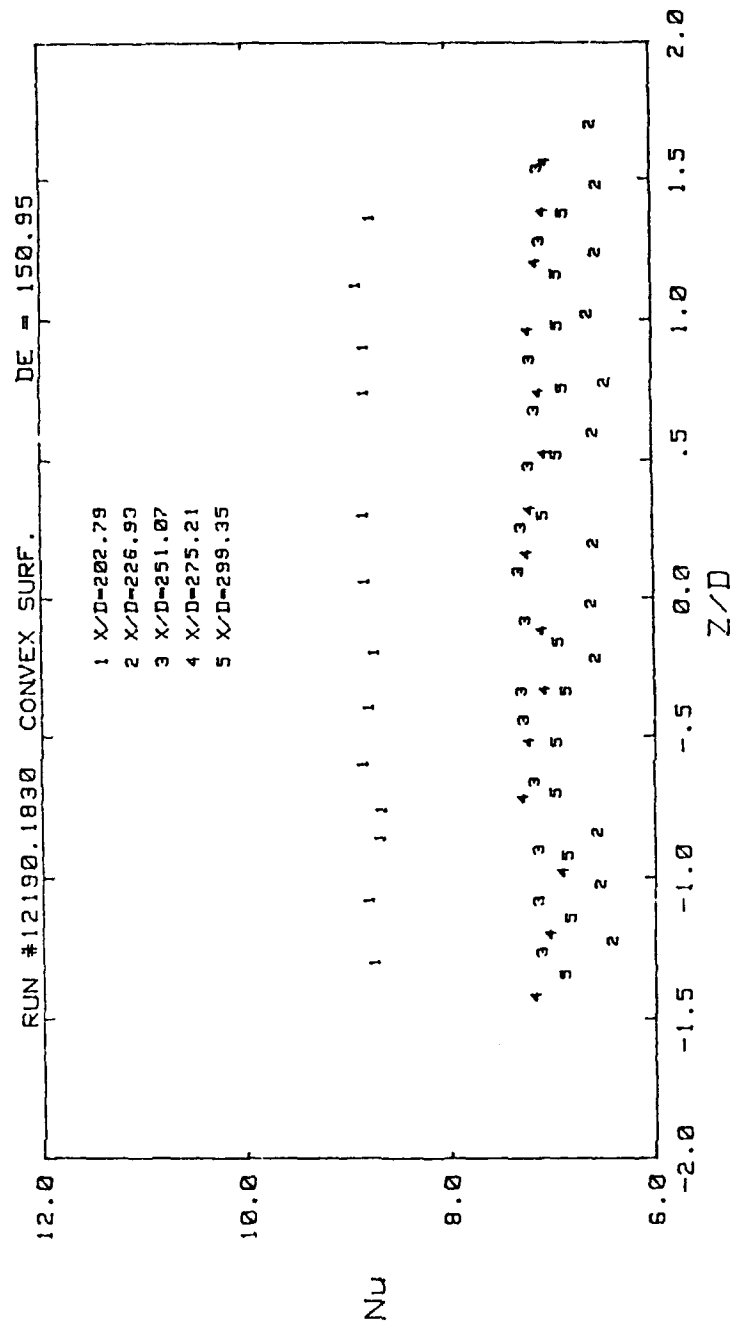
Figure 53. Spanwise Nusselt Number Distributions vs. z/d For
Curved Convex Surface, De = 150.9
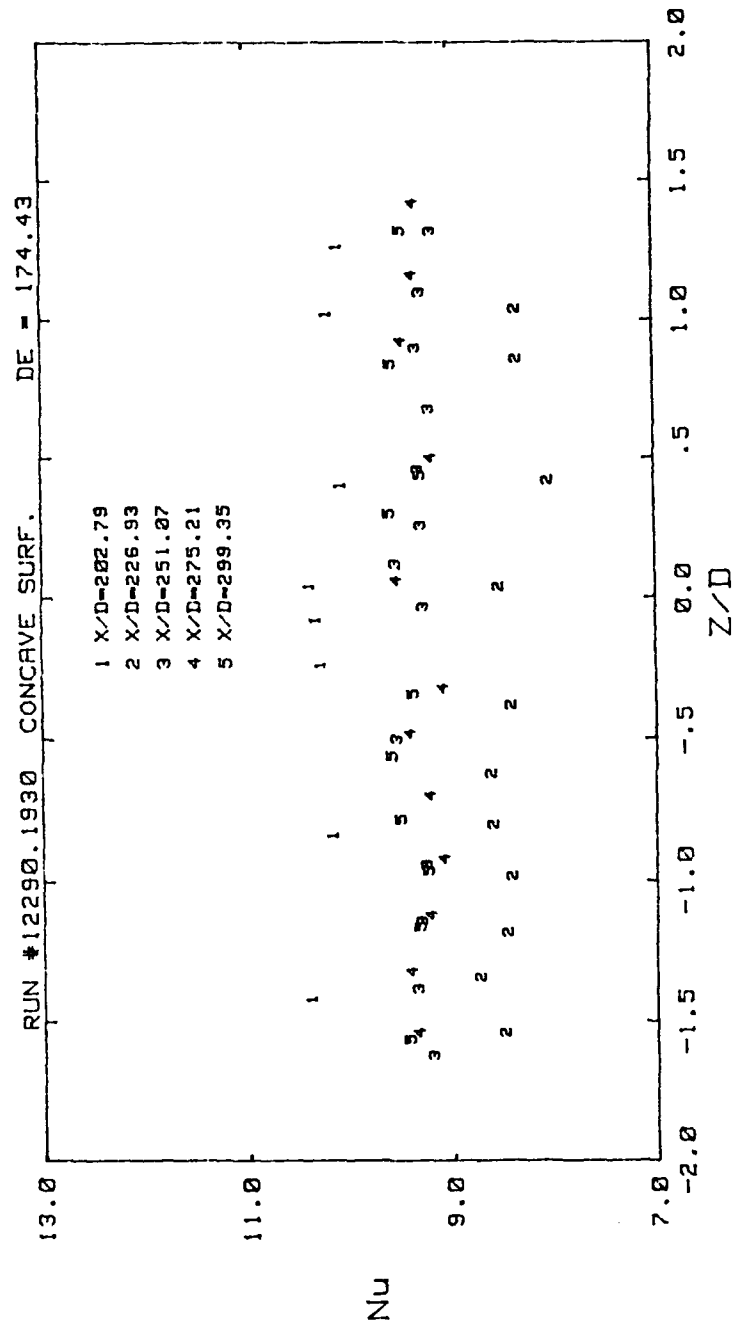
Figure 54. Spanwise Nusselt Number Distributions vs. z/d For Curved Concave Surface, De = 174.4

90
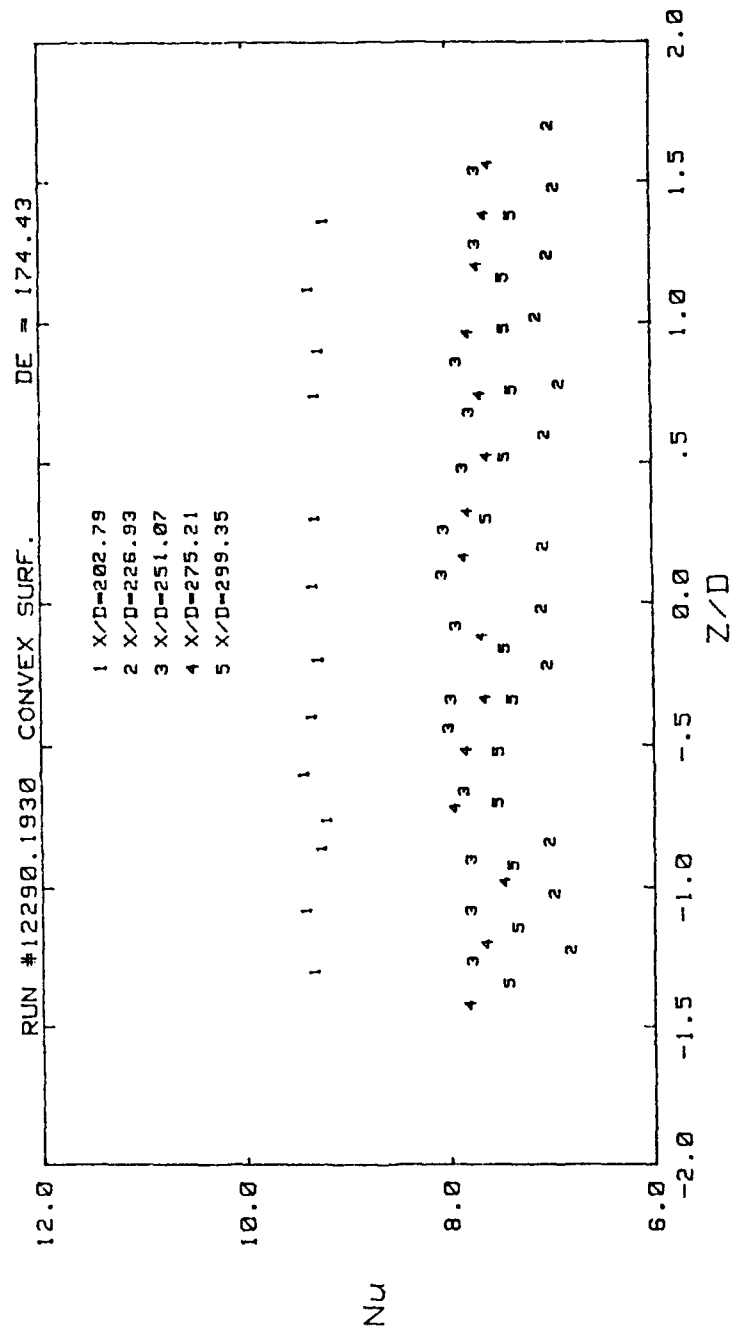
Figure 55. Spanwise Nusselt Number Distributions vs. z/d For
Curved Convex Surface, De = 174.4

91
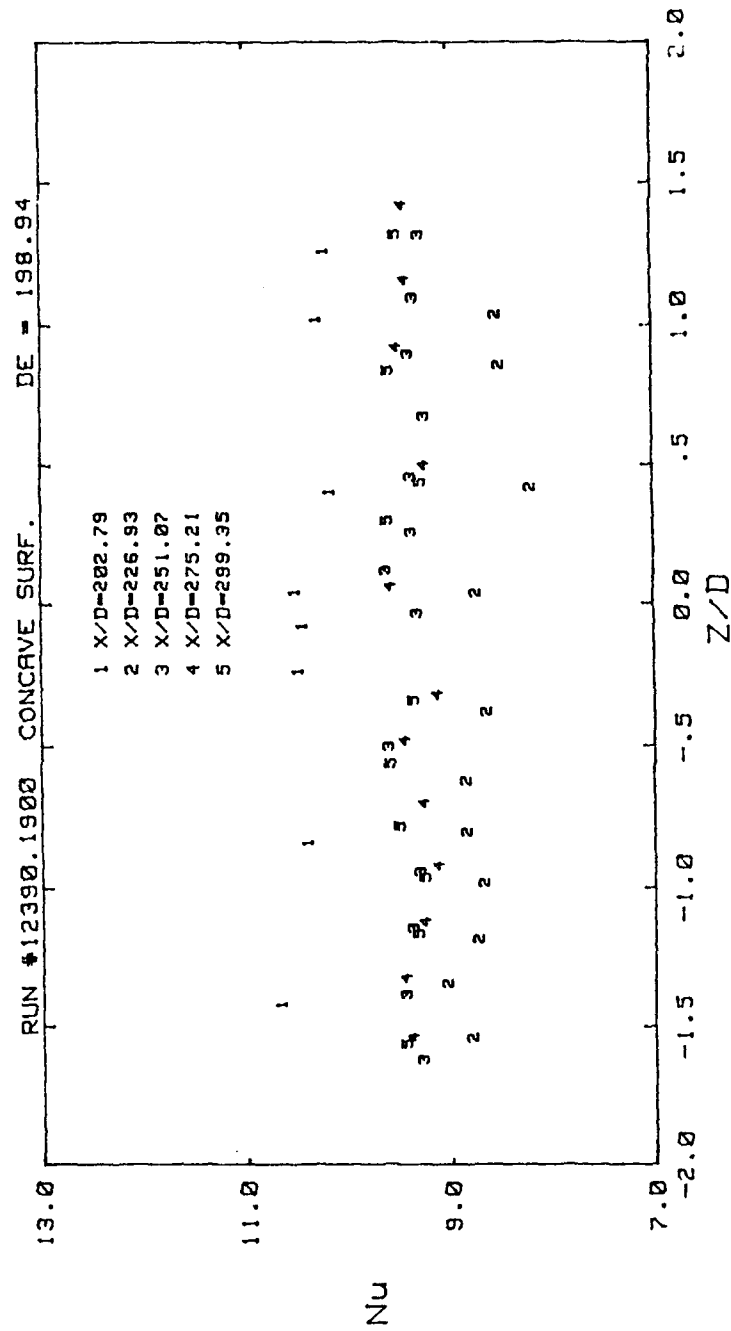
Figure 56. Spanwise Nusselt Number Distributions vs. z/d For
Curved Concave Surface, De = 198.9

92
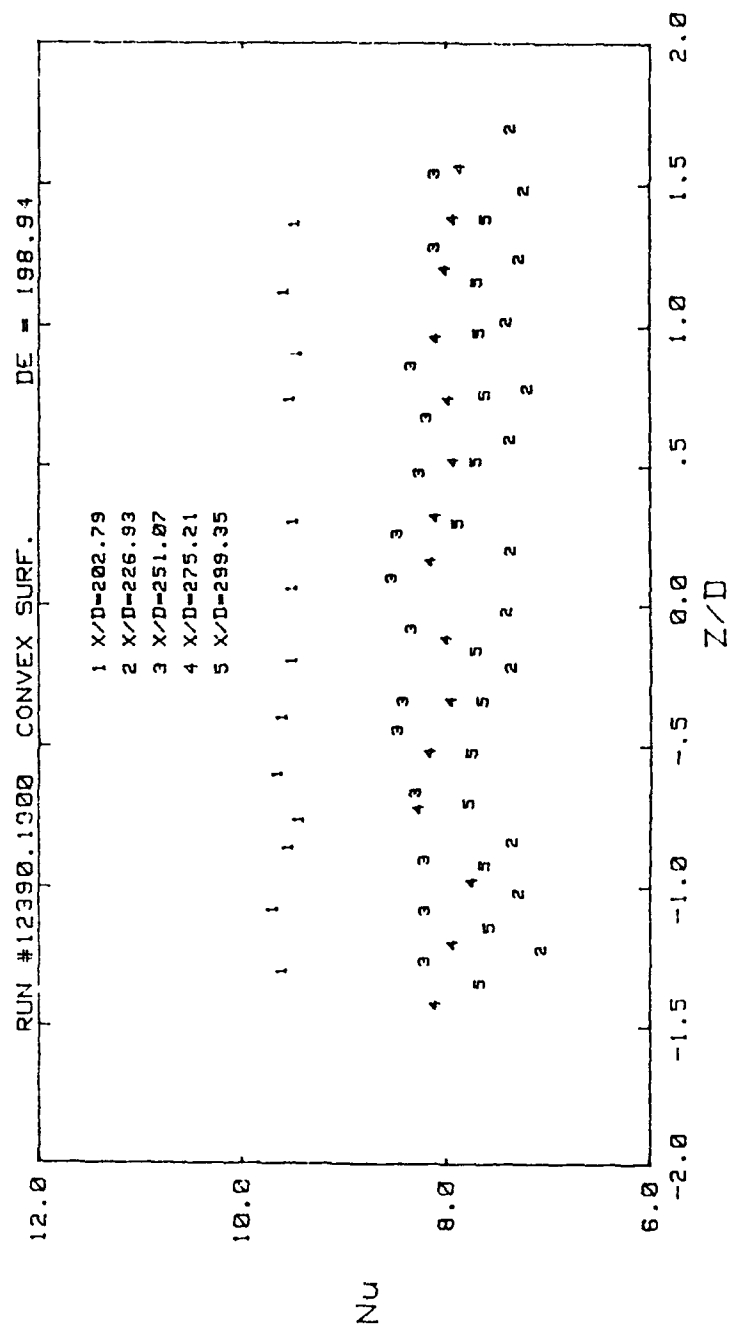
Figure 57. Spanwise Nusselt Number Distributions vs. z/d For
Curved Convex Surface, De = 198.9

93
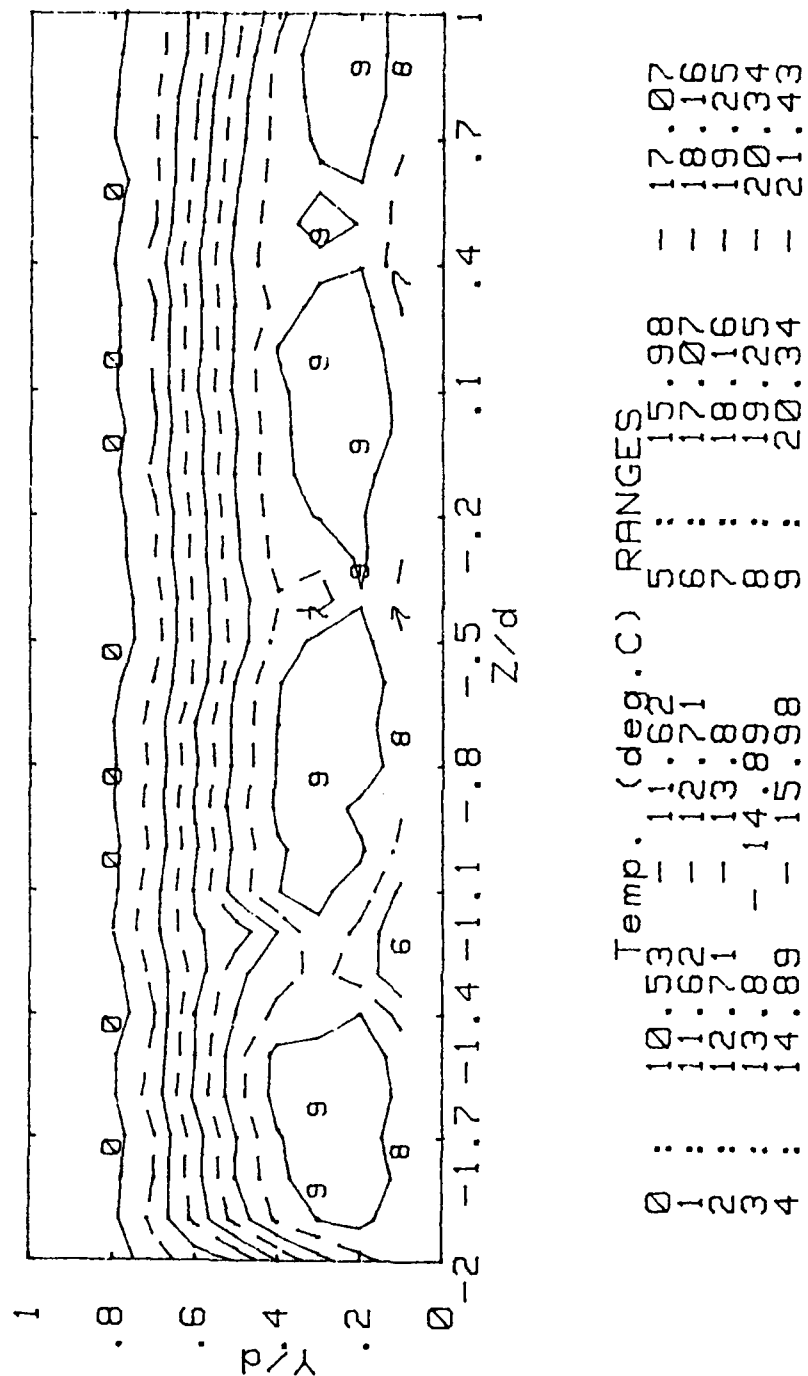
Figure 58. Measured Exit Local Mean Temperature Contours.
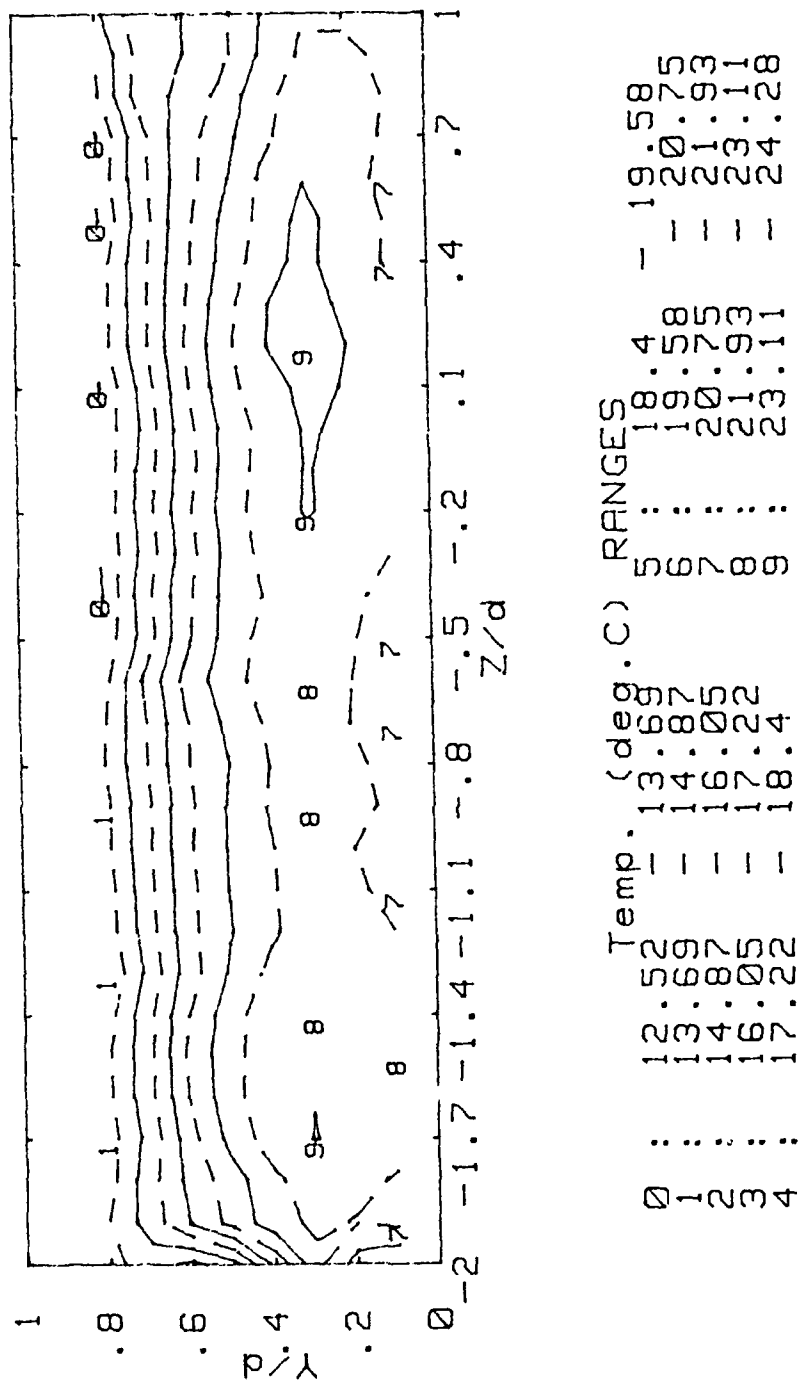De = 58.5

94
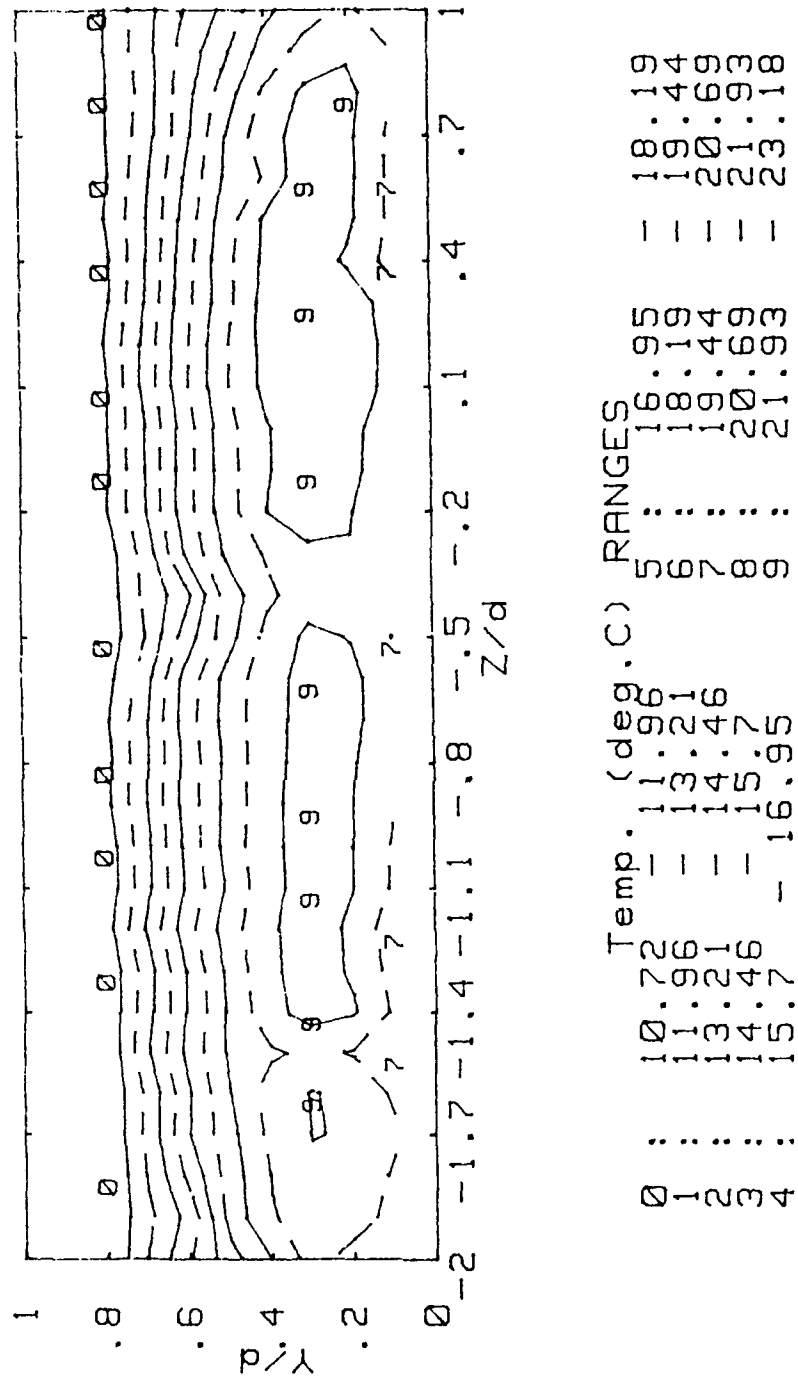
Figure 59. Measured Exit Local Mean Temperature Contours.
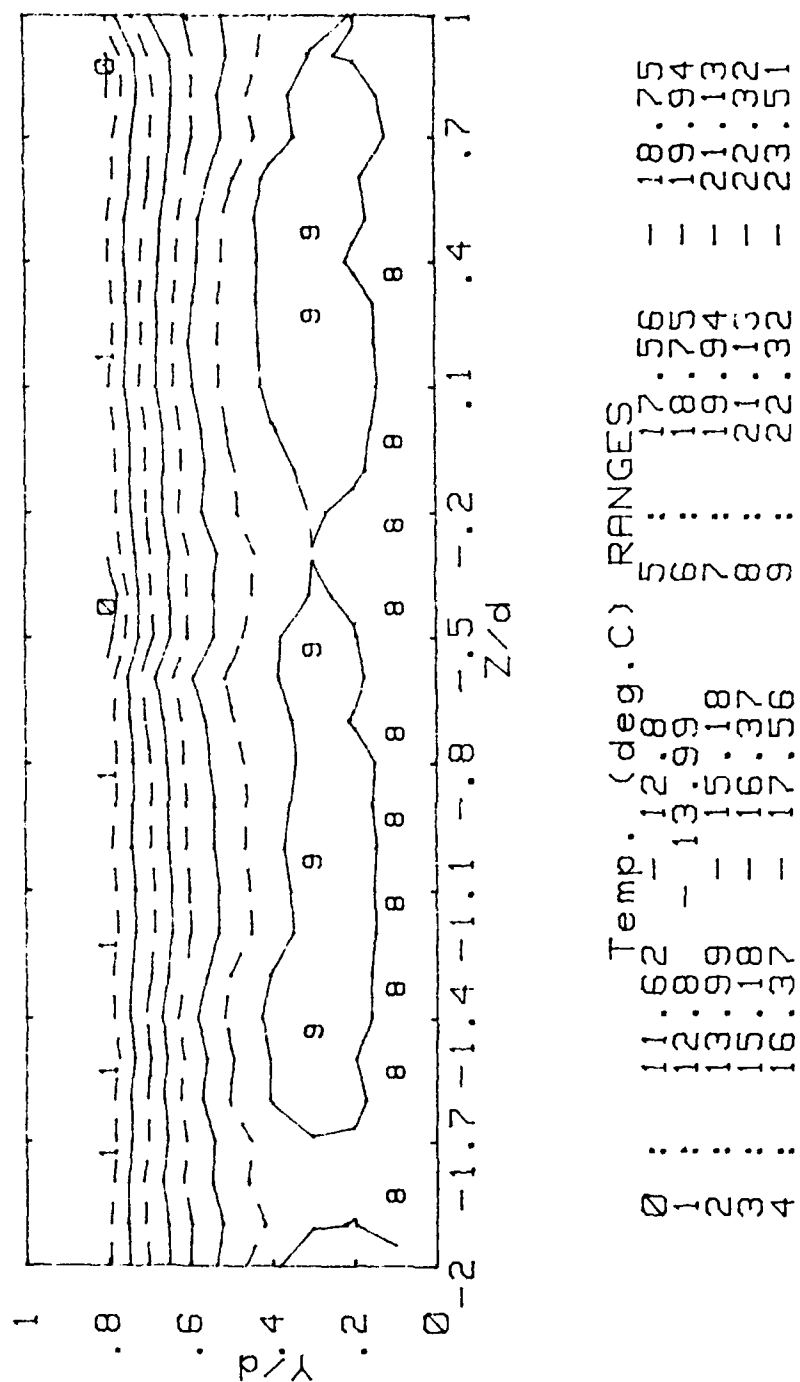De = 73.7

Figure 60. Measured Exit Local Mean Temperature Contours.
De = 98.1

Figure 61. Measured Exit Local Mean Temperature Contours.
De = 126.0

97
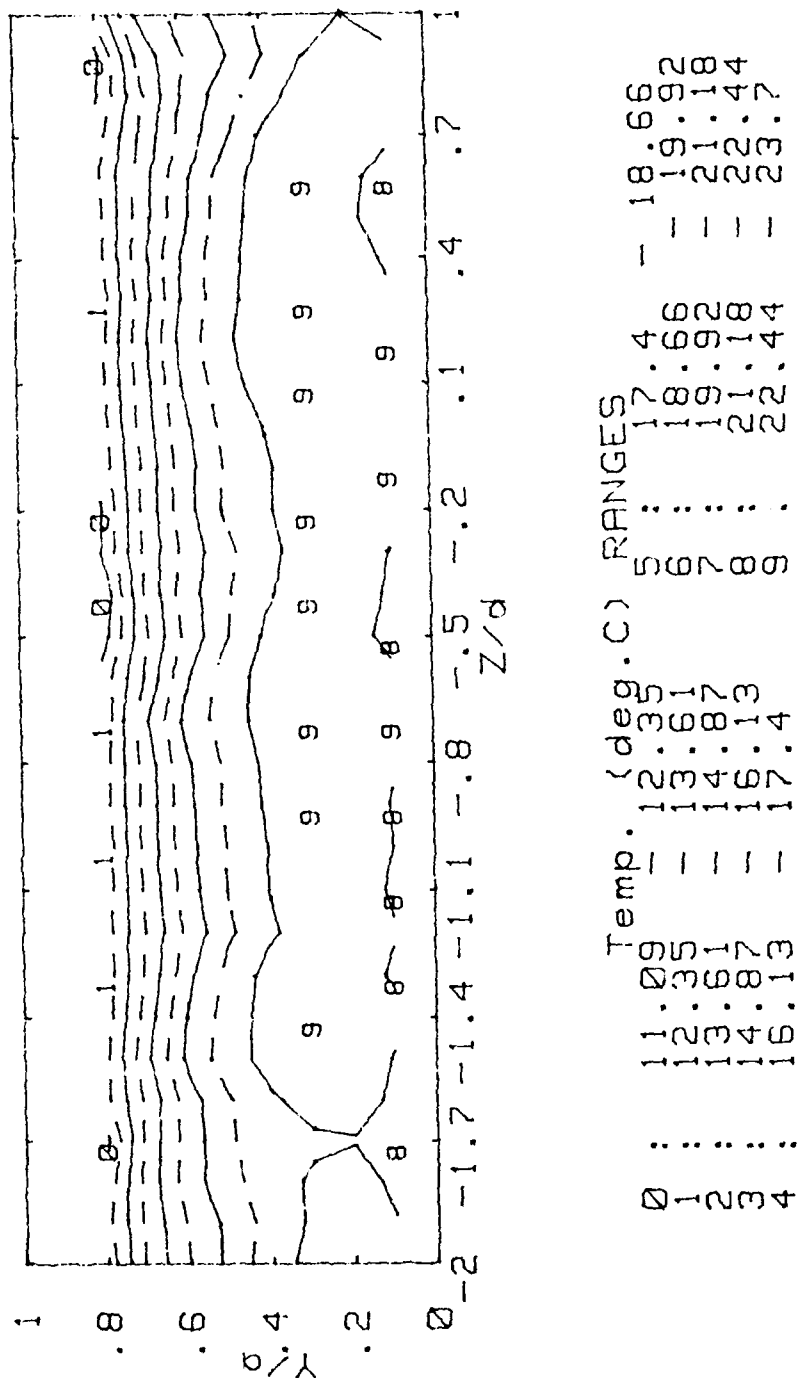
Figure 62. Measured Exit Local Mean Temperature Contours.
De = 149.8
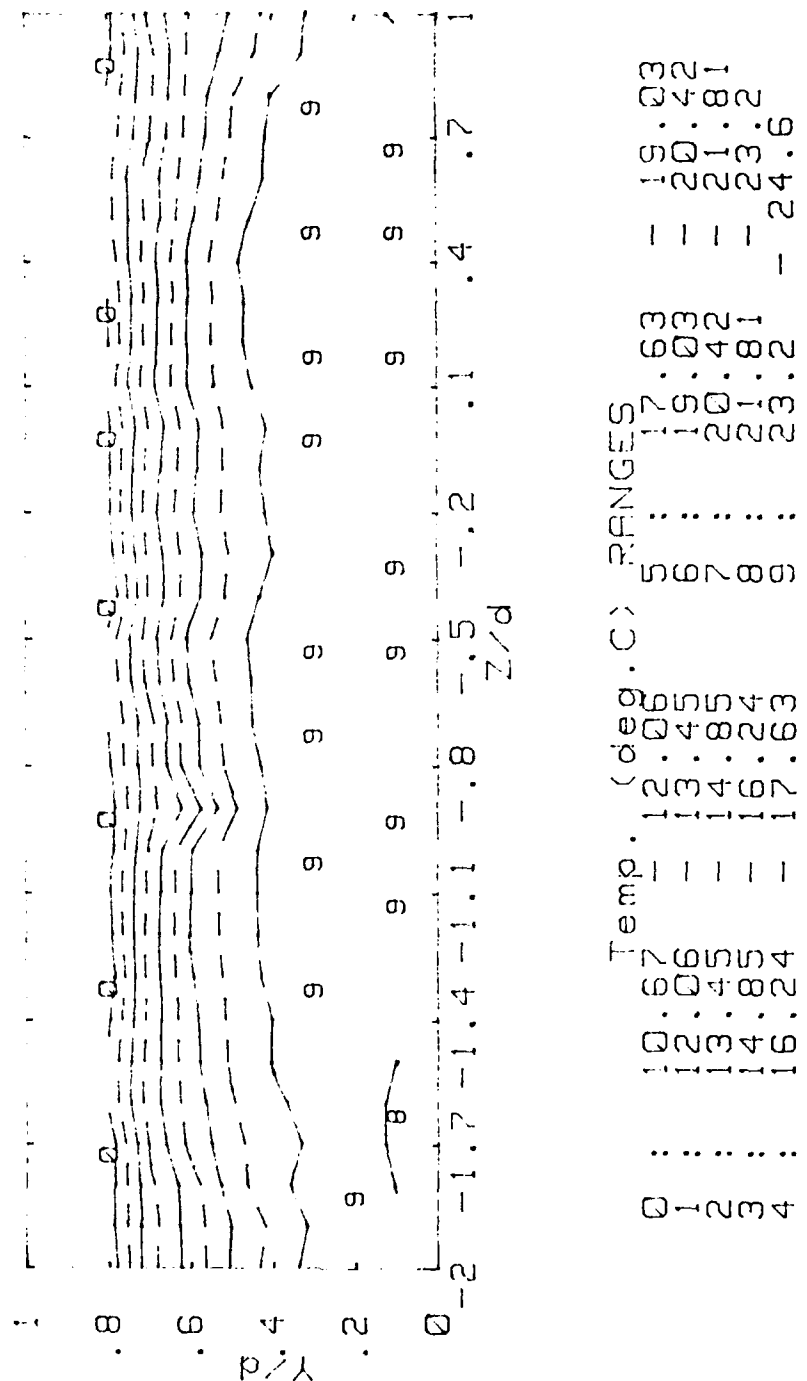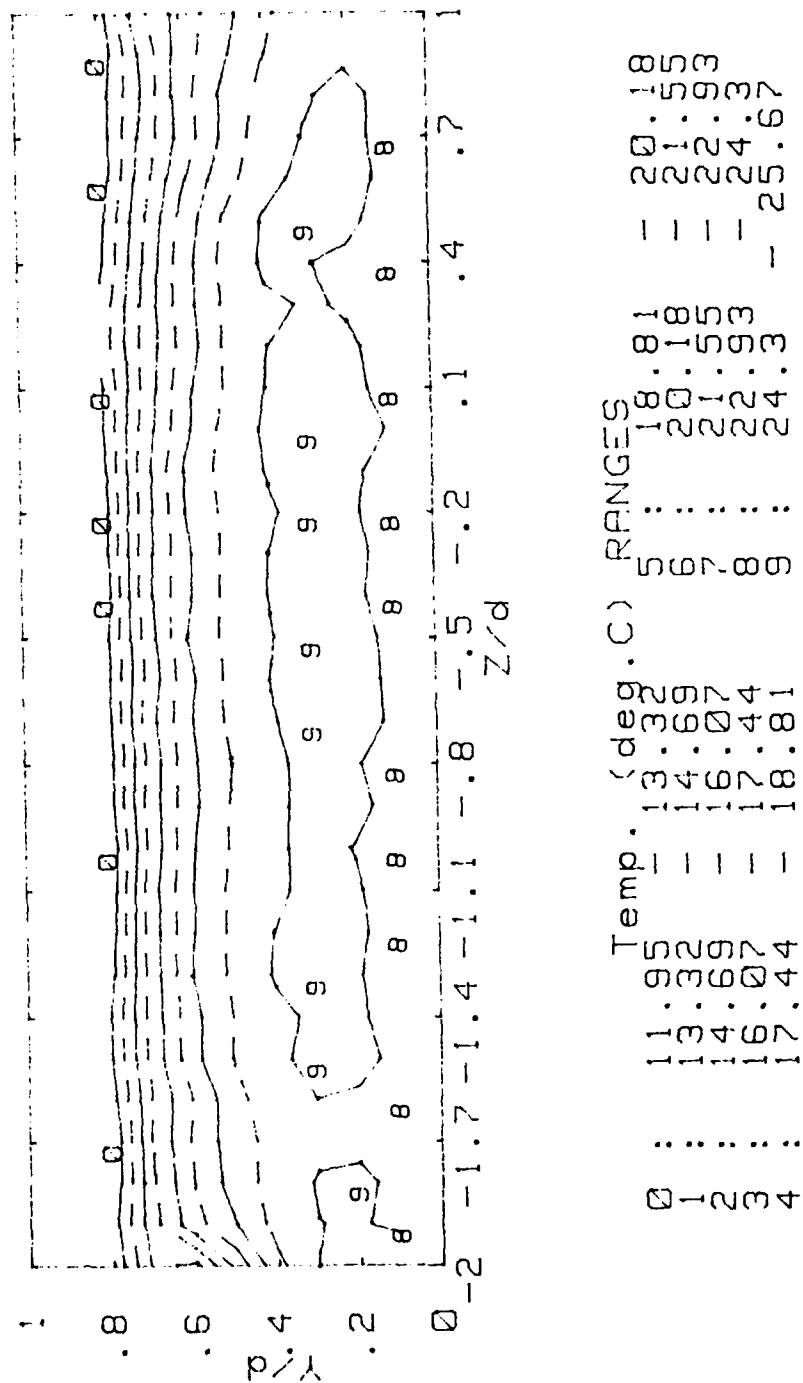
Figure 63. Measured Exit Local Mean Temperature Contours.
De = 173.5

99

Figure 64. Measured Exit Local Mean Temperature Contours.
De = 198.4

100
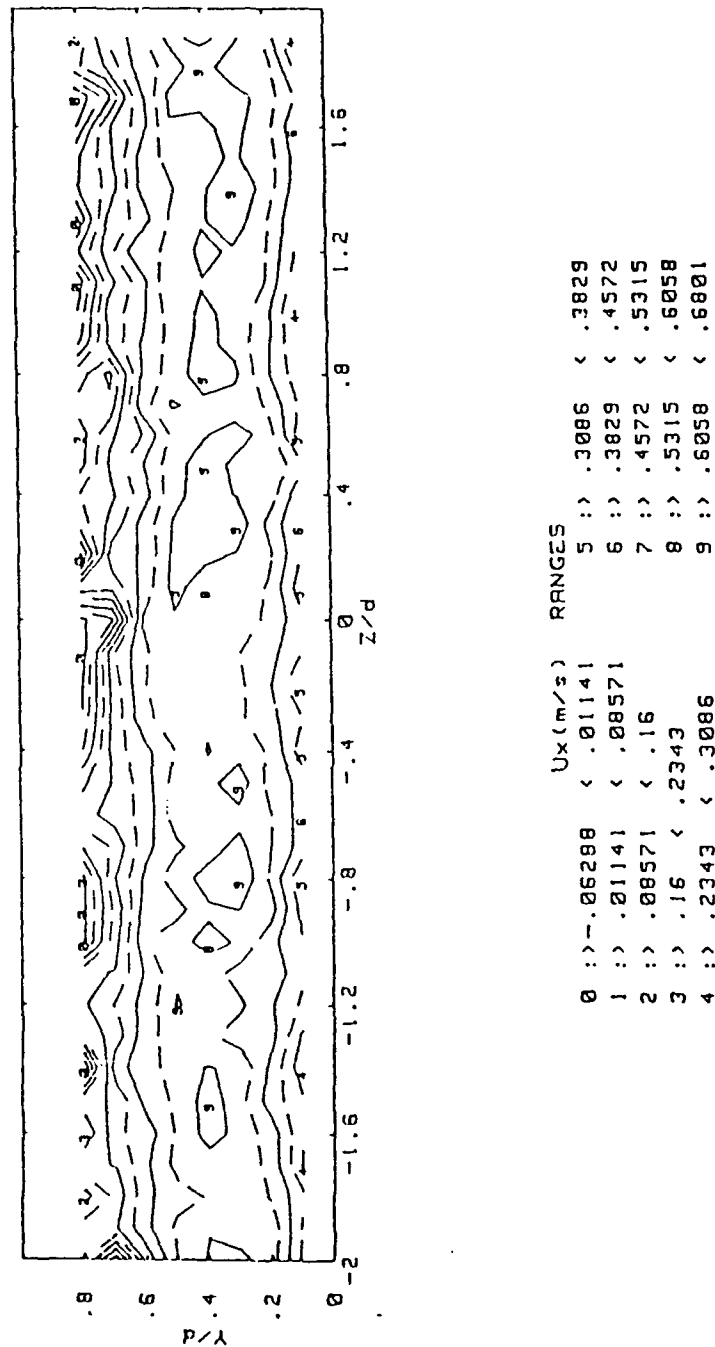
Figure 65. Mean Velocity Contours, De = 50
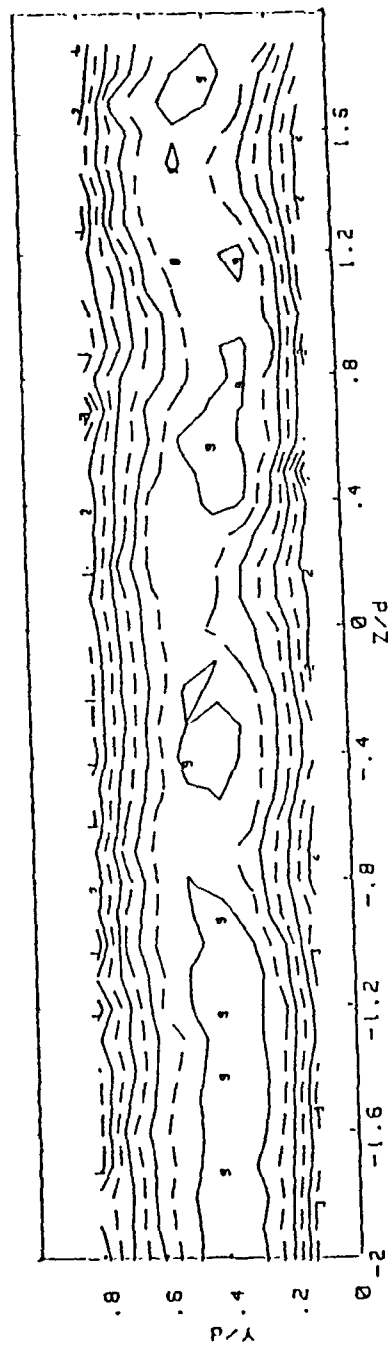
101

Figure 66. Mean Velocity Contours, De = 75
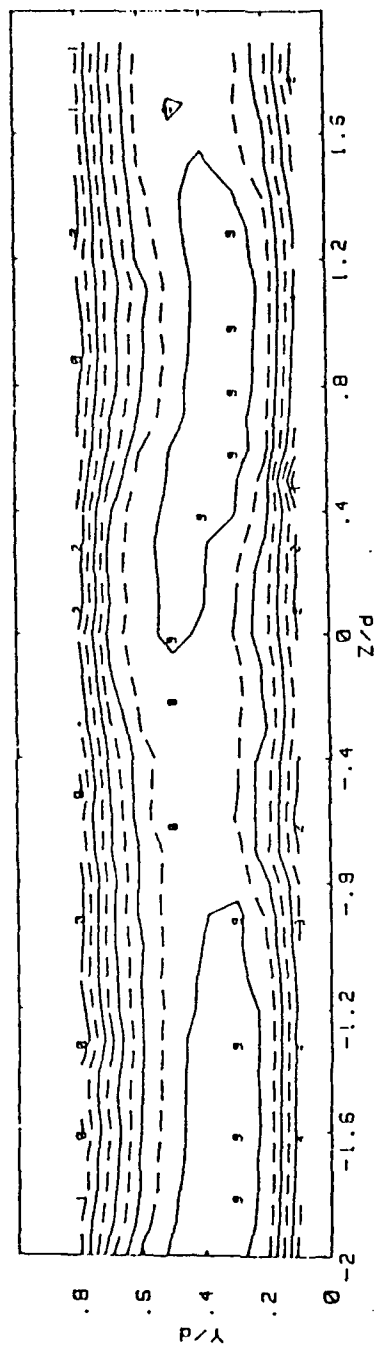
102

Figure 67. Mean Velocity Contours, De = 100
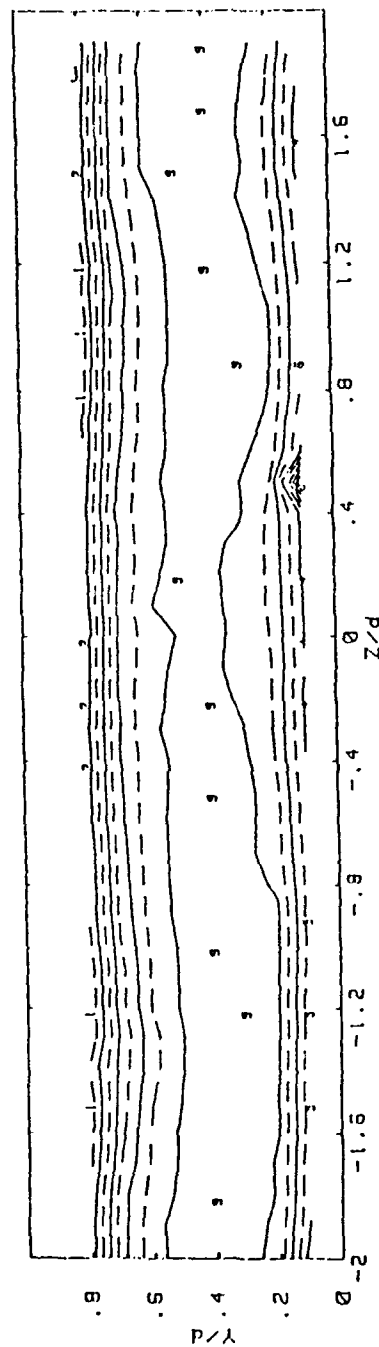
Figure 68. Mean Velocity Contours, De = 150
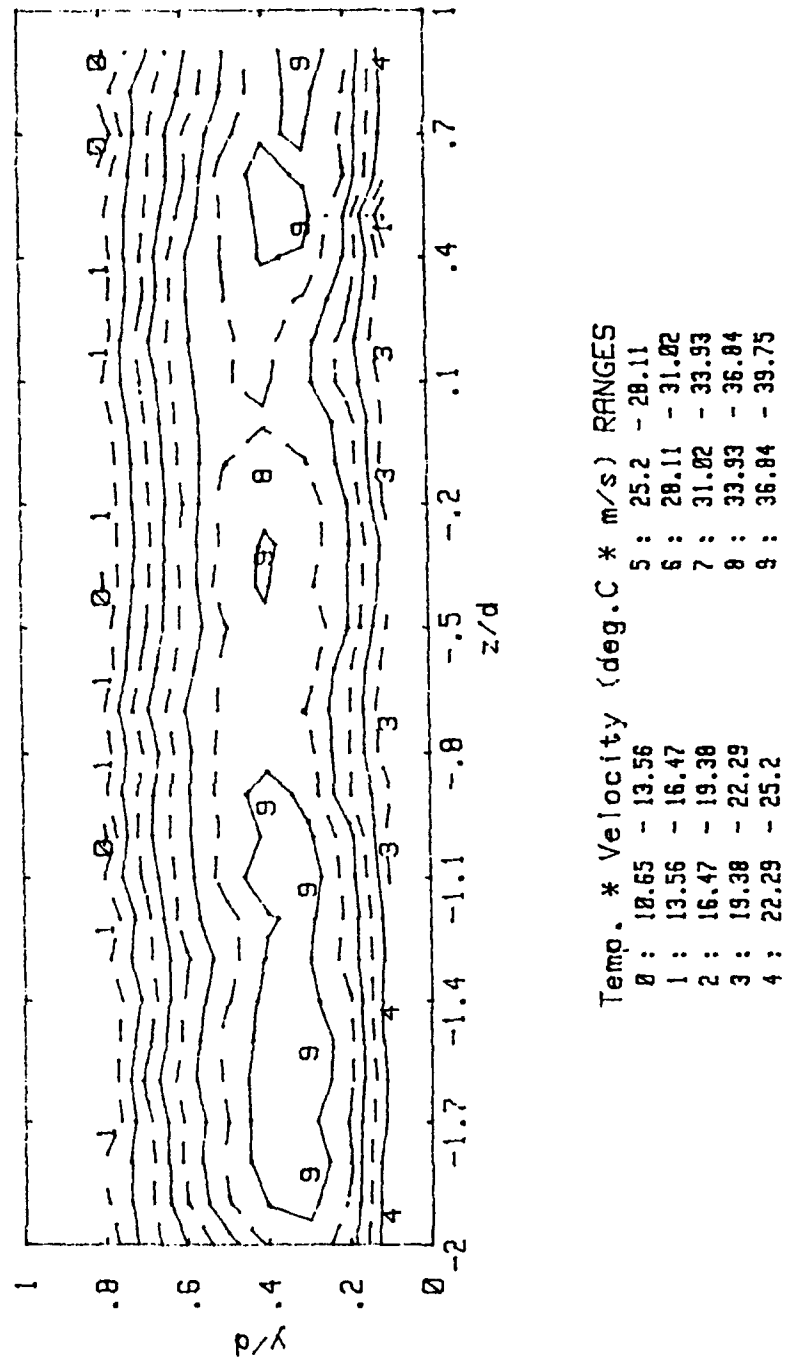
Figure 69. Mean Temperature/Mean Velocity Product Contours,
De = 58.5

105

RUN #11890.1945   De = 73.66
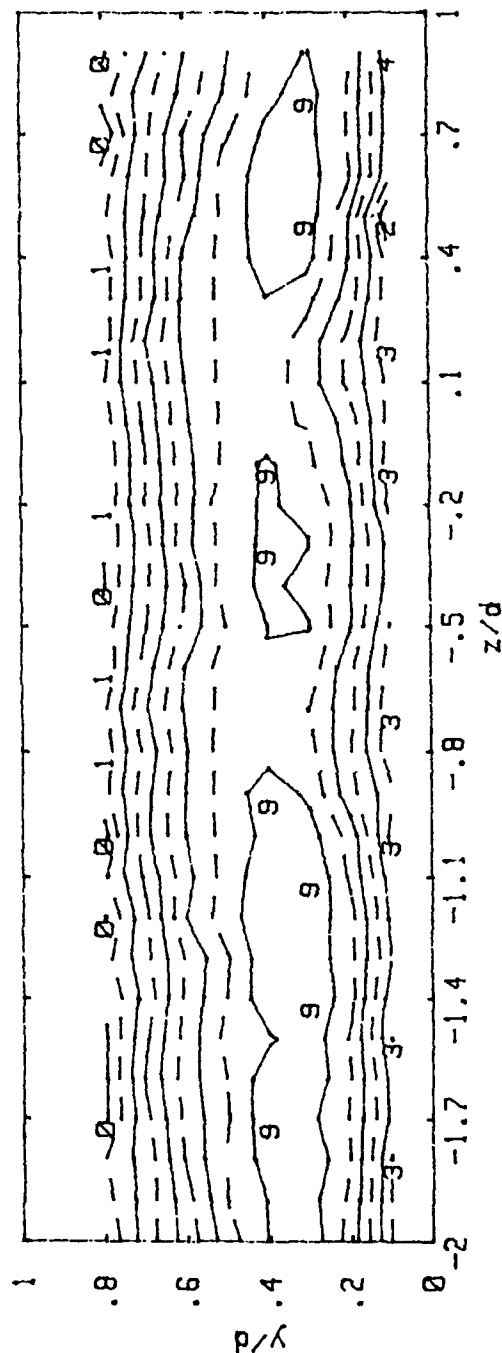
Temp. * Velocity (deg.C * m/s) RANGES

0 : 10.69 - 13.71   5 : 25.81 - 28.83
1 : 13.71 - 16.74   6 : 28.83 - 31.86
2 : 16.74 - 19.76   7 : 31.86 - 34.88
3 : 19.76 - 22.78   8 : 34.88 - 37.9
4 : 22.78 - 25.81   9 : 37.9 - 40.93

Figure 70. Mean Temperature/Mean Velocity Product Contours,
De = 73.7

106
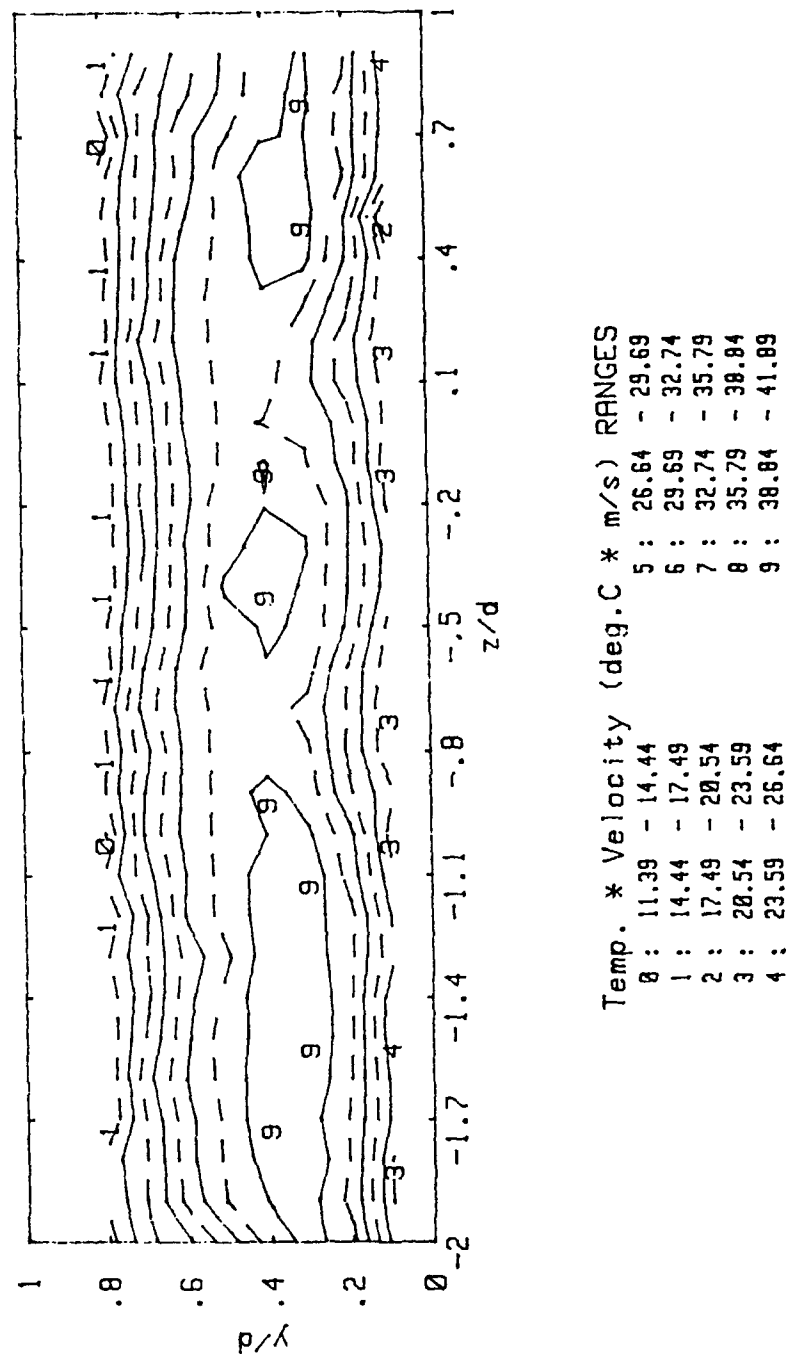
Figure 71. Mean Temperature/Mean Velocity Product Contours,
De = 98.1

Figure 72. Mean Temperature/Mean Velocity Product Contours, De = 126.0

108

Figure 73. Mean Temperature/Mean Velocity Product Contours,
De = 149.8

Figure 74. Mean Temperature/Mean Velocity Product Contours,
De = 173.5

110

Figure 75. Mean Temperature/Mean Velocity Product Contours,
De = 198.4

111

APPENDIX C
SOFTWARE DIRECTORY

This Appendix gives a listing of the various programs used in this thesis. Each program listing contains a summary of how the program is used, user inputs, program outputs and any additional features. Programs are listed in two groups; Nusselt number distributions and exit mixed-mean temperature measurement. All programs were written in BASIC 4.0 for use on the HP9836S computer.

I. NUSSELT NUMBER DISTRIBUTION PROGRAMS

A. TCHECK:

This program acquires multiple channel thermocouple data and performs temperature calibration equations to provide measurements in Degrees Celcius.

user inputs: thermocouple voltage readings, X

program output: provides monitor summary of thermocouple number, data aquisition channel number, voltage reading and corresponding temperature reading in Deg. C.

B. TEMCURV:

This program aquires multiple channel thermoucouple data and creates two files to be used in other programs for the curved heating channel. Primary purpose is to supply data for Nusselt number calculations.

user inputs: a) thermocouple voltage readings.

b) run number.

c) voltages across shunts for all four heaters, mvolts.

d) voltages across heaters, volts.

e) ambient pressure, inches of mercury.

f) pressure drop across orifice plate, inches of water.

program outputs: a) data file, Idata, provides data required to determine heat

input, conduction loss and Dean number; Runno, Amp1, Amp2,

Amp3, Amp4, Vh1, Vh2, Vh3, Vh4, Pamb, Deltap, Tmi,

Tccamb, Tcvamb, Ro.

b) data file, Tdata, provides temperature data in Deg. C for

determination of local Nusselt numbers.

C. NUCURV3B:

This program determines heat transfer coefficients and Nusselt numbers by

conducting surface energy balance. Heat flux inputs and conducted heat losses are

determined.

user inputs: a) reads data files Tdata and Idata from program TEMCURV.

b) estimated Dean number.

program outputs: a) data file, Hdata, of heat transfer coefficients, local Nusselt

numbers streamwise and spanwise locations, measured and

corrected temperatures as follows; H, Nus, X2, Z, T1 and T.

additional features: a) provides spanwise-averaged Nusselt numbers.

b) using energy balance, calculates local mean temperatures.

c) with estimated Dean number, performs iteration process to

determine actual Dean number.

D. NUSCCPL2

This program reads data file and plots spanwise variations of Nusselt numbers

by rows for concave section of curved heating channel utilizing thermocouples 31-115.

user inputs: local Nusselt numbers along with corresponding streamwise and spanwise

distances (output data file, Hdata, from program NUCURV3B).

program outputs: Nusselt number distribution contours for all rows of concave curved

section.

E.   NUSCVPL2

This program reads data file and plots spanwise variations of Nusselt numbers

by rows for convex section of curved heating channel utilizing thermocouples 116-120.

user inputs: local Nusselt numbers along with corresponding streamwise and spanwise

distances (output data file, Hdata, from program NUCURV3B).

program outputs: Nusselt number distribution contours for all rows of convex curved

section.

II. EXIT MIXED-MEAN TEMPERATURE MEASUREMENT

A.   TEMTRAV

Program for control of temperature traverse probe positioning and data

acquisition in the curved heating channel. Interfaces with MITAS controller to control the

probe position. Provides temperature difference between exit temperature and ambient inlet

temperature.

user inputs: a) estimate of Dean number

b) initial position of pressure probe.

c) number of y and z points to take data at.

d) resolution of data.

e) ambient inlet temperature channel number.

f) temperature probe channel number.

g) ambient pressure.

h) pressure drop across orifice plate.

i) delay time to start the experiment.

program outputs: a) data file, Temp, provides position and temperature data as

follows: Y, Z, temperature, inlet temperature, temperature

difference.

b) provides actual Dean number through iteration process.

B. TMXDMPLOTB

Program to plot time averaged traverses of temperature probe measurements.

Will plot up to ten radial traverses for different spanwise locations.

user input: a) temperature data file, TEMP (output from program TEMTRAV).

b) spanwise positions to plot.

program output: temperature traverse plot

C. TMXDMEAN

Modified version of TMXDMEAN to plot traverse of mean temperature, mean

velocity products. Will plot up to ten radial traverses, for different spanwise locations.

Program has been modified to determine exit mixed-mean temperature using process

described in Chapter 3, Section C, part 2.

user inputs: a) temperature data file, TEMP (output from program TEMTRAV).

b) velocity data file, VEL (output from program VELOCITY).

c) spanwise positions to plot.

program output: a) mean temperature, mean velocity traverse plot.

b) monitor output of exit mixed-mean temperature.

115

APPENDIX D
DATA FILE LISTING

A Summary of the data files and corresponding experimental parameters is given in two parts, the first of which involves the determination of all Nusselt number results and the second with the calculation of the measured exit mixed-mean temperature results.

A. NUSSELT NUMBER RESULTS.

The following lists of data were used for the determination of all Nusselt number data presented in this thesis. This includes both the spanwise-averaged Nusselt data and the local spanwise Nusselt number distributions.

experimental parameters:

Dean nnumber	58.9	74.2	98.6	126.4	150.9	174.4	198.9
Pressure drop (in water)	.031	0.05	0.09	0.15	0.215	0.29	0.38
Heat flux/heater (watts)	38.8	37.8	53.75	52.9	73.6	72.2	76.0
Max. surface temp. (TC#199, ^{o}C)	56.5	48.6	54.9	49.3	57.1	51.5	50.2

data file listings:

Tdata/Idata #	22-24	26-28	6-8	9-11	1-3	4-6	7-9
File number	9	9	9	9	10	10	10
Hdata # (file #19)	50	75	100	125	150	175	200

B. MEASURED MIXED-MEAN TEMPERATURE RESULTS

The following list of data provides the data information used in calculating the measured exit mixed-mean temperature and the plotting of the temperature traverse contours. Also included is the velocity file number, which is presented by Hughes [Ref. 8] and Tuzzolo [Ref. 14].

experimental parameters:

Dean number	58.5	73.7	98.1	126.0	149.8	173.5	198.4
Pressure drop (in water)	0.031	0.05	0.09	0.150	0.215	0.29	0.38
Heat flux/heater (watts)	40.0	47.2	56.7	63.3	73.2	81.9	92.2
Max. surface Temp. TC #199, $^{\circ}$C)	60.4	60.3	59.2	56.8	57.6	58.8	59.7

data file listing:

Tdata/Idata #	3,4	5,6	7,8	9,10	11,12	0,1	2,3
File number	15	15	15	15	15	17	17
Temp #	50	75	100	125	150	175	200
File number	15	15	15	15	15	17	17
Vel #	1	1	3	4	4	5	51

LIST OF REFERENCES

1. Ligrani, P. M. and Niver, R. D., "Flow Visualization of Dean Vortices in a Curved Channel with 40 to 1 Aspect Ratio," _The Physics of Fluids,_ V. 31, pp. 3605-3617, 1988.

2. Johnson, R. W. and Launder, B. E., "Local Heat Transfer Behavior in Turbulent Flow Around a 180 deg Bend of Square Cross Section," _The American Society of Mechanical Engineers,_ Presented at the 30th International Gas Turbine Conference and Exhibit, Paper No. 85-GT-68, 1985.

3. Chang, S. M., Humphrey, J. A. C., Johnson, R. W., and Launder, B. E., "Turbulent Momentum and Heat Transfer in Flow Through a 180 deg Bend of Square Cross Section," _Proc. 4th Turbulent Shear Flow Symposium,_ University of Karlsruhe, Karlsruhe, FRG, 1983.

4. Brinch, P. F., and Graham, R. W., "Flow and Heat Transfer in a Curved Channel," National Aeronautics and Space Administration, Technical Note D-8464, May 1977.

5. Gibson, M. M., Verriopoulos, C. A., and Nagano, Y., "Measurements in the Heated Turbulent Boundary Layer on a Mildly Convex Surface," _Turbulent Shear Flows,_ V. 3, 1982, p. 80.

6. Simon, T. J., and Moffat, R. J., "Heat Transfer Through Turbulent Boundary Layers-The Effects of Introduction and Recovery From Convex Curvature," ASME Paper No. 79-WA/GT-10, 1979.

7. Chang, S. M., Humphrey, J. A. C., and Modavi, A., "Turbulent Flow in a Strongly Curved U-Bend and Downstream Tangent of Square Cross Section," _Physico-Chemical Hydrodynamics,_ Vol. 4, 1983, p. 243.

8. Hughes, R. E., _Development, Qualification and Measurements in Two Curved Channels with 40 to 1 Aspect Ratio,_ Master's Thesis, Naval Postgraduate School, Monterey, CA., September 1989.

9. Schwartz, G. E., _Control of Embedded Vortices Using Wall Jets,_ Master's Thesis, Naval Postgraduate School, Monterey, CA., September 1988.

10. ASME Power Test Committee, _ASME Power Test Codes,(Supplement on Instruments and Apparatus),_ part 5,Chapter 4, p. 25, American Society of Mechanical Engineers, 1959.

11. Holman, J. P. and Gajda, W. J., Jr., Experimental Methods for Engineers, 4th Edition, pp. 238-247, McGraw-Hill, 1984.

12. Bella, D. W., Flow Visualization of Time-Varying Structural Characteristics of Dean Vortices in a Curved Channel, Master's Thesis, Naval Postgraduate School, Monterey, CA., September 1988.

13. Baun, L. R., The Development and Structural Characteristics of Dean Vortices in a Curved Rectangular Channel, Master's and Engineer's Thesis, Naval Postgraduate School, Monterey, CA., September 1988.

14. Tozzulo, M. F., Study of Vortex Arrays Induced Artificially and From Centrifugal Instabilities, Master's and Engineer's Thesis, Naval Postgraduate School, Monterey, CA., June 1989.

15. Kays, W. M. and Crawford, M. E., Convective Heat and Mass Transfer, Second Edition, p. 103, McGraw-Hill Book Company, 1980.

INITIAL DISTRIBUTION LIST

No. Copies

1. Defense Technical Information Center 2
   Cameron Station
   Alexandria, VA 22304-6145

2. Library, Code 0142 2
   Naval Postgraduate School
   Monterey CA 93943-5002

3. Professor Phillip M. Ligrani 6
   Code 069Li
   Department of Mechanical Engineering
   Naval Postgraduate School
   Monterey CA 93943-5000

4. Professor Chelakara S Subramanian 1
   Code 069Su
   Department of Mechanical Engineering
   Naval Postgraduate School
   Monterey CA 93943-5000

5. Department Chairman, Code 69 1
   Department of Mechanical Engineering
   Naval Postgraduate School
   Monterey CA 93943-5004

6. Lt Paul E. Skogerboe 2
   1281 Spruance Rd.
   Monterey, CA 93940

7. Naval Engineering Curricular Officer, Code 34 1
   Department of Mechanical Engineering
   Naval Postgraduate School
   Monterey CA 93943-5004

8. Dr. K. Civinskas 8
   Propulsion Directorate
   U.S. Army Aviation Res. and Technology Activity
   AVSCOM
   NASA-Lewis Research Center
   Cleveland, OH 45433